Effects of tissue-specific interferon-γ expression on local inflammatory responses

vorgelegt von
Diplom-Biochemiker
Markus Koch
aus Berlin

Von der Fakultät III – Prozesswissenschaften
der Technischen Universität Berlin
zur Erlangung des akademischen Grades

Doktor der Naturwissenschaften
- Dr. rer. nat. -

genehmigte Dissertation

Promotionsausschuss:
Vorsitzender: Prof. Dr. Ulf Stahl
Berichter: Prof. Dr. Stefan H.E. Kaufmann
Berichter: Prof. Dr. Roland Lauster

Tag der wissenschaftlichen Aussprache: 19.11.2003

Berlin 2003

D83

Content I

Abbreviations VI

Abbreviations

AA	amino acid
Ab	antibody
Ag	antigen
AHR	airway hyperresponsiveness
AMACO	an extracellular matrix protein containing VWA-like domains related to those in MAtrilins and COllagens,
AP	alkaline phosphatase
APC	antigen presenting cell
BAL	bronchoalveolar Lavage
BALF	bronchoalveolar Lavage Fluid
BCG	bacillus Calmette et Guérin
BCR	B cell receptor
BSA	bovine serum albumin
C57BL/6	C57BL/6 is the most widely used inbred mouse strain.
CD	Crohn's disease
CD#	"cluster of differentiation": international nomenclature for cell surface molecules (CD number)
CI-tgIFNγ-KO	IFNγ-KO mice with lung-specific IFNγ expression (CC10-IFNγ transgenic IFNγ-KO)
CLP	common lymphoid progenitor
CTL	cytolytic (cytotoxic) T lymphocyte
Cy5	Cy-Chrome 5, fluorescent dye for flow cytometry and microarray analysis
Cy3	Cy-Chrome 3, fluorescent dye for flow cytometry and Microarray analysis
DC	dendritic cells
DNA	deoxyribonucleic acid
DP	double positive
ELISA	enzyme linked immunosorbent assay
ER	endoplasmic reticulum
FACS	fluorescent activated cell sorting
FITC	fluorescein, fluorescent dye for FACS analysis
HCG	human chorionic gonadotropin
HSC	hematopoietic stem cell
IBD	inflammatory bowel disease
IEL	intraepithelial lymphocytes
ITF	intestinal trefoil factor
IFA	incomplete Freud's adjuvant
ifabp	intestinal fatty acid binding protein promoter

IFNγ	interferon γ
IFNγ-KO	interferon γ knockout; C57BL/6 mouse strain with a targeted deletion in the IFNγ locus
IL	interleukin
i.p.	intraperitoneal
LCMV	lymphocytic choriomeningitis virus
lfabp	liver fatty acid binding protein promoter
LPL	lamina propria lymphocytes
LPS	lipopolysaccharid
tgLI#4,23,31	lfabp-IFNγ transgenic mouse line number 4, 23 or 31
mAb	monoclonal antibody
M	mol per liter
MHC	major histocompatibility complex
NK	natural killer
ORF	open reading frame
OVA	ovalbumin (chicken egg albumin)
PBS	phosphate buffered saline
PCR	polymerase chain reaction
PE	phyco-erythrin, fluorescent dye for FACS analysis
PI	propidium iodide
PMS	pregnant mere serum
PMSF	phenylmethysulphonylflouride, common protease inhibitor
PTK	protein tyrosine kinase
RNA	ribonucleic acid
SCID	severe combined immunodeficiency
SDS	sodiumdodecysulphonate, common detergent
TAP	transporter associated with antigen presentation
TCR	T cell receptor
TdT	terminal deoxynucleotidyl transferase
Th1	T helper cell type 1
Th2	T helper cell type 2
TIN	tubulointerstitial nephritis
TLR	toll-like receptor
TNF	tumor necrosis factor
UC	ulcerative colitis
VWA	Von Willebrand factor A (aminoacid sequence common in extracellular matrix proteins)

1 Introduction

Mammals posses a variety of mechanisms to protect themselves against pathogens (e.g. bacteria and viruses) and tumors. Responsible for these protective mechanisms is the immune system, which consists of a large variety of soluble mediators and cells with specialized roles in the defense against infection. Upon infection, the coordinated cooperation of the mediators and cells leads to an immune response that is accompanied by inflammation and usually results in elimination of the invading microbe or the mutated cells. However, immune responses and especially the accompanying inflammation cause diseases when the responses are inappropriate or when they are uncontrolled. Key elements in the induction and coordination of the immune response are cytokines. Cytokines are soluble proteins that are released from cells and modify the behavior and development of the same cell that releases them (autocrine), of cells in the immediate surrounding (paracrine) or of distant cells (endocrine). One of these cytokines i.e. Interferon-γ (IFNγ) is the subject of this study. The many known functions and the involvement of IFNγ in almost all types of systemic and mucosal immune responses lead us to the analysis of its function in inflammation in two models with exclusively local IFNγ expression.

1.1 The cells of the immune system

The principal mediators of the immune system are specialized cells with a wide spectrum of different functions. All of these cells are derived from the same progenitors, the pluripotent hematopoietic stem cells, found in the fetal liver and the bone marrow (hematopoiesis). Hematopoiesis is regulated by cytokines from bone-marrow stromal cells or by cytokines of immune cells (Figure 1). Upon cytokine stimulation, hematopoietic stem cells differentiate into lymphoid and myeloid precursor cells. While the lymphoid precursor cells develop only into three distinct cell types, the T- B- and natural killer (NK) cells, the myeloid precursor cells further develop into macrophages, neutrophils, dendritic cells (DC), basophils / mast cells, eosinophils and red blood cells. The number and localization of the myeloid immune cells within the body largely depends on the presence of an immune response and the cytokines and chemokines produced thereby. Neutrophils are rare in tissues in the absence of infection. During infection, their number increases rapidly, and at the site of inflammation, they are a prominent cell type. Macrophages are located in all organs and connective tissues. High numbers can also be

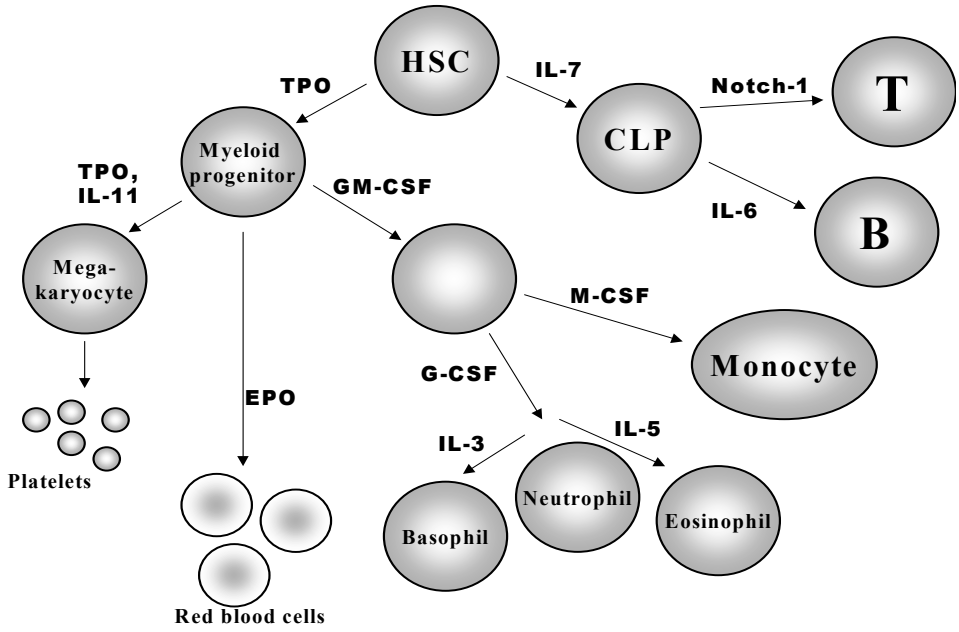

Figure 1: A schematic representation of hematopoiesis and its regulation by cytokines. HSC = hemapoietic stem cell; TPO = thrombopoietin; IL = interleukin; CLP = common lymphoid progenitor; GM-CSF = granulocyte macrophage colony stimulating factor; EPO = erythropoietin. The figure was modified from Kimball's Biology Pages (http://www.ultranet.com/~jkimball/BiologyPages/W/Welcome.html)

found in the spleen, the major site of immune responses to blood borne antigens. Dependent on the host tissue they reside in, macrophages can further differentiate into specialized tissue-specific macrophage like cells, e.g. Kupfer cells (liver) and microglia (brain). Immature dendritic cells are predominantly found in the epithelia of skin, the gastrointestinal and respiratory system, which are the main entry sites for antigen and microbes. Mature DC are mostly located in lymph nodes, where they interact with one of the descendants of the lymphoid progenitor cells, the T-cells.

T cells are divided into distinct classes based on the cell surface receptors they express. The majority of T cells express T cell receptors (TCR) consisting of α and β chains (α/β T cells). A small group of T cells express receptors made up of γ and δ chains (Bluestone et al., 1995). Within the α/β T-cell lineage there are two sublineages: those that express the coreceptor molecule CD4 ($CD4^+$ T cells) and those that express CD8 ($CD8^+$ T cells). $CD4^+$ and $CD8^+$ T cells differ fundamentally in how they recognize antigen and mediate different types of regulatory and effector functions.

T and B lymphocytes are found in the central lymphoid organs, the thymus (T cells), and bone marrow (B cells), where they undergo the developmental steps that equip them with the necessary receptors to mediate the responses of the mature immune system. Mature T and B lymphocytes are found in peripheral organized lymphoid tissues, such as spleen, lymph nodes, Peyer`s patches of the intestine and tonsils, where they further develop into cytokine secreting effector cells. Mature T and B cells are also found in the mucosa of the gut and in the event of an infection, effector T cells are usually a prominent cell type at the site of inflammation.

Lymphoid and myeloid cells interact and cooperate to eliminate invading microbes. However, there are two fundamentally different types of immune responses to infection, the innate (natural) and the acquired (adaptive) immune response.

1.2 The innate immune response

The innate immune response is initiated immediately after contact to foreign antigens, and in contrast to the adaptive immune response, innate responses remain unchanged regardless of how often the antigen is encountered. Both types of responses are initiated by the recognition of foreign, “non self”, structures by specific receptors of immune cells.

1.2.1 Receptors

A main distinction between the innate and the adaptive immune system lies in the receptors used for the recognition of foreign structures. In contrast to receptors of the adaptive immune response, receptors of the innate immune system are germline-encoded with genetically predetermined specificity. Many of these innate receptors evolved early in the development of immune systems, and structural components similar to these receptors can be found in many multicellular organisms (Medzhitov and Janeway, 1998). The receptors, e.g. toll-like receptors (TLRs), recognize conserved pathogen-associated molecular patterns (PAMPs) shared by large groups of microorganisms. Recognized molecular patterns include lipopolysaccharide (LPS) of gram-negative bacteria, and lipoteichoic acids of gram-positive bacteria (recognized by TLR-4 and TLR-2), double stranded RNA from certain viruses (TLR-3) and flagellin of flagella expressing bacteria (TLR-5). Microbial DNA is recognized by TLR-9 in the form of unmethylated cytosine–guanosine dinucleotide sequences flanked 5' by two purines and 3' by two pyrimidines (CpG motifs) (Bauer et al., 2001; Beutler, 2002; Janeway and Medzhitov, 2002; Kaisho and Akira, 2001; Medzhitov and Janeway, 2000b). Recognition of PAMPs allows the innate immune system not only to detect the presence of an infectious microbe, but also to determine the type of the infecting pathogen. Pattern recognition receptors activate conserved host defense signaling pathways that control the expression of immune response genes in a wide variety of cells.

1.2.2 Effector cells

The main effector cells of the innate immune system towards infections with bacteria and parasites are neutrophils, which appear early at the site of infection, and macrophages, which migrate more slowly than neutrophils and therefore appear later. Infections by numerous types of viruses are initially controlled by NK-cells, which directly kill virus infected host cells. Macrophages and neutrophils have the ability to phagocytose and then kill invading microorganisms. Macrophages possess receptors, which facilitate phagocytosis, e.g. for carbohydrates that are not normally exposed on the cells of vertebrates, such as mannose, and therefore can discriminate between "foreign" and "self" molecules (Medzhitov and Janeway, 2000a; Stahl and Ezekowitz, 1998). Additionally phagocytic receptors, expressed on macrophages and neutrophils, are those for antibodies and complement, so that the coating of microorganisms with antibodies or complement, enhances phagocytosis (McKenzie and Schreiber, 1998; Zhang et al., 1997).

1.2.3 Development of inflammatory responses

Stimulation of macrophages via TLRs and/or cytokine receptors, e.g. the IFNγ-receptor, results in efficient killing of the engulfed microorganism and the secretion of several cytokines e.g. tumor necrosis factor α (TNF-α), interleukin 12 (IL-12) and IL-18, and a wide variety of chemokines. The local high concentration of chemokines and cytokines induces the recruitment of leukocytes to the site of infection. Different cytokines and chemokines serve multiple overlapping functions in the recruitment of leukocytes. TNF-α induces the expression of further chemokines but also the upregulation of adhesion molecules like E-selectin, intercellular adhesion molecule 1 (ICAM-1) and vascular cell adhesion molecule 1 (VCAM-1) by endothelial cells, which enables leukocytes to leave the blood vessels and cross into the tissue. Chemokines are also involved in this process of endothelial cell activation, but mainly induce the chemotaxis of leukocytes along a concentration gradient towards the sites of infection or inflammation.

Because different cytokines induce different chemokines, and different chemokines attract different types of leukocytes, the type of infiltrate is controlled by the cytokines secreted at the site of infection.

The initially secreted cytokines i.e. TNF-α, IL-12 and IFNγ also have the ability to activate infiltrating cells, especially macrophages and neutrophils. In macrophages and neutrophils this activation leads to the production of various toxic molecules, including reactive oxygen intermediates (ROI), reactive nitric oxide intermediates (RNI), antimicrobial peptides, and lysozyme, which are essential to efficiently kill phagocytosed microbes. However, these toxic molecules do not distinguish between self-tissue and microorganisms. If macrophages and neutrophils are strongly activated, e.g. by cytokines like IFNγ, the antimicrobial products can be secreted into the extracellular environment where they cause injury of the surrounding normal host tissue. Together with the intentional secretion of tissue-modulating factors by activated macrophages and neutrophils, this whole process of infiltration and activation causes inflammation (Ricevuti, 1997).

1.2.4 Linking innate and adaptive immunity

Additionally to their role in the induction of inflammation, cytokines expressed by the effector cells of the innate immune system, also induce and coordinate the appropriate type of adaptive immune response. IFNγ activates DC, which are the cellular link between innate and adaptive immune responses (Fearon and Locksley, 1996; Trinchieri and Gerosa, 1996). DC constantly endocytose extracellular soluble antigens and when TLRs on their surface recognize distinctive PAMPs or they encounter cytokines like IFNγ, DC become activated and differentiate into mature antigen-presenting cells (APC). They present peptides of foreign antigens complexed with MHC molecules (major-histocompatibility-complex) on their surface. In addition, they upregulate costimulatory molecules like CD40, CD80 and CD86. Recognition of the MHC-peptide complex on mature DC by naïve T cells with the appropriate TCR results in activation of these T cells and in the development of an adaptive immune response (Banchereau and Steinman, 1998; Lanzavecchia and Sallusto, 2001; Liu, 2001; Mellman and Steinman, 2001).

1.3 The adaptive immune response

The adaptive immune response is based on the activation and clonal expansion of B and T cells following recognition of their cognate antigen. B cells recognize soluble antigens via the B-cell receptor (BCR), a membrane bound form of antibodies. Upon antigen recognition B cells start to proliferate and differentiate into IgM secreting effector cells, the plasma cells. In a T-cell dependent process, a subpopulation of activated B cells differentiates to plasma cells producing other antibody isotypes. A fraction of the activated B cells matures to long-living memory B cells and enables a fast and highly specific response to further infection with antigen.

The T-cell response is initiated by the interaction of the TCR/CD3 complex of naïve T lymphocytes with MHC-peptide complexes presented by APCs. In the presence of costimulatory molecules this interaction leads to the activation and clonal expansion of the T cells, and the generation of effector and memory T cells. Although the processes that generate effector T cells and B cells take much longer than the immediate responses of macrophages and neutrophils at the site of infection, they generate a high number of highly specific and efficient effector T cells and B cells. In contrast to the innate immune system, the generation of memory T cells and B cells enables the adaptive immune system to respond to a secondary infection with the immediate generation of the appropriate effector mechanism. The basis for these processes is the high specificity of the T- and B-cell receptors that enable them to detect any possible foreign structure.

1.3.1 Receptors

In contrast to the receptors of the innate immune system, the receptors of the adaptive immune system, are not genetically predetermined. The functional receptors of T and B-cells are generated in immature T and B cells by the rearrangement of germline gene segments. Each of the rearranged segments is randomly selected from a large pool of suitable exons, leading to a highly diverse repertoire of T and B cells each with unique antigen-specific receptors. Although the human genome only contains 3-4 x 10^5 genes, as much as 2.5 x 10^7 different TCRs and about the same number of BCRs can

be generated (Bretscher, 1992; Bretscher, 1975; Madrenas et al., 1996; Schwartz, 1996). The enormous number of possible TCRs and BCRs also has a negative side effect. It allows the adaptive immune system to recognize not only pathogen derived but also host derived structures. To limit the possibility of an adaptive immune response against self (autoimmune reaction), developing T and B cells are negatively selected against almost all proteins expressed in the host.

1.3.2 Prevention of autoimmune responses

Negative selection, however, is not perfect and further mechanisms exist that control possibly self reactive T or B cells. Recognition of self antigens on non-professional APCs, which lack costimulatory molecules like CD80 and CD86, induces anergy in the T or B cells, a state of functional inactivation, (Ohashi et al., 1991; Wucherpfennig and Strominger, 1995). The physical separation of naïve self-specific T or B cells from the antigen also prevents their activation (ignorance). Probably most important in the prevention of pathology by either autoreactive T cells or during exaggerated immune responses are regulatory T cells (T_{reg}). Many lymphocyte populations have been shown to exhibit regulatory functions. However, only $CD4^+$ $CD25^+$ T cells were shown to possess regulatory functions independent of the experimental system. These cells inhibit autoimmune diabetes in mice, prevent inflammatory bowel disease (IBD), prevent the expansion of effector T cells *in vivo* and inhibit T cell activation *in vitro*. Although the regulatory mechanism remains unclear, secretion or expression of either IL-10, TGF-β, CTLA-4 or a combination of these molecules appears to be involved (Annacker et al., 2001; Curotto de Lafaille and Lafaille, 2002; Hara et al., 2001; Read et al., 2000; Sakaguchi et al., 1995; Shevach, 2000; Stephens and Mason, 2000). However, in human and mouse many types of autoimmune diseases are known, indicating neither of these mechanisms is fail-safe.

1.3.3 Two types of CD4$^+$ T cells; two types of adaptive responses

The interaction of naïve CD4$^+$ T cells with professional APCs causes differentiation of the CD4$^+$ T cells into one of two principal directions (Figure 2). Dependent on the type of APC, the costimulation and the cytokine milieu present at the site of activation, the naïve T cell is either committed to the Th1 or the Th2 linage. While the presence of IL-12 promotes the development of Th1 cells, presence of IL-4 induces the development of Th2 cells.

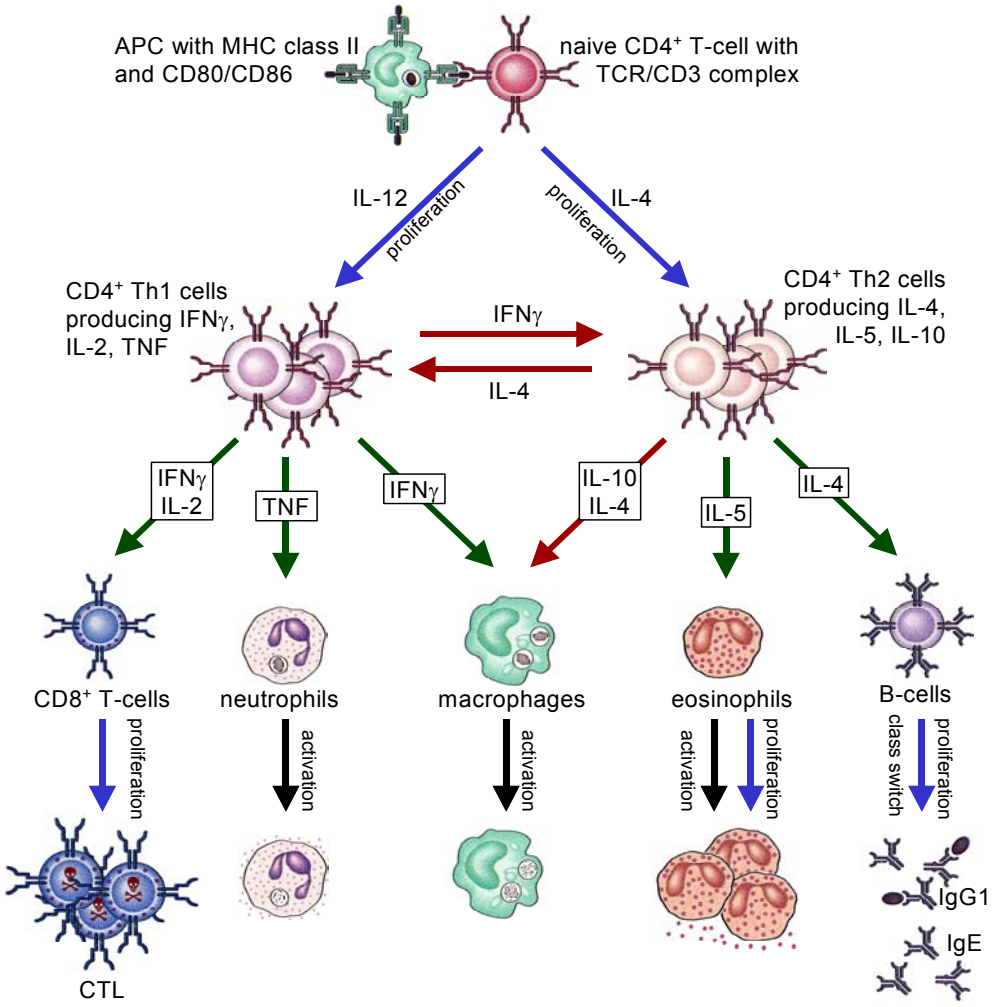

Figure 2: Schematic representation of Th1 and Th2 cell development and selected effector functions. Naïve CD4$^+$ T cells differentiate into Th1 or Th2 cells dependent on the presence of IL-12 or IL-4 at the time of APC contact. Cytokines secreted by the two CD4$^+$ T cell types are indicated with their positive (green arrows) or negative (red arrows) effect on proliferation (blue arrows) or activation (black arrows) of other cells of the immune system. Parts of this figure were adapted from the book Cellular and Molecular Immunology by A.K. Abbas, A.H. Lichtman and J.S. Pober (Abbas et al., 2000).

Th1 and Th2 cells mediate different types of immune responses, by secreting different sets of cytokines. Th1 cells produce TNF-α, IL-2, IFNγ and lymphotoxin (LT), and thereby initiate a cell mediated response involving enhancement of microbicidal activity of monocytes and macrophages and the development of cytotoxic T-lymphocytes (CTLs). Th2 cells secrete IL-4, IL-5, IL-6 and IL-13, which induce a humoral response by activating B cells. Furthermore, Th2 cells promote the production of IgE and the development of eosinophils and mast cells (Farrar et al., 2002; Jacobs and Bross, 2001; Jankovic et al., 2001; Mosmann and Coffman, 1989; Oltz, 2001; Romagnani, 1991; Weill and Reynaud, 1996).

The cellular response preferentially develops during infections with intracellular bacteria and viruses and has been shown to be critically involved in the clearance or containment of infections with pathogens, like *Salmonella*, *Listeria* and *M. tuberculosis* (Hahn and Kaufmann, 1981; Kaufmann, 1993). Nevertheless, cellular responses can lead to severe inflammation, by activating neutrophil and macrophage effector mechanisms as described in innate immunity and by activating CTLs. If a cellular response is wrongfully induced or insufficiently controlled, this can lead to diseases like insulin dependent diabetes mellitus and probably also one form of inflammatory bowel disease, namely Crohn's disease (Fuss et al., 1996; Singh et al., 1999).

Humoral responses are generated during infections with parasites, e.g. helminths, and are the principal protective response against extracellular bacteria. Antibodies produced during a humoral response can neutralize bacteria, enhance their uptake by phagocytes via Fc Receptors or following complement fixation/opsonization via complement receptors. Complement fixation can also cause direct lysis of some bacteria.

A humoral response can also cause inflammation and if inappropriately induced or uncontrolled it leads to immediate hypersensitivity reactions responsible for allergies and also asthma. Central mediators of inflammation during immediate hypersensitivity reactions are mast cells, neutrophils and eosinophils. Mast cells and eosinophils express Fcε receptors and thereby recognize IgE complexed antigen. When they are activated via these Fcε

receptors they secrete a variety of tissue damaging and modulating effector molecules and enzymes. Mast cells e.g. secrete histamine, which stimulates smooth muscle cells, and a variety of prostaglandins and leukotriens, which lead to bronchoconstriction and mucus secretion. These cells also produce cytokines like IL-4, IL-5, IL-13 and TNF-α and thereby induce endothelial cell activation and promote Th2 differentiation (Boyce, 2003; Finkelman and Urban, 2001; Kay, 1989; Kay, 1991; Kips, 2001).

Although the cytokines produced by Th1 and Th2 cells antagonize each other and decrease the development of the respective other T-cell subset, many infections and allergic diseases involve both types of responses for their development or control (Maziak, 2003; Nabel, 2002; Szabo et al., 2003).

1.4 The mucosal immune system

Alongside, and partially separated from the immune system of inner organs exists a highly sophisticated mucosal immune system with all the necessary lymphoid tissues and some very specialized cells. Mucosal immune responses are induced in the Gut-Associated Lymphoreticular Tissues (GALT) for the gut mucosa, and the Nasopharyngeal-Associated Lymphoreticular Tissues (NALT), for the respiratory tract. There is only limited information on the airway-associated mucosal immune response that is induced in the NALT. In contrast, the gastrointestinal immune response and its induction in the GALT has been extensively studied.

1.4.1 Immune system of the gastrointestinal tract

Central GALT are Peyer`s patches (PP) and mesenteric lymph nodes (MLN). While MLN are identical in overall structure to other peripheral lymph nodes, PP have a dome-like structure and are separated from the intestinal lumen only by a single layer of cuboidal epithelial cells and M cells. M cells mediate the uptake and transport of antigen from the gut lumen into the PP, but also serve as entry points for pathogens (Jones et al., 1994; Neutra et al., 1996). Within the PP, the anatomical appearance resembles that of classical secondary lymphoid organs, with clearly defined T and B cell areas (Kelsall and Strober, 1996). The lamina propria and the epithelium adjacent to the intestinal lumen (Figure 3-B/C) are the effector tissues of gut-associated mucosal immune responses. The lamina propria is highly populated by IgA secreting plasma cells, B cells and conventional $CD4^+$ T cells of the Th1 as well as the Th2 type and $CD8^+$ T cells (James et al., 1986). In contrast to the lamina propria lymphocytes, many of the intraepithelial lymphocytes (IEL) express the γ/δ-TCR and more than 90% of the IEL are $CD8\alpha^+$ (Kaufmann, 1996; Lefrancois, 1991). IEL are located between the epithelial cells adjacent to the basement membrane and it is likely that the epithelial cells interact with the IEL (Figure 3-C) (Brandeis et al., 1994; Mowat and Viney, 1997). Epithelial cells are capable of antigen processing and presentation and express costimulatory molecules and adhesion molecules, enabling them to function as APCs (Kvale et al., 1992; Ye et al., 1997). Their APC-like function

is possibly regulated by the surrounding IEL e.g. by IEL IFNγ secretion or by the activation of TLRs, which have been reported to be expressed on the epithelial cells of the intestine (Akira et al., 2001).

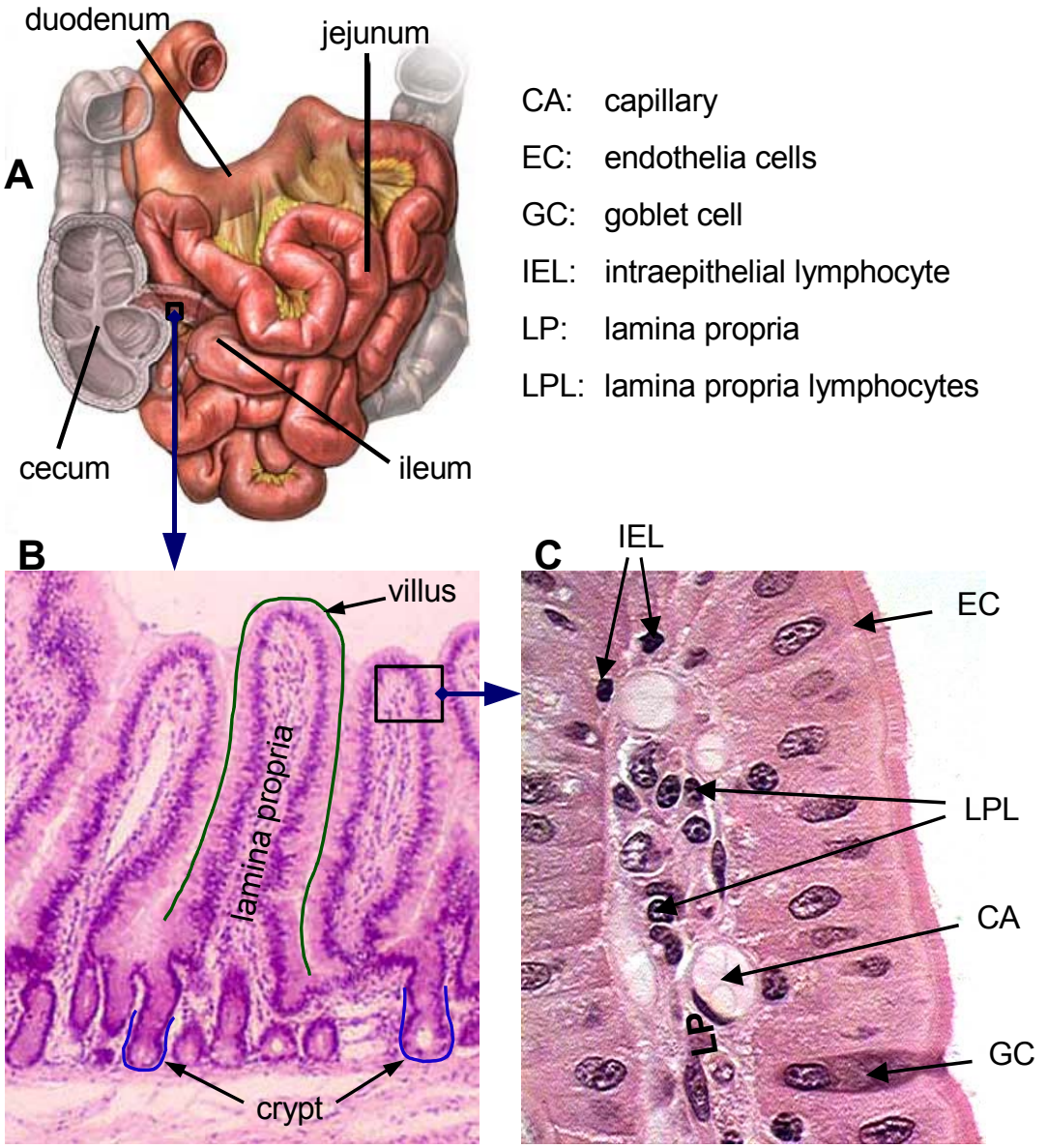

Figure 3: Schematic representation of the small intestine (A), beginning at the duodenum, followed by the jejunum, and ending in the ileum, which ends at the cecum and opens into the large intestine. (B) Histologic picture of the ileum mucosa. Villi, reaching into the intestinal lumen, and crypts, adjacent to the submucosa are indicated. Within the villi and between the crypts lies the lamina propria. (C) Higher magnification of a villus with columnar epithelium that represents the boarder to the intestinal lumen an the lamina propria within it. The epithelium consists of endothelial cells (EC), goblet cells (GC) and embedded intraepithelial lymphocytes (IEL). Within the lamina propria (LP) are capillaries (CA), lymphocytes (LPL), macrophages and B cells. The figure was created with pictures from David G. King`s histology webpages at Southern Illinois University School of Medicine (www.siumed.edu/~dking2/), P. B. Bell´s and B. Safiejko-Mroczka´s histology pages at the University of Oklahoma (casweb.cas.ou.edu/pbell/Histology/histo.home.html) and with a picture from the website of A.D.A.M. Inc. (www.adam.com).

1.4.2 Immune system of the respiratory tract

Only little is known about the mucosal immune system of the respiratory tract. Nevertheless, it is believed that it shares many features with the intestinal immune system. In humans, the IEL density in the epithelium of the respiratory tract is similar to the IEL density in the intestine, although the predominance of $CD8^+$ T cells compared to $CD4^+$ T cells is less strong in the lung and almost all T cells express the α/β TCR (Cerf-Bensussan and Guy-Grand, 1991; Fournier et al., 1989; Goto et al., 2000). Like in the intestine, the lamina propria of the bronchus-associated lung epithelium is highly populated by IgA secreting plasma cells and conventional $CD4^+$ T cells. In contrast to the intestine, high numbers of DC have been found in the airway epithelium in humans (Holt et al., 1989). However, large differences between animal species exist. A significant amount of IEL in murine lung e.g. expresses the γ/δ-TCR (Goto et al., 2000) and in pigs, in contrast to humans and rodents, huge numbers of intravascular macrophages have been found (Pabst, 1996).

Macrophages that reside within the lumen of alveoles (alveolar macrophages) constitute the primary defense mechanism of the lung (Figure 4-C). They efficiently phagocytose particles, like dust and bacteria, that escaped the dust traps of the nose, trachea and bronchioles. The phagocytic activity of these macrophages keeps the surface of the lung essentially sterile. It has been suggested that these macrophages are capable of reentering the lung and that they represent a transport mechanism for antigens from the bronchoalveolar lumen to draining lymph nodes (Corry et al., 1984; Harmsen et al., 1985).

The most prominent difference between the respiratory and the intestinal mucosal immune system is the lack of structures similar to the Peyer´s patches within the lung. Additional organized bronchus-associated lymphoreticular tissues (BALT) are also missing in lungs of healthy humans and mice, although they can be found constitutively in other animal species and appear in humans and mice during chronic inflammation of the airways (Pabst and Gehrke, 1990; Sato et al., 1992). BALT is therefore not considered to be a major component of the pulmonary immune system in

healthy adult humans and it has been suggested that other parts of the respiratory tract carry out some of the BALT functions. The generation of IgA secreting plasma cells e.g. might be directly induced in the epithelium of the airways (Salvi and Holgate, 1999).

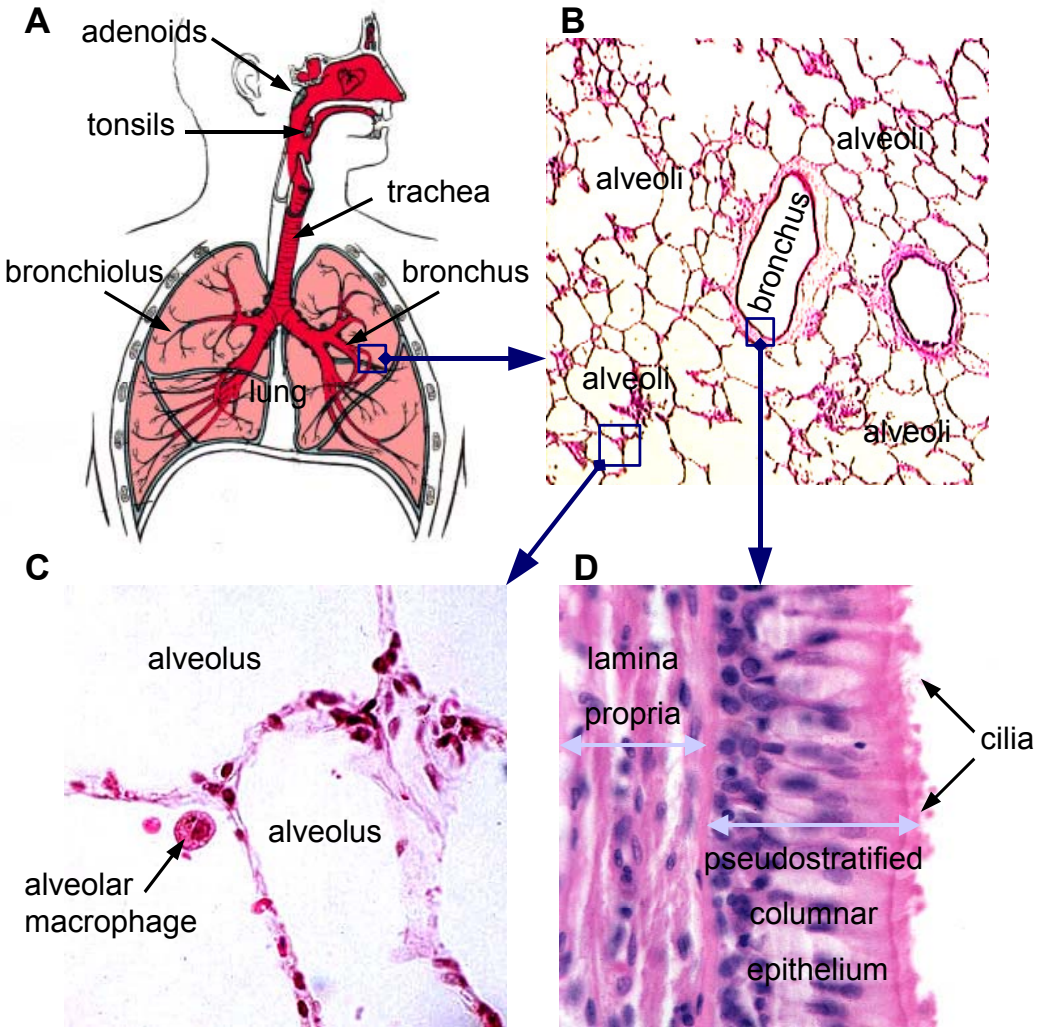

Figure 4: Schematic representation of the human respiratory tract with indicated location of adenoids and tonsils (A). The mouth and nose cavities end in the throat, which seperates into the trachea and the esophagus. The trachea ends in the mediastinum where it separates into two bronchi that lead into the left and right lung. Within the lungs, bronchi further separate into smaller bronchi, than into bronchioles and finally end in alveoli (A,B). The trachea, bronchi and larger bronchioles are lined by pseudostratified columnar epithelium, consisting of goblet cells, ciliated epithelial cells and clara cells, and an underlying lamina propria, which contains mast cells, plasma cells, DC, lymphocytes and scattered mucous glands (D). Aleveoli are lined by a thin layer of simple squamous epithelium, allowing gas exchange with blood flowing through underlying capillaries (C). Within the alveolar lumen are macrophages that phagocytose particles and bacteria, which escaped from the dust trap and export functions of the nose, trachea and bronchi. The figure was created with pictures from D.G. King`s histology webpages at Southern Illinois University School of Medicine (www.siumed.edu/~dking2/), T.A. Godwin`s webpages on the resipartoy system (edcenter.med.cornell.edu/CUMC_PathNotes/Respiratory/Respiratory.html) and with a picure from the Canadian Lung Association`s website (www.lung.ca).

The central inductors of airway-associated mucosal immune responses in humans appear to be NALT. In humans NALT consist of the palatine tonsils and adenoids, which together form a physical barrier termed Waldeyer´s ring. This ring is located at the transition of the mouth to the oropharynx, where NALT encounter inhaled as well as ingested antigens (Figure 4-A). Palatine tonsils are considered the equivalent of PP for the respiratory mucosal immune system. They contain crypts with M cells around the bases enabling them to take up antigen and their general structure is similar to that of secondary lymphoid organs, with lymphoid follicles and distinct T and B cell areas (Gebert, 1995; Nave et al., 2001). T and B cells leaving the tonsils are believed to home to their primary effector site, the respiratory tract.

1.4.3 Control of the mucosal immune system

Because of the constant exposure of all cells of the mucosal and specifically the intestinal immune system to enteric bacteria and food derived antigens, the system must be efficiently controlled (Hooper and Gordon, 2001; Neurath et al., 2002). A cytokine fundamentally involved in this control is IL-10. Mice lacking IL-10 expression develop inflammation in the intestine, which is strictly dependent on the presence of enteric bacteria (Kuhn et al., 1993; Sellon et al., 1998). Regulatory T cells that express IL-10 have been identified in the intestinal mucosa, and it is possible that these cells mediate tolerance to enteric bacteria and food antigens (Chen et al., 1994; Maloy and Powrie, 2001; Shevach, 2000). Overall, the mucosal immune system represents a balanced system with a highly controlled cell composition and cytokine milieu. Accordingly, it is likely that shifts in the expression level of cytokines can have detrimental consequences for mucosal tolerance. In fact, most inflammatory diseases involving the mucosal immune system, including that of the airways, are associated with either elevated levels of Th1 cytokines (e.g. inflammatory bowel disease), or elevated levels of Th2 cytokines (e.g. asthma) (de Jong et al., 2001; Neurath et al., 2002; Strober et al., 2002). One of the cytokines, whose presence or absence appears to be fundamentally involved in the development or perturbation of inflammatory diseases is IFNγ.

1.5 Interferon-γ (IFNγ)

The important role of IFNγ in the immune system and its regulation is mirrored by its early discovery. IFNγ and its relatives the type I interferons were first recognized more than 30 years ago based on their antiviral activity. Since IFNγ was found to utilize a different receptor and to induce a different response than all other interferons known, it was termed type II interferon or immune interferon.

1.5.1 Producers and inducers

The only sources of IFNγ were long thought to be NK-cells, $CD4^+$ T cells of the Th1 type and $CD8^+$ CTLs. Recent findings indicate that also macrophages, B cells and $CD8\alpha^+$ DC produce IFNγ (Munder et al., 1998; Ohteki et al., 1999; Yoshimoto et al., 1997). While $CD4^+$ T cells need to be primed by the recognition of antigen presented by DC in the presence of IL-12 before they start producing IFNγ, macrophages, NK cells, B cells and $CD8^+$ T cells can produce IFNγ independent from antigen recognition. In these cells, IFNγ expression is induced by other proinflammatory cytokines like TNF-α, IL-18 and IL-12 or IFNγ itself, as macrophages and NK-cells additionally dispose of a positive autocrine feedback mechanism for IFNγ (Di Marzio et al., 1994; Hardy and Sawada, 1989). Interestingly, macrophages are also the main source of TNF-α, IL-18 and IL-12, which they rapidly produce upon TLR stimulation or infection with intracellular bacteria and which are critically involved in the activation of NK-cells, the main source of IFNγ in the absence of an adaptive immune response.

1.5.2 The receptor and its signals

The IFNγ receptor is expressed on all cells except erythrocytes and consists of two subunits named IFNγR-1 and IFNγ-R2. Because biologically active IFNγ is a homodimer, binding of IFNγ to its receptor is believed to induce the dimerization of IFNγR-1, which than allows the recruitment two units of IFNγR-2. Homodimerization of the receptor leads to the Janus-Kinase (JAK) mediated phosphorylation of STAT1 (Signal Transducer and Activator of

Transcription 1), which then translocates into the nucleus where it binds to specific promoter sequences and thereby activates transcription of primary response genes and of more than 40 transcription factors, which regulate the expression of numerous secondary response genes. Interestingly, the JAK/STAT1 pathway is shared with the signaling of type I interferons, and resulting from this, many of the genes transcribed upon receptor activation are similar between the type I interferons and IFNγ. However, type I interferon signaling predominantly utilizes STAT2, which leads to significant differences in the pattern of genes that are activated in interferon type I or type II exposed cells (Foxwell et al., 1992).

1.5.3 Effects of IFNγ-receptor stimulation

The composition of genes that are eventually activated upon IFNγ binding, is dependent on the cell type and the activation status of other cytokine or chemokine signaling pathways. So far, more than 500 IFNγ directly and indirectly activated genes have been described and were classified into 37 functional categories (de Veer et al., 2001). Many of these genes code for intracellular proteins that have important cell cycle regulating functions or are involved in apoptosis (Chawla-Sarkar et al., 2003). A prominent IFNγ induced class of intracellular proteins are the 47 kDa and 65 kDa GTPase families and the Mx-GTPase. Infection experiments with animals, in which genes of members of these families were rendered non-functional or deleted (KO mice), implicate an important role of these ubiquitously induced proteins in intracellular defense mechanisms (Boehm et al., 1997; Carlow et al., 1998; Collazo et al., 2001); and unpublished data by Jens Zerrahn, MPIIB Berlin).

Additional functions of IFNγ include stimulation and coordination of many features of the adaptive and innate immune response. IFNγ is the main activator of professional phagocytes, especially of macrophages. In these cells, IFNγ increases receptor mediated phagocytosis and leads to the production of antimicrobial substances and enhances their ability to efficiently kill engulfed microbes. The enhanced antimicrobial activity is due to expression of enzymes like inducible nitric oxide synthase (iNOS) and

enabling the assembly of the enzyme complex phagocyte oxidase (phox), which then produce RNI and ROI respectively, the most potent mediators of phagocytic killing. IFNγ also promotes fusion of phagosomes with lysosomes and expression of the natural resistance-associated macrophage protein (NRAMP) family, which has been shown to inhibit microbial growth in the phagosome (Boehm et al., 1997; Bogdan et al., 2000). Additionally, macrophages and neutrophils release a variety of tissue-modulating chemokines and enzymes. Neutrophils, for example, release a variety of matrix metalloproteinases (MMP) e.g. elastase and collagenase, which modify the surrounding extracellular matrix.

Since the IFNγ-receptor is ubiquitously expressed, IFNγ also has the ability to directly modulate normal tissue cells. IFNγ activates vascular endothelial cells and promotes the expression of ICAM-1 in these cells, an adhesion molecule primarily used by monocytes to infiltrate into tissue. In keratinocytes and endothelial cells, IFNγ induces the expression of interferon-inducible protein 10 (IP10 / CXCL10), which together with the IFNγ-induced I-TAC (macrophage derived chemokines interferon-inducible T cell alpha-chemoattractant / CXCL11) and Mig (monokine induced by gamma-interferon / CXCL9), leads to the infiltration of leukocytes that express the CXCR3 receptor, namely macrophages, neutrophils and activated T cells. (Boztug et al., 2002; Dufour et al., 2002; Narumi et al., 1997). The induced infiltration and the activation of neutrophils and macrophages to produce further activating cytokines, chemokines and effector molecules like MMPs, RNI and ROI, which damage normal tissue, leads to inflammation in the affected tissue.

The ability of the adaptive immune system to respond to foreign antigen is also stimulated by IFNγ. IFNγR signaling induces or increases the expression of MHC class II on cells of the immune system and MHC class I on all nucleated cells, which promotes the activation of $CD4^+$ T cells (MHC class II) and $CD8^+$ T cells (MHC class I). This process is further stimulated by the induction of different subunits of the proteasome and the stronger expression

of transporter associated with antigen processing (TAP), leading to a better processing of antigen (Boehm et al., 1997; Fruh and Yang, 1999; Tanaka, 1994).

Upregulation of MHC class II on DC and macrophages promotes the activation of $CD4^+$ T cells, which will differentiate to Th1 cells in the presence of IFNγ. IFNγ induces Th1 differentiation indirectly via the induction of IL-12, which represents the main stimulator of Th1 cell development. Additionally, IFNγ also impedes the proliferation of Th2 cells (Agnello et al., 2003).
The diverse functions and effects of IFNγ in the immune system make it one of the key cytokines for the control of infections, but also for the development of inflammatory diseases like inflammatory bowel disease and asthma.

1.6 IFNγ and infection

The most dramatic evidence for the fundamental importance of IFNγ in the control of intracellular bacteria comes from human individuals with a hereditary IFNγ-receptor deficiency. These people cannot control infections with intracellular bacteria and if untreated, even vaccination with *Mycobacterium bovis* BCG leads to their death (Jouanguy et al., 1997; Newport et al., 1996). The importance of IFNγ for the generation and the effector function of a cellular immune response, has been analyzed in several infection studies in mice that contain a targeted deletion of the IFNγ or the IFNγ-R gene. Uninfected, these mice have a normal hematopoietic system and are in physical appearance, aging and behavior similar to control mice. Interestingly, the ability to generate a delayed-type hypersensitivity response is only impaired and not abolished in IFNγ-KO mice, indicating that other proinflammatory cytokines like TNF-α and IL-18 also mediate effector functions similar to IFNγ in inflammatory responses (Cooper et al., 1993). However, IFNγ-KO mice are extremely susceptible to low doses of the intracellular pathogen *M. tuberculosis* and even die from infection with the

non-virulent strain *M. bovis* BCG. (Cooper et al., 1993; Dalton et al., 1993; Flynn et al., 1993; Pearl et al., 2001). IFNγ-KO and IFNγR-KO mice are also severely sensitive to infections with other intracellular bacteria, like *Listeria monocytogenes* and *Salmonella enterica* var. Typhimurium, which mainly results from the lack of efficient macrophage mediated killing of these pathogens during the innate immune response (Dalton et al., 1993; Hess et al., 1996; Kaufmann, 1993; van den Broek et al., 1995). The adaptive immune response is also impaired in these mice, but in the case of an *L. monocytogenes* infection, it is sufficient to control a secondary infection if the mice had been vaccinated with an avirulent *L. monocytogenes* strain. In this case, the protective immune response was mediated by CTLs and additional macrophage activating cytokines like IL-18 and TNF-α (Harty and Bevan, 1995). Conversely, treatment with IFNγ protects wild type mice from otherwise lethal doses of *L. monocytogenes* (Kiderlen et al., 1984).

In all of these studies, the systemic immune response was the main focus of investigation. However, *Salmonella* and *Listeria* are food borne pathogens and their primary route of infection is through the intestine, where they cross the epithelial cell barrier and disseminate into deeper organs. It is known that the first line of defense are neutrophils and macrophages (Hughes und Galan, 2002), and that $CD4^+$ IFNγ producing T cells are fundamentally involved in the local adaptive immune response against these pathogens (Hess et al., 1996; Bao et al., 2000). Yet, it is not clear, what role IFNγ plays in this local immune response and how these local responses are involved in protection from or control of infection with these pathogens.

1.7 Inflammatory bowel disease

The immune system of the gastrointestinal tract represents an effective barrier to pathogenic microbes. However, the gastrointestinal tract also contains a high diversity of foreign antigens, derived from enteric bacteria and ingested food, which the intestinal immune system has to tolerate. It is therefore not surprising that the mucosal immune system is controlled by a complex, not fully understood network of cells and cytokines. It is believed that the disturbance of this tight regulatory network can lead to intestinal inflammation. This concept is supported by findings of increased expression of proinflammatory cytokines in the gut-associated mucosa of humans that suffer from chronic inflammation of the gut, i.e. the inflammatory bowl disease (IBD) (Monteleone et al., 2002). There are two forms of IBD, Crohn`s disease (CD) and ulcerative colitis (UC). Both are characterized by infiltration and disruption of the intestinal mucosa by various immune cells, but differ in the site of inflammation. While UC is usually associated with the colon, CD is most commonly associated with the small intestine.

IBDs in humans are complex chronic inflammatory disorders of largely unknown etiology, but recently several mouse models have been developed that allow new insights into the processes that lead to IBD (Strober et al., 2002; Wirtz and Neurath, 2000). These models led to the assumption that IBD is not a classical autoimmune disease, but probably involves antigens derived from food and enteric bacteria, which are ubiquitously present in a normal gastrointestinal environment. In most of the models of CD, dysregulated $CD4^+$ T cells of the Th1 type produce inflammatory cytokines like IFNγ and TNF-α in response to luminal bacterial antigens. Only few models, those representing UC, are associated with increased expression levels of the Th2 cytokines IL-4 and IL-5 (Iqbal et al., 2002; Strober et al., 2002; Takeda et al., 1999). Similarly, there is evidence that human CD is associated with a Th1 and human UC with a Th2 cytokine pattern of inflammation (Fuss et al., 1996; Parronchi et al., 1997; Strober et al., 2002). However, the mechanisms that lead to inflammation and particularly the role of IFNγ are largely unknown.

1.8 Asthma

A human disease, in which the absence of Th1 cytokines and particularly of IFNγ have been implicated, is asthma. Asthma is a chronic inflammatory human disease that has increased dramatically over the past two decades. It is characterized by hyperresponsiveness of the airways towards unspecific bronchoconstrictors and allergens (airway hyperresponsiveness : AHR) (i), variable airflow obstruction (ii) and strong infiltration of the airways that leads to high numbers of eosinophils in bronchoalveolar lavage fluid (BALF) (iii). Although the fundamental mechanisms that underlie the development and perturbation of the asthmatic state remain elusive, it is known that a dysregulated Th2 response is fundamentally involved (Gerblich et al., 1991; Robinson et al., 1992; Walker et al., 1992). To gain further insights into this disease, experimental animal models have been established and proven very useful in the analysis of the mechanisms that lead to asthma. In these models, an asthma like reaction is induced, by the sensitization and subsequent challenge of mice with a foreign protein antigen. These experiments have shown that the Th2 cytokines IL-4, IL-5, IL-13 and the Th2-associated IgE antibodies are critically involved in the development of the asthma like reactions (Leong and Huston, 2001; Wills-Karp, 2000). The different cytokines play distinct roles in the induction of asthma. Especially important for the development of inflammation are IL-5 and IL-4. IL-5 leads to the recruitment and activation of eosinophils and IL-4 promotes the Ig class switch towards IgE in B-cells. The IL-4-related cytokine IL-13 has been specifically implicated in the development of AHR (Brusselle et al., 1995; Finkelman et al., 1988; Foster et al., 1996; Rankin et al., 1996; Walter et al., 2001; Wang et al., 1989; Wills-Karp et al., 1998; Zhu et al., 1999). However, the exact mechanisms by which these cytokines induce the asthma-associated airway changes and AHR remain elusive.

It is also not completely clear, what mechanisms underlie the development of the dysregulated Th2 response. Human asthma is caused by infections or allergen exposure in genetically predisposed individuals. At least twelve polymorphic genes have been implicated in asthma development, including

genes that control IgE, cytokine and chemokine production and tissue remodeling (Cookson, 1999; Fahy et al., 2000). Although, the genetic composition of the population has not changed in the last 20 years, the incidence of asthma has nearly doubled in industrialized countries since 1980. It has been hypothesized that improved hygiene is the major reason for this increase of asthma. According to this theory, infections early in life normally lead to changes in the immune system that protect from allergies and asthma. Many epidemiological studies have supported this theory (Ball et al., 2000; McKeever et al., 2002; Riedler et al., 2001). In an extension of this theory certain infections that elicit a Th1 immune response have been specifically implicated. Such infections are thought to generate a rather Th1 dominated immune system, which e.g. through IFNγ expression prevents the development of an inappropriately strong humoral immune response. Infections with or exposure to *M. tuberculosis* have been explicitly implicated in the prevention of asthma development (von Hertzen et al., 1999). For example, skin test reactivity to *M. tuberculosis* antigens was significantly lower in asthmatic individuals than in healthy controls (Shirakawa et al., 1997). Studies in the mouse model have further supported this theory (Herz et al., 1998; Major et al., 2002) and specifically implicated IFNγ production of mycobacteria-specific Th1 cells in the observed reduction of allergic airway inflammation (Erb et al., 1998). A protective effect of IFNγ was additionally shown in multiple experimental systems, where mice were treated with IFNγ prior or during the induction of the asthma-like reaction (Coyle et al., 1996; Flaishon et al., 2002; Li et al., 1996; Rais et al., 2002; Yoshida et al., 2002). However, the mechanisms by which IFNγ mediates the reduction of asthma in these models are unclear. Furthermore, there are also contradicting results about the effects of IFNγ or IFNγ inducing cytokines on the development of asthma like reactions in mice (Hessel et al., 1997; Kumano et al., 1999; Thomas et al., 2002; Wild et al., 2000). Therefore, the exact role of IFNγ in the development or reduction of an allergic airway inflammation remains elusive.

2 Aims of this thesis

The goal of this work was to analyze the effects of tissue-specific IFNγ expression in the development of inflammation-associated diseases in the respective tissue. We focused on two different models of inflammatory responses, in which controlled IFNγ expression is believed to play a pivotal role. In the first model we analyzed the inflammatory response that develops in the lung of mice after Ovalbumin (OVA) sensitization and subsequent intranasal challenge with OVA and resembles a model of allergic asthma. To exclude the influence of systemic IFNγ and thus allow us the analysis of the effects of only local IFNγ presence in the lung during the development of allergic airway inflammation, we employed a previously generated mutant mouse line with low lung-specific transgenic IFNγ expression and a non-functional endogenous IFNγ gene.

In the second model we aimed to develop an IBD model by generating mice that express IFNγ specifically in the gut, thus allowing the analysis of the effects of IFNγ on the homeostasis of the mucosal immune system and the induction of IBD. We also planned to estimate the effects of local gut-specific IFNγ expression on infection with food borne pathogens.

Specific aims were:

1.1 To test the hypothesis that IFNγ in the lung is a key suppressor of asthma-associated inflammation and the resulting AHR.

1.2 To investigate the effector mechanism of this hypothesized effect.

2.1 To generate a transgenic mouse line with gut-specific IFNγ expression.

2.2 To estimate the effects of gut-specific IFNγ expression on the homeostasis of the intestinal immune system and the possible induction of IBD by this IFNγ expression.

2.3 To analyze the effects of gut-specific IFNγ expression on inflammatory responses of the intestinal immune system during infection.

3 Material

Addresses and contact information for suppliers are attached in section 10.2. Standard laboratory chemicals used to prepare buffers were purchased from *Sigma, Merck* or *Roth* in per analysis quality.

3.1 Enzymes

T4 DNA ligase reverse transcriptase superscript II DNAse I RNAse H	*Gibco*
Restriction endonucleases Calf intestine alkaline phosphatase (CIAP)	*New England Biolabs (NEB)*
Pfu DNA polymerase DNA polymerase I, large fragment (Klenow)	*Stratagene*
Taq DNA polymerase	*Gene Craft*
Proteinase K Collagenase II, III, VII Hyaluranidase	*Sigma*
2x SYBR-Green PCR master mix	*Applied Biosystems*

3.2 Equipment

PCR thermocycler ABI DNA-Sequencer A377 ABI Prism 7000	*Applied Biosystems*
FACS-Calibur	*Becton Dickinson*
Protein electrophoresis chambers Electrophoresis Power Supply	*Bio-Rad*
Microinjection pressure unit Thermoblock Microcentrifuge	*Eppendorf*
Phospho-Imager: FLA-2000	*FujiFilm*
Biofuge 15	*Heraeus Instruments*
Ultra Turrax T8 tissue homogenizer	*IKA Labortechnik*
ELISA-Reader SpectraMax 250	*Molecular Devices*
Table micrometer HM315	*Microm*
Microinjection moving table and microscope	*Olympus*

CO_2-incubator Nuaire Autoflow	*Zapf, Saarstedt,*
Microscopes	*Zeiss*
Cytospin	*Shandon*
AHR measurement equipment	*HSE Harvard Apparatus*
Metabolism cages	
Cryostat	*Leica*
UV crosslinker	*Stratagene*
2100 bioanalyzer system DNA microarray laser scanner	*Agilent*

3.3 Other material

Dialysis filter, Type VS, 0.0025 µm	*Millipore Corporation*
Hybond-N (+)-membrane ECL hyperfilm γ32P [ATP] (5000 Ci/mmol)	*Amersham*
Sterile filters and membranes	*Schleicher & Schüll*
Flasks, plates and sterile vials	*Nunc*
Trizol Reagent	*Gibco*
Alum (Al(OH)3)	Serva
OVA Grade VII	*Sigma*
Nitrocellulose membrane	*Bio-Rad*
Dif-Quik	*Roche*
Ketamin	*Curamed*
Xylazin	*Bayer*
Quikhybe Solution	*Stratagene*
G 50 Probe Quant microcolumns	*Amersham Pharmacia*

3.4 Kits

Plasmid Minipreparation Kit Plasmid Maxipreparation Kit QiaQuick Gel Extraction Kit RNeasy mRNA extraction Kit SuperFect	*Qiagen*

Lipifectamin TOPO-TA-cloning	*Invitrogen*
PCR-Script-Amp "prime-it II" labeling-kit	*Stratagene*
Universal Genome Walker Kit	*Clontech*

3.5 Plasmids

Plasmid name	Description
pBluescript KS+	Standard cloning vector *Stratagene*
PCR2.1	TA-cloning and sequencing vector *Invitrogen*
pCR-Script-Amp	Cloning and sequencing vector for PCR-fragments amplified with PFU-polymerase *Stratagene*
pcDNA3.1/Zeo	Expression vector with human CMV promoter and a second expression cassette containing the Zeocin resistance gene under the control of a SV40 promoter. *Invitrogen*
pcDNA3.1/Zeo-ΔCMV	Similar to pcDNA3.1/Zeo with the CMV promoter deleted by BamHI and BglII digestion and ligation.
pEP-lfabp	Contains bp –596-+21 of the liver fatty acid binding protein promoter A kind gift from J.I. Gordon and colleagues
p9kb_aatII	Contains the villin promoter. A kind gift from D. Pinto and colleagues

3.6 Primers

The table below, shows the sequences of the synthetic oligonucleotides used for cloning (C), screening of genomic DNA (S) or semi-quantitative RT-PCR (R). All primers were obtained from *Metabion* and diluted to 100 µM stock solutions. The working solutions were prepared from stock solutions according to the requirements. Standard primer sequences were chosen using the web-based software Primer3.

Primer-name	5'-3' sequence	Application
Lfabp-BamHI-fw	CCGCGGTGGATCCCGCTCTAGAACTAGTGGAT CGATC	C
Lfabp-NotI-rev	GGG GAG TTG GGC CTT GCG GCC GCC CCT GAC CAC AAC AGC	C
IFNγ-XhoI-fw	CTG CGG CCT AGC TCG AGA CAA TGA ACG CTA CAC ACT GC	C
IFNγ-ApaI-rev	GGG ACA ATC TCT TCC CGG GCC CGA ATC AGC AGC GAC TCC	C
IFNγ-AatII-fw	GCT CTG AGA CAA TGA CGT CAA ACG CTA CAC ACT GC	C
IFNγ-NotI-rev	GGG ACA ATC TCT TCC CGC GGC CGC ATC AGC AGC GAC TCC	C
TP-IFNγ-ex2-fw	CTC AAG TGG CAT AGA TGT GGA AG	S
TP-IFNγ-ex3-rev	CTT GGC AAT ACT CAT GAA TGC ATC C	S
TP-IFNγ-neo-fw	CGC CTT CTT GAC Gag TTC TTC TG	S
Neo-323-fw	CTC CTG CCG AGA AAG TAT CCA	S
Neo-628-rev	CAC AGT CGA TGA ATC CAG AAA AG	S
β-actin-fw	TGG AAT CCT GTG GCA TCC ATG AAA C	R
β-actin-rev	TAA AAC GCA GCT CAG TAA CAG TCC G	R
GAPDH-fw	GCA ACT CCC ACT CTT CCA CCT TC	R
GAPDH-rev	CCT CTC TTG CTC AGT GTC CTT GCT	R
IFNγ-68-fw	ACG GCA CAG TCA TTG AAA GCC TA	R
IFNγ-168-rev	CTC ACC ATC CTT TTG CCA GTT CC	R
lfabp-IFNγ-(-18)-fw	GGG CGG CCG CTC GAG ACA	R
lfabp-IFNγ-(+179)-rev	TCC TTT TGC CAG TTC CTC CAG ATC TCC AA	R
IL-4-44-fw	TCG AAT GTA CCA GGA GCC ATA TCC	R
IL-4-192-rev	CTC TGT GGT GTT CTT CGT TGC TGT	R
IL-5-224-fw	ATC AAA CTG TCC GTG GGG GTA CT	R
IL-5-324-rev	TCT CTC CTC GCC ACA CTT CTC TTT	R
IL-10-183-fw	GGA CAA CAT ACT GCT AAC CGA CTC CT	R
IL-10-423-rev	CTG CTC CAC TGC CTT GCT CTT ATT	R
IL-13-129-fw	CAC ACA AGA CCA GAC TCC CCT GT	R
IL-13-284-rev	GGT TAC AGA GGC CAT GCA ATA TCC	R
Eotaxin1-28-fw	CTG CTG CTC ACG GTC ACT TCC T	R
Eotaxin1-178-rev	CAG GGT GCA TCT GTT GTT GGT G	R
iNOS-2536-fw	GAC GAG ACG GAT AGG CAG AGA TTG	R
iNOS-2725-rev	CCT GGG AGG AGC TGA TGG AGT AG	R
IP-10-17-fw	CCG TCA TTT TCT GCC TCA TCC T	R
IP-10-142-rev	GCT TCC CTA TGG CCC TCA TTC T	R
IIGP-672-fw	GCC ACC AAT CTT CCT GCT CTC TAA C	R

Primer-name	5'-3' sequence	Application
IIGP-856-rev	CTT CCA GCC AAA TCC TCT GCT TC	R
AMACO-79-fw (A-0)	CGG CTT TGT TCG CTT TGT CC	R
AMACO-269-rev (A-1)	CTC CCG GTT CAC ATG CAC TTC	R
AMACO-318-fw (B-3)	GCG GTC GAC ATC CTG TTT CTG	R
AMACO-469-rev (B-4)	GGA GTG GAA CCA AAC TGC AAG G	R
AMACO-944-fw (C-7)	GTG CTG GAG AGG ATC AAG GCA AG	R
AMACO-1045-fw (C-8)	CTG TAG CAG TTG GCA GGG TGT G	R
AMACO-1634-fw (D-10)	GAA GAT CAC CGG TAG CCC GAA G	R
AMACO-1805-rev (D-11)	CTC ACG TCC CAC AGA GGC AGA	R

3.7 Cells and cell culture media

Dulbecco´s Modified Eagle´s Medium (DMEM), RPMI 1640 medium, fetal bovine serum, penicillin/streptomycin solution, L-glutamine, HEPES, sodium pyruvate and non-essential amino acid solution were obtained from *Biochrom*. M2 and M16 media were purchased from *Sigma.* Zeocin was purchased from *Invitrogen*. The cell line used for *in vitro* transfection studies was the human colon carcinoma cell line CaCo2 (obtained from *ATCC*).

phosphate buffered saline (PBS):

8g	NaCl
0.2g	KCl
0.2g	KH_2PO_4
1.3g	Na_2HPO_4
ad 1000 ml	

Standard DMEM and RPMI medium:

10%	FCS
0.2mM	L-glutamine
10U/ml	penicillin and streptomycin

CaCo2 DMEM

DMEM plus	
1x	non essential amino acids
15%	FCS
10U/ml	penicillin and streptomycin
1mM	Sodium Pyruvate
0.2mM	L-glutamine

Collagenase digestion media

Standard RPMI plus	
1x	non essential amino acids
10mM	Hepes
1mM	Sodium Pyruvate
150 U/ml	collagenase II
850 U/ml	Hyaluranidase

Erylysis buffer	1 Part:	2.06g Tris pH 7.65 in 100 ml H_20;
	9 parts	2.075 g NH_4Cl in 250ml H_20

3.8 Antibodies

An overview of the monoclonal antibodies (mAb) used is given in the table below**.** Monoclonal antibodies (mAb) marked with an asterisks (*) were purified from hybridoma supernatants by protein-G sepharose. The mAb used for flow cytometry were conjugated with the fluorescent dyes FITC, PE or Cy-5. The mAb marked with a number sign (#) were used as isotype controls. Western blot is abbreviated WB and *in vitro* restimulation is abbreviated IVR.

Specificity	Clone	Application	Source
CD3	145-2C11	FACS, IVR	Pharmingen
CD4	YTS191.1	FACS	ATCC*
CD8α	YTS169	FACS	ATCC*
CD25	PC61	FACS	ATCC*
CD28		IVR	ATCC*
CD62L	MEL-14	FACS	Pharmingen
CD69	H1.2F3	FACS	Pharmingen
IL-4		FACS	Pharmingen
IL-5		FACS	Pharmingen
IL-10		FACS	Pharmingen
IFNγ	XMG1.2	ELISA, WB	ATCC*
IFNγ	R4-6A2	ELISA, WB	ATCC*
IgE		ELISA	Pharmingen
αOVA-IgE		ELISA	Pharmingen

3.9 Buffers and solutions

Solutions were made up in H_2O prepared with a *Millipore* water purifier, unless stated otherwise. Where indicated, solutions were sterilized by autoclaving for 25 min at 121°C, or filter-sterilized through a 0.2 µm membrane.

3.9.1 Buffers used in molecular biology

TE :	10 mM Tris-HCl (pH 7.6); 1 mM EDTA (pH 8.0)	TAE running buffer :	36 mM Tris-HCl 30 mM Na_2HPO_4/NaH_2PO_4
TBE :	90 mM Tris 90 mM Boric acid 20 mM EDTA	10x MOPS :	87.6 g MOPS in 800 ml 125 mM NaAc pH to 7.0 20 ml 0.5 M EDTA, pH 8.0
DNA loading buffer:	50% (v/v) glycerol 1 mM EDTA 0.4% (w/v) bromophenol blue 0.4% (w/v) xylene cyanol	RNA loading buffer :	50% (v/v) glycerol 1mM EDTA 0.25% w/v bromophenol blue 0.25% w/v xylene cyanol
Injection buffer :	10mM Tris 0.1mM EDTA adjusted to pH7.5	SSC (20x) :	3 M NaCl 0.3 M Na-Citrate
Tail-lysis buffer :	100 mM Tris, pH 8.5 5 mM EDTA 200 mM NaCl 0.2% SDS 100 mg/ml Proteinase K		

Solutions used for small scale DNA preparation (Miniprep):

Solution 1:	50 mM Glucose 10 mM EDTA 25 mM Tris-HCl, pH 8.0
Solution 2:	0.2 mM NaOH 1% SDS
Solution 3:	3 M K-Acetate pH 4.8

Solutions for the preparation of competent *E. coli* cells

Solution 1 :	50 mM $MnCl_2$ 50 mM $CaCl_2$ 10 mM MES pH 6.3
Solution 2:	50 mM $MnCl_2$ 50 mM $CaCl_2$ 10 mM MES, pH 6.3 15% glycerol

3.9.2 Buffer used for SDS gel electrophoresis, immunoblotting and ELISA

Cell lysis buffer	0.5% Triton X-100 300mM NaCl 50mM TrisCl, pH 7.6 0.5 mM PEFA-block 1mM leupeptin 1mM pepstatin A	Sample buffer (3 x)	187.5 mM Tris-HCl, pH 6.8 6% SDS 0.9 mM EDTA 30% glycerol 0.03% bromophenol blue 7.5% b-mercaptoethanol
Separating gel buffer (4x)	90.75g Tris Base 20ml 10% SDS volume to 460mls pH to 8.8 with HCl Q.S. to 500ml	Stacking gel buffer (4x)	12.12g Tris Base 8ml 10% SDS bring volume to 180mls pH to 6.8 with HCl Q.S. to 200ml
Running buffer	25 mM Tris-HCl 0.1% SDS 192 mM glycine, pH to 8.3	Transfer buffer	20% methanol 39 mM glycine 48 mM Tris 0.0375% SDS
Fixing Solution	20% methanol 10% acetic acid	Destain Solution	10% methanol 7.5% acetic acid
Coomassie Blue Stain	0.25% Coomassie Blue 50% methanol 7.5% acetic acid	Blocking Buffer	5% milk powder 0.5% Tween 20 0.1% sodium azide in 1x PBS
Antibody Solution	1 % BSA 0.1% Tween 20 0.1% sodium azide in 1x PBS	Diethanolamine buffer	48.5 ml diethanolamine 400 mg MgCl2 100 mg NaN3 Q.S. to 500ml
ELISA coating buffer	100 mM Na carbonate / hydrogencarbonate titrated to pH to 9.6	ELISA wash buffer	0.1% BSA 0.05 % Tween 20 in PBS

3.9.3 Buffer used for the perfused lung in AHR measurement

Sterile Krebs-Henseleit-hydroxyethylamylopectin buffer was obtained from Serag-Wiessner (*Naila*). The buffer contained 120 mM NaCl, 4.3 mM KCl, 1.1 mM KH_2PO_4, 24 mM $NaHCO_3$, 2.4 mM $CaCl_2$, 1.3 mM $MgCl_2$ and 2.4 g/l of glucose as well as 5 % (wt/vol) hydroxyethylamylopectin (mol wt 200,000) as an oncotic agent.

3.9.4 Bacterial culture medium

Luria Bertani (LB) medium: 1% (w/v) Bacto-Tryptone, 0.5% (w/v) yeast extract and 85.5 mM NaCl were dissolved in autoclaved water, the pH was adjusted to 7.5 with NaOH and the medium was autoclaved. Were indicated the appropriate antibiotics were added. Ampicillin was used at 50-100 mg/l. kanamycin was used at 25-50 mg/l. Both stock solutions were made in 50 % water and 50% ethanol and stored at –20°C. For plates 1.5 % (w/v) agar was added prior to autoclaving.

3.10 Software

Tables, calculations, statistic	GraphPad Prism 3.0 (*GraphPad Software*)
	Excel (*Microsoft*)
Graphics	PowerPoint (*Microsoft*)
	Photoshop (*Adobe Systems*)
Flow cytometric analysis	Cell Quest 3.0 (*BD*)
	FCS Express 1.0 (*De Novo Software*).
DNA sequence analysis	Clone manager 5.0 (*Scientific Software*)
	Chromas (Copyright Conner McArthy)
Densitometry	Image Gauge 1.0 (*FujiFilm*)
Text	Word (*Microsoft*)
Microarray analysis	Resolver (*Rosetta Inpharmatics*)

3.11 Web resources

DNA sequence identification:

http://www.ncbi.nlm.nih.gov/BLAST/

http://www.celera.com/

DNA sequence comparison:

http://www.ncbi.nlm.nih.gov/gorf/bl2.htlm

http://www.ebi.ac.uk/clustalw/

Oligonucleotide-primer design:

http://www-genome.wi.mit.edu/cgi-bin/primer/primer3_www.cgi

4 Methods

4.1 Molecular biological methods

The general molecular biological methods like *E. coli* cultivation, agarose gel preparation, DNA electrophoresis, DNA precipitation, measurement of DNA / RNA concentration and DNA digestion were performed according to *Molecular Cloning: A Laboratory Manual* (Sambrook and Russell, 2001). DNA sequencing was performed at the sequencing core facility of the MPIIB. Sequences were verified using the program Chromas and compared using the web-based program Blast 2 Sequences (http://www.ncbi.nlm.nih.gov/gorf/bl2.html)

4.1.1 Preparation of competent *E. coli* cells for the $CaCl_2$ method

A single bacterial colony was grown to an overnight culture in 5 ml LB medium at 37°C. Two ml of this culture were used to inoculate 200 ml LB containing 15 mM $MgCl_2$. This culture was grown to an OD600 = 0.6 equaling a bacterial concentration of ca. 6 x 10^8 cells/ml. The culture was cooled on ice for 10 min and centrifuged at 4°C for 5 min at 5000 rpm. The pelleted cells were carefully resuspended in 60 ml cold solution 1 and centrifuged at 6000 rpm for 10min at 4°C. Finally, the cells were resuspended in 12 ml cold solution 2. Aliquots (0.2 ml) were shock-frozen in liquid nitrogen and kept at –80°C until use.

4.1.2 Transformation of plasmid DNA into competent *E. coli* cells

Competent cells were slowly thawed on ice. Plasmid DNA (ca. 0.1 pmol) was mixed with 200 µl (2x10^8) bacteria and incubated on ice for 30 min. Subsequently, the cells were heat-shocked at 42°C for 45 sec. Then, cells were cooled on ice for 2 min and 1 ml LB medium (37°C) was added. After incubation at 37°C for 30-60 min at 200 rpm, an aliquot was plated on selective (antibiotic-containing) LB-agar.

4.1.3 Covalent connecting DNA fragments using T4 DNA ligase

DNA-ligase catalyses the formation of phosphodiester bonds between terminal 3`-hydroxy- and 5´-phosphoryl-groups of double stranded DNA.
DNA preparations were ligated in a volume of 20 µl using a 3x molar excess of insert and 1 unit T4 DNA ligase (S*tratagene*) in the corresponding ligase buffer. The reactions were carried out for 4 hours at room temperature (RT) or overnight at 16°C. 10 µl of the ligation solution were subjected to transformation into competent *E. coli*.

4.1.4 Isolation and purification of plasmid DNA

The principle of most protocols used for the purification of plasmid DNA is based on the fact that genomic DNA renatures intermolecularly and forms high-molecular, netlike structures while plasmid DNA renatures intramolecularly. Therefore, subsequent centrifugation allows the pelleting of genomic DNA, denatured proteins and cellular debris while plasmid DNA remains in solution (Birnboim and Doly, 1979).
For large scale preparations (maxiprep) and to archive clean DNA, anionic ion exchange columns were purchased from *Qiagen* together with necessary buffers. The principle of these columns is based on the fact that due to its charge, DNA can be purified with anion exchange chromatography. The protocol for a maxiprep was performed according to the manufacturer`s instructions.
Small scale preparations (miniprep) for exclusively analytical purposes were carried out starting with pelleting the cells from 1.5 ml culture. After resuspending the pellet in 250 µl of solution 1, 250 µl of solution 2 were added to lyse the cells and denature the DNA, RNA and proteins. Five min later 350 µl of solution 3 were added and the mixture was centrifuged 10 min at 20,000 rpm and 4°C. Plasmid DNA within the supernatant was then precipitated with 900 µl ethanol. Finally the pellet was air-dried and resuspended in 50 µl water or TE.

4.1.5 Isolation and purification of genomic DNA

Tail biopsies (0.5 cm) were incubated in 500 µl of tail-lysis buffer overnight at 56°C and 900 rpm. Following centrifugation for 10 min at 12,000xg the supernatant was transferred into a new tube and the DNA was precipitated by adding 500 µl of isopropanol. The DNA was pelleted by a 20 min centrifugation at 300xg and the pellet washed twice with 70% ethanol, air-dried, dissolved in water and quantified.

To achieve cleaner DNA more suitable for Southern blotting, a chlorophorm/phenol extraction was performed. Tail biopsies were lysed and centrifuged as described above, but the supernatant was thoroughly mixed with an equal volume of phenol (pH 7). This mixture was centrifuged in order to obtain two separated phases with the lower phenol phase and the interphase containing denatured proteins. To remove the remaining phenol from the upper aqueous phase a second extraction using an equivalent volume of chloroform/isoamylalcohol (24:1) was performed. The genomic DNA was precipitated with cold ethanol and resuspended in an appropriate volume of water or TE.

4.1.6 Locating the transgene integration site

To find the genomic sequence adjacent to the integrated transgene, genome walking was performed using the Universal Genome Walking Kit (*Clontech*). The method is based on annealing of known linkers to digested genomic DNA fragments and subsequent PCR amplification of the area between the linker and the transgene, previously described by Siebert and colleagues (Siebert et al., 1995). Briefly, multiple samples of highly purified genomic DNA were digested in 100 µl volume at 37°C overnight using multiple restriction enzymes known to cut frequently in murine genomic DNA (ApaI, BglII, PvuII, DraI, EcoRV and StuI). DNA from each digest was than purified using phenol/chloroform extraction and subsequent DNA precipitation with ice cold 95% ethanol, 3M NaOAc and 20 µg glycogen. After an additional 75 % ethanol wash, the linker (supplied with the kit) was annealed by overnight ligation with T4 DNA ligase, to achieve the fragment library. Then, two subsequent PCRs were performed with each library, using a primary linker-

specific primer and a primary transgene-specific primer in the first PCR and a nested linkerspecific and nested transgene-specific primer in the second PCR. The first PCR consisted of seven cycles with denaturing for 25 sec at 94°C and annealing plus extension for 3 min at 72°C followed by 32 cycles with annealing and extension at 67°C. The nested PCR was done with five cycles annealing and extension at 72° followed by 20 cycles with annealing plus extension at 67°C. All PCRs were carried out using hot start Advantage Genomic Polymerase (*Clontech*). Aliquots of the PCR mixture were then run on a 1% agarose gel, bands were excised, purified with *Qiagen* Gel extraction Kit and cloned into the sequencing vector pCR2.1 using the TOPO-Cloning Kit (*Invitrogen*). Sequences obtained were analyzed by BLAST searches in the NCBI or Celera mouse genome database.

4.1.7 Southern blot

Genomic DNA was digested overnight at 37°C with restriction enzymes and 0.1 µg/µl RNAse. The digested DNA probe was loaded on a 0.8 % agarose gel and separated at 100 V for 4 hours. The gel was then prepared for Southern blotting by denaturing the DNA using 0.5 M NaOH for 45 min and equilibrating the whole gel in 1 M Tris, 1.5 M NaCl pH 8.0 for 45 min. The DNA was transferred overnight onto a nylon membrane using the capillary force of paper towels and SSC buffer as transfer buffer. The transfered DNA was permanently crosslinked onto the nylon membrane by UV light in a *Stratagene* UV crosslinker or by 2 hours incubation at 80°C.

The blot was pre-hybridized for 10 min with 6 ml Quikhybe Solution (*Stratagene*) at 68°C in a hybridization oven. In parallel, the probe was prepared using the *Stratagene* "prime-it II" kit according to the manufacturer's instructions. Briefly, 25 ng of a 300-800 bp DNA fragment in 26 µl H_2O were boiled for 5 min together with 10 µl of random nonamer. Ten µl of dCTP buffer containing a dNTP mixture (0.1 M each) without dCTP, 1 µl of Klenow polymerase (5 U/µl) and 2.5µl (50 µCi) of α-dCT^{32}P were added and incubated for 10-15 min at 37°C. The reaction was stopped by the addition of 0.5 M EDTA, pH 8.0 and the unincorporated nucleotides were separated from the probe using a spin column (G 50 Probe Quant microcolumns).

Twohundred µl of denatured herring sperm DNA (10mg/ml) were added to the remaining probe and the mixture was boiled for 5 min before it was added to the prehybridized blots. The hybridization was carried out at 68°C for 4 hours or over night and subsequently washed twice for 15 min at RT with 2x SSC and 0.1% SDS and for a high stringency wash an additional 30 min wash at 60°C with 0.1x SSC and 0.1% SDS was performed. The blot was wrapped in plastic foil and left overnight on a phosphoimager plate or film.

4.1.8 Isolation and purification of RNA from tissue

RNA was isolated by the Trizol Reagent RNA preparation method (*Gibco*). Briefly, 100 mg tissue were homogenized in 1 ml of Trizol Reagent with a Ultra Turrax T8 tissue homogenizer (*IKA Labortechnik*). The mixture was left for 5 min at 20°C, before 0.2 ml chloroform were added and mixed for 15 sec. Following 3 min incubation at 20°C, the suspension was centrifuged at 4°C for 15 min at 10,000xg. Subsequently, 0.5 ml isopropanol were added and after a 10 min incubation at 20°C, RNA was precipitated by centrifugation for 10 min at 10,000xg at 4°C. The RNA pellet was washed in 75% ethanol, air-dried and dissolved in RNAse free water. The purified RNA was stored at -80°C.

4.1.9 Northern blot

For Northern Blotting, a 1% agarose gel containing formaldehyde was prepared. For this, 1.2 g agarose were boiled in 87.4ml water and left to cool to 60°C. Then 21.6 ml of formaldehyde (37%) and 12 ml 10x MOPS buffer were added and the gel was poured. The RNA (10-20 µg) was prepared by the addition of 11 µl H_2O, 9 µl formaldehyde, 25 µl formamide and 5 µl 10x MOPS followed by a 15 min 65°C incubation. Before loading the sample onto the gel, 10 µl RNA loading buffer were added. After the gel was run for 3 hours at 80 V, using 1x MOPS as running buffer, the gel was denatured using 0.5 M NH_4Ac twice for 20 min. The denatured gel was then briefly immersed in 12x SSC and the RNA was blotted onto nylon membrane using 12x SSC as transfer buffer. Blotting, hybridization and washing were performed exactly as described for Southern blotting.

4.1.10 Generation of cDNA

Initially purified RNA samples were treated with DNAse (*Gibco*) to eliminate genomic DNA contamination. For this, 8 µg of RNA in 16 µl H_2O and 1 µl of 10x reaction buffer were incubated with 2 µl of DNAse I for 15 min at RT. The reaction was stopped by the addition of 2 µl 25 mM EDTA and the DNAse was inactivated by incubating the mixture at 65°C for 15 min. While 12 µl of this mixture were stored and later analyzed for the completion of the DNAse digestion, 10 µl of it were used for reverse transcription. For that 1 µl random hexamer primers (200 µg/ml) was added, the mixture was incubated for 10 min at 65°C and then placed on ice. After 5 min on ice, a reaction mix containing 4 µl 5x first strand buffer, 1 µl 10 mM dNTPs and 2 µl 0.1 M DTT were added and following a 10 min incubation at RT 1 µl of superscript reverse transcriptase was added. This mixture was immediately incubated for 50 min at 42°C and finally incubated for 15 min at 70°C in order to inactivate the reverse transcriptase and to stop the reaction.

4.1.11 PCR and RT-PCR

The selective amplification of DNA sequences was performed as described previously (Mullis et al., 1986). For analytical PCRs BioTherm Taq polymerase (*Gene Craft*) was used and for cloning PCRs Pfu polymerase (*Stratagene*) was used.

The standard protocol was as follows:

PFU or Taq Buffer (with $MgCl_2$)	5 µl	
DNA template	1 µl	(20-200 ng)
Forward and reverse Primer	0.2 µl	(20 pmol)
dNTPs	0.5 µl	(10mM each)
PFU or Taq Polymerase	0.5 µl	(2U)
Water	Ad 50 µl	

Standard cycle conditions were:

30 cycles of		
denaturation	95°C	40 sec
annealing	55-60°C	40 sec
extension	72°C	1.0 min/kb for Taq polymerase 2 min/kb for Pfu polymerase.

For RT-PCR cDNA was used as template for semiquantitative amplification. The number of cycles necessary to produce enough PCR-product for detection but small enough to not exceed the logarithmic phase of the PCR was determined by serial dilutions of cDNA or multiple PCRs with different numbers of cycles. To compare the amount of cDNA used in each reaction, β-actin primers were included. Possible contamination with genomic DNA was estimated using 1:5 diluted DNAse digested not reverse transcribed RNA as template.

4.1.12 Real-time RT-PCR

Quantification of DNA using real-time PCR is based on the measurement of amplified products after each cycle of the PCR using fluorescent dyes interacting only with double stranded DNA. The more template is present at the beginning of the reaction, the lower the number of cycles it takes to reach a point in which the fluorescent signal is first recorded as statistically significant above background, which is the definition of the threshold cycle (Ct). Comparison of the threshold cycle for a specific template in each sample leads to semi-quantitative evaluation of original template concentration. For semi-quantitative real-time PCR total RNA was extracted from organs as described in section 4.1.8 and transcribed to cDNA as described in section 4.1.10. All PCRs were run for 40 cylces with 20 sec 94°C and 60 sec 60°C in the ABI Prism 7000 Sequence Detection System (*Applied Biosystems*) using ABI PRISM optical 96-well plates (*Applied Biosystems*). When possible primers were designed to span large introns and to produce product sizes between 100 and 200 bp. Reaction mixtures were set up in 30 µl final volume using 15 pmol of each primer, 5 µl template cDNA and 15 µl 2x SYBR-Green PCR Master mix (*Applied Biosystems*). For the quantification of GAPDH and β-actin, 5 µl of 1:150 diluted cDNA were used as template in each reaction and for the quantification of cytokines, eotaxin and AMACO, 5 µl of 1:15 diluted cDNA were used. Each quantification was performed at least twice with independent cDNA samples and in duplicates for each cDNA and primer pair. Data analysis was performed using the ABI Prism 7000 SDS Software and *Microsoft* Excel. The threshold cycle was

determined for each sample and fold differences relative to the expression level in one of the analyzed cDNA samples was calculated for each cDNA sample and primer pair (fold-difference=$2^{-\Delta Ct}$). Resulting fold differences for cytokines, eotaxin and AMACO expression levels were corrected for different amounts of cDNA by multiplication with the average fold difference of GAPDH and β-actin expression within the same sample. When IFNγ expression levels were measured, 5 µl of 1:10 diluted DNAse digested not reverse transcribed RNA was used as template in separate reactions, to control for genomic contamination.

4.1.13 RNA microarray

Microarray experiments were done as two-color hybridizations. Total RNA was extracted from whole lungs of at least five mice in each sensitized and challenged group 24 hours after the last i.n. challenge and from at least five only sensitized animals from each group as described in section 4.1.8. Total RNA was purified in a second step using the RNeasy Kit (*Qiagen*), and was then quantified and integrity was determined with the 2100 bioanalyzer system (*Agilent Technologies*). An amount of 4 µg total RNA was reverse transcribed with an oligo-dT-T7-promotor primer by a fluorescent linear amplification reaction (*Agilent Technologies*) and cRNA was labeled either with Cyanine 3-CTP and Cyanine 5-CTP (*NEB Life Science Products*) in a T7 polymerase amplification reaction according to the supplier's protocol. In order to compensate specific effects of the dyes, e.g. incorporation and to ensure statistically relevant data analysis, a color swap was performed. The RNA samples were labeled vice verse with the two fluorescent dyes (fluorescence reversal). After precipitation, purification and quantification, 1.25 µg of each labeled cRNA was mixed, fragmented and hybridized to the 8.4 K custom *'in situ'* mouse array according to the supplier`s protocol (*Agilent Technologies*). Scanning of microarrays was performed with 5 µm resolution using a DNA microarray laser scanner (*Agilent Technologies*). Features were extracted with an image analysis tool Version A4.045 from *Agilent Technologies* using default settings. Data analysis was carried out on the Rosetta Inpharmatics platform Resolver Built 3.0.0.3.22.

4.2 Generation of transgenic mice

4.2.1 Cloning strategies

Three transgene constructs were created, each with a different gut-specific promoter and all containing the IFNγ cDNA (villin-IFNγ-BGHpA, ITF-IFNγ-BGHpA, lfabp-IFNγ-BGHpA).

The IFNγ cDNA was isolated by RT-PCR from C57BL/6 spleen cDNA and cloned into the sequencing vector pCR-Scrip-Amp. After verification of the inserted IFNγ sequence, this plasmid was used as template for further PCR with primers containing restriction sites for further cloning. To exclude any influence of non-coding IFNγ mRNA on expression, all restriction sites added during further PCR amplifications were immediately upstream of the start codon or downstream of the stop codon.

villin-IFNγ-BGHpA: The villin-IFNγ-BGHpA cassette was constructed by amplifying the IFNγ cDNA with primers containing an AatII restriction site upstream and a NotI restriction site downstream of the coding sequence. The resulting PCR product was then digested appropriately and cloned into the equally treated vector p9kb-aatII, which contained the 9kb villin promoter upstream of an AatII site. This vector was kindly provided by Pinto and colleagues (Pinto et al., 1999). After verification of the amplified IFNγ cDNA sequence, the villin promoter together with the IFNγ cDNA was cloned into the vector pcDNA3.1-Zeo-ΔCMV using the KpnI and NotI restriction sites. The vector pcDNA3.1-Zeo-ΔCMV is based on the plasmid pcDNA3.1-Zeo, but lacks the CMV promoter. It contains a bovine growth hormone polyadenylation (BGHpA) signal sequence downstream of a multicloning site and also contains a Zeocin resistance cassette.

ITF-IFNγ-BGHpA: The pcDNA3.1-Zeo-ΔCMV backbone was also used to construct the ITF-IFNγ-BGHpA cassette. For this, the IFNγ cDNA was amplified using primers containing XhoI and ApaI restriction sites. The PCR product was inserted into the pcDNA3.1-Zeo-ΔCMV vector by restriction digest with XhoI and ApaI and subsequent ligation with equally treated vector. The ITF promoter was inserted using the EcoRI and XhoI restriction

sites adjacent to the ITF promoter sequence and still present in the vector, 5´ of the IFNγ sequence. The final construct pcDNA3.1-Zeo-ΔCMV-ITF-IFNγ was then verified by sequencing.

lfabp-IFNγ-BGHpA: The lfabp-IFNγ-BGHpA cassette was constructed by introducing PCR amplified IFNγ cDNA, containing XhoI and ApaI restriction sites, into the complete pcDNA3.1-Zeo vector, yielding a vector with IFNγ-cDNA under the control of the CMV promoter. This intermediate vector was used as positive control for transfection studies (pcDNA3.1-Zeo-CMV-IFNγ-BGHpA). To introduce the lfabp promoter and delete the CMV promoter the lfabp promoter sequence was PCR amplified from the plasmid pEP-lfabp using primers that introduced a BamHI restriction site upstream and a NotI restriction site downstream of the promoter sequence. The plasmid pEP-lfabp was kindly provided by J.I. Gordon (Simon et al., 1997). The resulting PCR product was cloned into the IFNγ containing pcDNA3.1-Zeo vector using the appropriate restriction enzymes and leading to the replacement of the CMV promoter with the lfabp promoter. Before further use, the complete sequence of the transgene cassette was verified.

4.2.2 Stable transfection of CaCo2 cells

Prior to transfection, the constructs (5 µg of DNA) were linearised by restriction enzyme digestion and purified over agarose gels. Transfection was performed with *Qiagen* SuperFect according to the manufacturer`s instructions. Briefly, the CaCo2 cells were cultured until they reached 40-80% confluency. Five µg of total DNA were mixed with CaCo2 tissue culture medium without fetal calf serum (FCS) or antibiotics in total volume of 150 µl. To this, 20 µl of SuperFect transfection reagent was added and mixed. The mixture was incubated for 5-10 min at room temperature while the cells were washed once with PBS. One ml of complete CaCo2 medium was then added to the transfection mix, which was transferred onto the cells and incubated for 4-6 hours at 37°C and 8% CO_2. DNA lipid complexes were removed by two consecutive washes with PBS and fresh medium was added. The cells were left for 24-48 hours before they were trypsinized and passaged at a ratio of 1:15 in medium containing 300 µg/ml Zeocin (*Invitrogen*) until colonies

appeared. Single colonies were transferred to 96 well plates and expanded. After multiple rounds of expansion, $1x10^6$ cells originating from 1 single clone were plated on 10 cm dishes and supernatants from this culture were analyzed by ELISA as described below.

4.2.3 DNA preparation for transgene injection

Each plasmid designated for injection was cut with suitable restriction enzymes, separating the plasmid-backbone from the construct. The digested DNA was separated using an ethidium bromide free preparative gel and the linearized constructs were eluted in 2 mM Tris pH7.5 using the QiaQuick protocol. For injection, the DNA was diluted in injection buffer to a final concentration of 3-5 ng/µl.

4.2.4 Superovulation and oocyte preparation

For superovulation, 6-8 weeks old IFNγ-KO females were injected intraperitoneal (i.p.) with 5U of PMS (*Sigma*) and exactly 48 hours later, again i.p. injected with 5U of HCG (*Sigma*). Then they were mated with IFNγ-KO males. The following morning, mated females were analyzed for vaginal plugs and if present approximately at 10a.m. the oocytes were prepared. Females were sacrificed by cervical dislocation, the lower part of the peritoneum was opened and the uterus and both of the oviducts and ovaries were carefully excised. The oviducts were separated from ovaries and uterus and were transferred into a dish containing warm M2 medium (*Sigma*). Using a microscope, the swollen part of the oviduct (ampulla) containing a cloud of oocytes surrounded by cumulus cells, was opened with two forceps and the oocytes liberated into the medium. The oocytes were then collected and transferred into 300 µg/ml hyaluronidase containing M16 medium using a pulled out Pasteur pipette equipped with a tube and a mouth pipette. They were incubated for 5 min at 37°C and 5% CO_2 to remove the cumulus cells. The single oocytes were washed twice in M2 Medium and once in M16 and then allowed to recover in pre-warmed M16 medium for at least 1 hour at 37°C and 5% CO_2.

4.2.5 Holding and injection needle preparation

Capillary needles (*Hilgenberg*) for holding the oocytes and for DNA microinjection were pulled out to the correct diameter in a horizontal pipette puller (*Bachofer*). The needles were bent to an angle of 20° near the tip and the holding pipette was first broken and then closed to a diameter of 40 to 50µm in a microforge in order to generate a smooth glass surface and to allow firm adhesion of the oocyte for successful manipulation. The injection needle was filled by capillary forces with a droplet of DNA solution.

4.2.6 Pronuclear injection

The injection needle containing transgene DNA was fixed to the *Eppendorf* microinjector and the oocytes were transferred into a pre-warmed droplet of M2 medium on a glass coverslip under the microscope. (*Olympus* IX70, fitted with Narishige Micromanipulators). Using the holding pipette, each oocyte was adjusted until the male pronucleus was in the centre of the oocyte and the polar bodies out of the route of the injection needle. The injection needle was inserted into the pronucleus and a small amount of DNA (<1 fmol, equivalent to a few hundred copies) was injected. The injected oocytes were transferred back into warm M16 medium and incubated at 37°C and 7% CO_2 overnight.

4.2.7 Oviduct transfer into pseudopregnant foster mothers

The next day, eggs, which had survived injection and had proceeded into the 2-cell stage, were implanted into the oviduct of foster mothers. To generate foster mothers for the oocytes, 8-10 week old CD1 female mice were mated with vasectomized CD1 males on the day of the oocyte preparation and DNA microinjection. For the implantation, females showing a vaginal plug after 24hours were anaesthetized by an injection of 500 µl of Avertin i.p and the dorso-lateral side was opened by a small incision. The ovary and part of the uterus were pulled out and 8-10 2-cell embryos were transferred into the infundibulum of each oviduct with a mouth pipette. Following transfer, the ovary and uterus were carefully relocated into the peritoneum and the incision closed with a metal clamp.

4.2.8 Genotyping of putative transgenic animals by PCR

At the age of 3-4 weeks, mice were weaned and genders were separated. At the same time, they were ear marked and a 5 mm tail biopsy was cut off to prepare a sample of genomic DNA from each potential founder. Transgene-carrying mice were identified by PCR of tail biopsy DNA and Southern blotting. Since multiple IFNγ expressing transgene constructs were injected into homo and heterozygous IFNγ-KO animals, a PCR protocol was developed to discriminate between homozygous and heterozygous IFNγ-KO and IFNγ transgenic animals. The targeted IFNγ locus consists of exon-1 and most of exon-2 before a stop cassette and the inverted neomycin resistance-gene. This is followed by the complete intron-2 and exon-3. To discriminate between the transgenic and wild-type untargeted IFNγ gene, primers complimentary to the beginning of exon-2 and the end of exon-3 were designed. With these primers, a wild-type endogenous IFNγ locus lead to a 330bp PCR-product. If a IFNγ transgene was present in the genome a 290bp PCR-product was amplified since all constructed cassettes contained the IFNγ cDNA lacking the introns. As a PCR control for IFNγ-KO animals a third primer complementary to the end of the neomycin resistance-gene was designed. This primer in conjunction with the exon-3 reverse primer described above produced a 850bp fragment if an IFNγ-KO allele was present.

4.3 Immunologic methods

4.3.1 Histology

Organs were embedded in tissue-tek (*Shandon*), snapfrozen in liquid nitrogen and subsequently kept at -80°C. Using a Cryostat (*Shandon*), 5 µm sections were cut, air dried, fixed in acetone for 10 min and stained with hematoxylin and eosin or used in immunoperoxidase staining (section 4.3.2). For each organ, multiple stained sections were analyzed microscopically and digital pictures taken using a digital video system (*Microvid*).

4.3.2 Immunoperoxidase staining of cryosections

After 10min acetone fixation and two PBS washes, sections were incubated for 3 min in peroxidase block, containing 0.3 % saponin, washed in PBS and blocked with 5% rat serum for 10 min. Sections were then stained with primary antibody (anti-IFNγ mAb) for 60 min, subsequently washed five times in PBS and incubated for 40 min with the secondary peroxidase coupled antibody (goat anti-rat), followed by the peroxidase detection with an AEC substrate chromogen system (AEC; 3-amino-9-ethylcarbazole).

4.3.3 Single cell isolation from different tissues

Spleen cells were isolated by homogenization using an iron mash sieve and subsequent red blood cell lysis using erylysis buffer and two washes with a 1:1 mixture of complete RPMI and PBS.

Lung lymphocytes were obtained by homogenizing the lung using an iron mash sieve and lysing the red blood cells using erylysis buffer. Following two washes in complete RPMI medium, cell suspensions were filtered through a 70 µm nylon sieve and centrifuged to pellet the cells. To further purify these cells, a 40%/70% Percoll gradient was performed for 30 min at 600xg.

Intraepithelial lymphocytes (IEL) from small and large intestines were isolated as previously described by Bonhagen and colleagues with some modifications (Bonhagen et al., 1996). Briefly, after excision of the Peyer's patches, large and small intestines of mice were cut open and washed twice in PBS, 1% BSA. Intestines were stirred at 37°C for 20 min in complete RPMI

medium and then washed twice by shaking in complete RPMI medium for 0.5 min. Supernatants were filtered through a 70 µm nylon sieve and centrifuged to pellet the cells. Cells were resuspended and further purified over a 40%/70% Percoll gradient.

Lamina propria lymphocytes (LPL) were isolated from small and large intestines by a modified version of the protocol published by Bonhagen et al. (Bonhagen et al., 1996). After IEL isolation, intestines were cut into 5 mm pieces and digested for 60 min at 37°C in complete RPMI medium supplemented with Collagenase D (*Roche*) and Collagenase Type VIII (*Sigma*). Resulting cell suspensions were filtered through a 70 µm nylon sieve and centrifuged to pellet the cells. Cells were washed in complete RPMI medium and further purified over a 40%/70% Percoll gradient.

Intestinal epithelia cells (IEC) were isolated using an 15%/30%/70% gradient, instead of the 40%/70% gradient after primary purification of intestinal cells. IEL, LPL and lung lymphocytes were collected at the interface of the 40%/70% or 30%/70% gradient and IEC were collected at the interphase of the 15%/30% gradient. Collected cells were washed twice in complete RPMI medium and counted. Viability of the cells was determined by Trypan blue exclusion.

4.3.4 Flow cytometry

To measure intracellular cytokines, $2x10^6$ cells were cultured for 5 hours in 1 ml of complete RPMI medium. During this incubation, cells were either stimulated with 3 µg of anti-CD3 mAb and 5 µg of anti-CD28 mAb or left alone. During the final 4 hours of culture, 10 µg/ml of Brefeldin A (*Sigma*) was added. After the incubation, cells were washed and incubated with rat serum and anti-CD16/CD32 mAb to block non-specific antibody binding. Ten min later, cells were stained with FITC-conjugated anti-CD4 mAb. After 30 min on ice, cells were washed with PBS and fixed for 20 min at room temperature with PBS, 4% paraformaldehyde (*Sigma*). Cells were washed with PBS, 0.1% BSA, permeabilized with PBS, 0.1% BSA, 0.5% saponin (*Sigma*) and incubated in this buffer with rat serum and anti-CD16/CD32 mAb for 5 min. To stain the intracellular cytokines PE-conjugated anti-IL-10 mAb

and APC-conjugated anti-IL-5 mAb, or APC- and PE-conjugated isotype control mAb were added. After 20 min at room temperature, cells were washed with PBS and fixed with PBS, 1% paraformaldehyde.

To measure surface expressed proteins, $2x10^6$ cells were incubated in 200 µl PBS with conjugated antibodies for 20 min on ice, washed in PBS and resuspended in 300 µl PBS containing 0.1% BSA. Counting of stained cells was performed with a FACS Calibur (*Becton Dickinson*) and the software FCS-express and Cell Quest were used to analyze the data (Figure 5 and Figure 6).

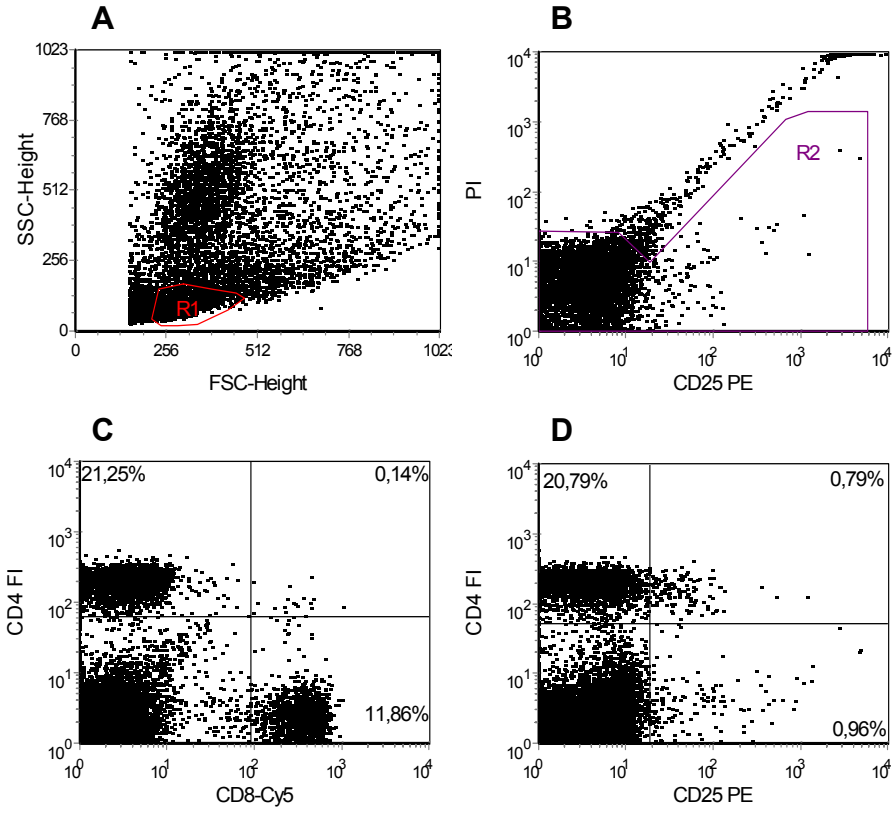

Figure 5: Flow cytometric analysis of $CD4^+$, $CD8^+$ and $CD4^+$ $CD25^+$ lung lymphocyte populations, determination of frequencies. Lung lymphocytes were isolated from each animal as described in section 4.3.3 and stained with Cy5-conjugated anti-CD8α mAb, FITC-conjugated anti-CD4 mAb and PE-conjugated anti-CD25 mAb. Cells were analyzed by four-color flow cytometry after the addition of propidium iodide. Figures show lymphocyte gating in FSC/SSC dot blot (A) and propidium iodide gating in the FL2/FL3 dot blot (B) to exclude dead cells. Gates from A and B were combined in C and D, where therefore life $CD4^+$ versus $CD8^+$ lymphocytes (C) and life $CD4^+$ versus $CD25^+$ lymphocytes (D) were plotted.

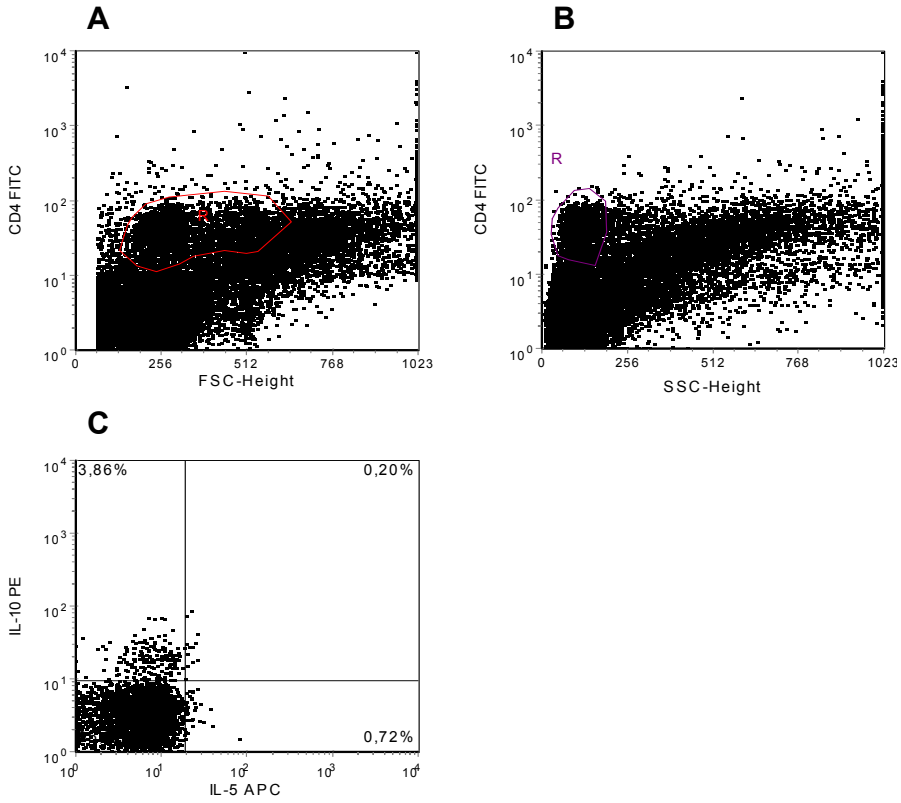

Figure 6: Flow cytometric analysis of IL-4$^+$, IL-5$^+$ CD4$^+$ lung lymphocyte populations. To analyze the frequencies of IL-4 and IL-5 producing CD4$^+$ cells, isolated lung cells were incubated with Brefeldin A in the absence or presence of anti-CD3 mAb and anti CD28 mAb and afterwards stained with FITC conjugated anti CD4 mAb and intracellularly with PE conjugated anti-IL-10 mAb and APC conjugated anti-IL5 mAb. Figures A and B represent CD4$^+$ lymphocyte gating using size and granularity. Gates of A and B were combined and assigned to C, where therefore IL-10$^+$ CD4$^+$ vs. IL-5$^+$ CD4$^+$ cells were plotted.

4.3.5 IEC culture and *in vitro* restimulation of lymphocytes

For *in vitro* lymphocyte restimulation, 5x10^5 freshly isolated lymphocytes originating from lung or spleen, were incubated in 200 µl complete RPMI, with or without 3 µg/ml anti-CD3 mAb and 5 µg/ml anti-CD28 mAb. After 72 hours supernatants were collected, centrifuged and used for ELISA analysis. IEC supernatant was collected from 2x10^6 IEC cultured for 48 hours in 500 µl complete RPMI supplemented with glucose and insulin. Before their use in ELISA or protein dot blot (section 4.4.4), supernatants were freed of cells and debris by centrifugation.

4.3.6 Bronchoalveolar lavage and cytospin

To collect bronchoalveolar lavage fluid (BALF) mice were carefully killed by cervical dislocation and median sternotomy was performed. The trachea was dissected free from surrounding soft tissue and a 0.6 mm syringe was inserted through a small incision. Bronchoalveolar lavage fluid (BALF) was collected by perfusing the lung with 1 ml of PBS and gently aspirating the fluid back. This was repeated three times each time recovering ca. 0.9 ml. The samples were pooled, centrifuged and cell numbers were determined. While the cell free BALF was stored at –80°C, cells were spun onto glass slides at 666 rpm for 3 min using a Cytospin (*Shandon*). Cells on glass slide were then stained with the hematoxylin and eosin like fast stain Hema-Schnellfaerbung (*Labor + Technik*) and differential counts were performed microscopically using standard histologic criteria.

4.3.7 Blood smear

Droplets of fresh blood were spread out on microscope slides and stained with Hema-Schnellfaerbung (*Labor + Technik*). The different kinds of blood cells were determined by microscopy and counted using standard histologic criteria.

4.4 Biochemical methods

4.4.1 ELISA

Immuno-Maxisorp ELISA plates (*Nunc*) were coated with the primary antibody in 50 µl/well coating buffer and left overnight at 4°C. Plates were washed four times using ELISA wash buffer and blocked for 2 hours at 37°C in 200 µl/well PBS containing 1% BSA. After repeating the washing step, standards and samples were diluted in tissue culture medium, 50 µl added to each well and left at 4°C overnight for optimal binding of the cytokine of interest to the primary antibody. Plates were then washed prior to the addition of 50 µl/well of the secondary antibody diluted to the appropriate concentration in PBS / 1% BSA and incubated in a moist chamber at 37°C for 1 hour. After repeated washing, 50 µl/well streptavidin-conjugated alkaline phosphatase (*Dianova*) diluted 1:1000 in PBS / 1% BSA was added and incubated for 1 hour at 37°C. After further washing, 50 µl of the phosphatase substrate (*Sigma*) in 10 µl diethanolaminebuffer was added. The reaction was allowed to proceed for 20 min in the dark before being stopped by addition of 50 µl 0.5 M EDTA, pH8.0. The plate was read by a Spectramax ELISA reader (*Molecular Devices*) and analyzed by Softmaxpro software. Control wells were left untreated with the primary or secondary antibody or filled with medium only. For IFNγ ELISA, primary antibody was R4-6A2, used at 2 µg/ml and secondary antibody was XMG1.2-biotin used at 2 µg/ml. The standard recombinant IFNγ was purchased from *R&D* and diluted from 200 U/ml in two fold dilutions. The IFNγ ELISA was linear in the range from 6 U/ml to 100 U/ml. For anti OVA IgE detection, plates were coated with ovalbumin (OVA) grade VII (*Sigma*) and anti-OVA-IgE was specifically detected by the monoclonal antibody anti-mouse IgE-HRP clone LO-ME3 (*Biosource*).

4.4.2 SDS polyacrylamide gel electrophoresis

Cells ($1x10^8$) were washed twice in PBS and lysed in cell lysis buffer on ice. Nuclei and cell debris were removed by centrifugation of the lysate for 10 min at 10.000xg and 50 µg of protein were separated on a discontinuous SDS-

PAGE according to Laemmli using vertical slab gels (Laemmli, 1970). Samples were prepared in SDS-containing sample buffer and heated to 95°C for 3 min before electrophoresis. Proteins were visualized either with Coomassie Blue staining or immunoblotting (Western Blot).

4.4.3 Western blot

Proteins were transferred from SDS polyacrylamide gels to nitrocellulose membranes (*Bio-Rad*) using a semi-dry electrophoresis apparatus (LKB multiphor II) according to the manufacturer's instructions. After electrophoresis membranes were stained with Ponceau S to visualize total protein. Molecular weight standards were marked with a pencil. The membrane was then washed twice in blocking buffer and blocked for 1 hour at RT or 12 hours at 4°C. After blocking, the membrane was incubated with primary antibody (anti-IFNγ mAb XMG1.2) in a dilution of 1:1000 for 45 min and subsequently washed four times in PBS. The membrane was then incubated for 1 hour with the appropriate secondary antibody conjugated to horse-radish peroxidase (HRP) at a dilution of 1:5000 and washed as before.

4.4.4 Protein dot blot

Nitrocellulose membranes (*Bio-Rad*) were fixed in the dot blot apparatus (*Bio-Rad*) and vacuum was applied. Fivehundred µl of medium containing serial diluted recombinant IFNγ or 500 µl of supernatant were gradually poured into each well, in which the vacuum sucks the liquid through the nitrocellulose membrane while proteins stay trapped on the membrane. After all supernatants had been applied, membranes were treated as described for western blot (section 4.4.3).

4.4.5 ECL detection

The *Amersham* ECL system was used for the detection of HRP according to the manufacturer's instructions. The membranes were exposed to pre-flashed films (*Amersham*), using exposure times between 10 seconds and 30 min depending on the intensity of the signals.

4.5 Animal procedures

4.5.1 Mouse strains, housing and breeding

All transgenic animals, C57BL/6 mice and IFNγ-KO mice were bred in our facility at the Federal Institute for Health Protection of Consumers and Veterinary Medicine (BGVV) in Berlin. Mice were kept under specific pathogen-free (SPF) conditions in filter bonnet cages with food and water ad libidum. The experiments were conducted according to the German animal protection law.

4.5.2 Measurement of urine volume and urine test

Each mouse was kept for 24 hours in a metabolism cage where urine and feces were collected separately. For urine tests *Roche* Combur urine test strips were used. These test strips measure approximate leukocyte numbers, protein, glucose, bilirubin, hemoglobin concentrations, pH and presence of nitrate and ketones. Water consumption was measured by weighing the supplied drinking water before and after the 24 hour single housing. To control that the calculated water consumption was not due to a leaking bottle, the collected urine was also weighed.

4.5.3 Induction of allergic airway inflammation

Mice were sensitized and challenged with chicken OVA grade VII (*Sigma*) as previously described with some modifications (von Bethmann et al., 1998). Briefly 6 to 8 week old homozygous CC10-IFNγ-tg-IFNγ-KO, C57BL/6 and IFNγ-KO animals were immunized to OVA by intraperitoneal injection of 20 µg OVA emulsified in 100 µl Alum (*Serva*) on day 0 and 14. Where indicated, mice were challenged intranasally with 100 µg OVA in 25 µl endotoxin-free PBS on days 28, 29 and 30. Mice were sacrificed and analyzed on day 31.

4.5.4 Measurement of airway hyperresponsiveness

Twentyfour hours after the last challenge, mouse lungs were prepared, ventilated and perfused as previously described by Denzler and colleagues (Denzler et al., 2000). Briefly, mice were deeply anesthetized with Ketamin (160 mg/kg) and Xylazin (20 mg/kg). Mice were placed into a 37°C chamber (*Harvard Apparatus*). A tracheotomy was performed and the animals were room-air ventilated (positive pressure ventilation, PPV) with a rotary vane compressor pump (VCM*; Harvard Apparatus*) with 90 breaths/min and a tidal volume of approximately 150 µl. After laparotomy and removal of the diaphragm, the animals were heparinized, exsanguinated and the abdomen was removed. A sternotomy was performed and a cannula was placed into the left atrium, followed by insertion of an arterial cannula into the pulmonary artery. Lungs were perfused with 37°C sterile Krebs-Henseleit-hydroxyethylamylopectine buffer at a constant flow rate of 1 ml/min (generated by a peristaltic pump, *Ismatec MS Reglo*) in a non-recirculating manner. In parallel with the onset of artificial perfusion, the gas supply was changed to a mixture of 5% CO_2, 21% O_2 and 74% N_2, and the perfusate was equilibrated with the same gas mixture. Left atrial pressure was adjusted at +2.2cm H_2O. Then the chamber lid was closed and negative pressure ventilation (NPV) was started with the chamber pressure oscillating between –4.5 and –9.0 cm H_2O in order to achieve a tidal volume (V_T) of approximately 150 µl. Hyperinflation (-24cm H_2O) was performed at 4 min intervals. Artificial thorax chamber pressure was measured with a differential pressure transducer (MPX 399/2*; Harvard Apparatus*) and airflow velocity was measured with a pneumotachograph tube connected to a differential pressure transducer (DP 45-14*; Validyne*). Arterial and venous pressure were continuously monitored by pressure transducers (P75/379*; Harvard Apparatus*) that were connected with the cannulae ending in the pulmonary artery and the left atrium, respectively. All data were amplified (CFBA*; Harvard Apparatus*) and analyzed with Pulmodyn software (*Harvard Apparatus*). The data for lung mechanics were analyzed applying the following formula: $P = 1/C * V + R_L * dV / dt$, where P is chamber pressure, C is pulmonary compliance, V is volume and R_L is pulmonary resistance.

Each experiment consisted of an initial period of baseline measurement and three treatments with increasing doses of the unspecific bronchoconstrictor methacholine, 12 min apart to allow the relaxation and recovery of bronchial musculature. From the data gathered during the baseline measurement, airway resistance and dynamic compliance were calculated for each analyzed lung and to allow the comparison between lungs, the values were designated as 100% resistance or compliance of the respective lung. For each dose of methacholine the calculated resistance and compliance were then put into relation to the baseline level.
All AHR measurements were performed by Martin Witzenrath at the Medizinische Klinik mit Schwerpunkt Infektiologie, Universitätsklinikum Charité.

4.6 Statistical analysis

Statistical significance of results was determined with the unpaired t-test or the Newman-Keuls post-hoc test included in the GraphPad Prism program (*GraphPad Software*).

5 Results

5.1 Lung-specific IFNγ expression in a murine model of allergic airway inflammation

5.1.1 Lung-specific IFNγ expression in CC10-IFNγ-tg-IFNγ-KO mice

The CC10-IFNγ-tg-IFNγ-KO mouse line was generated in our laboratory by Christine Reuter, in her PhD thesis. In these mice IFNγ expression is driven by the CC10-promoter exclusively in Clara cells of the lung (Stripp et al., 1992). Due to a targeted deletion of the IFNγ-gene in these mice (Dalton et al., 1993), IFNγ is constitutively and exclusively expressed by the transgene. The IFNγ-KO background was chosen because the highly inducible endogenous IFNγ promoter would interfere with the analysis of the effects of a strictly defined spatial and temporal expression of IFNγ. Dependent on the immune status, different amounts of IFNγ would be produced, possibly masking the effect of the locally produced low amounts of IFNγ.

IFNγ expression in the lung of CC10-IFNγ-tg-IFNγ-KO mice can be detected by northern blotting (Figure 7). Despite the fact that the amount of IFNγ-protein in the lungs of these mice is below the detection limit of an ELISA or a western blot, active IFNγ protein is produced, because the expression of multiple known IFNγ responsive genes like IIGP,

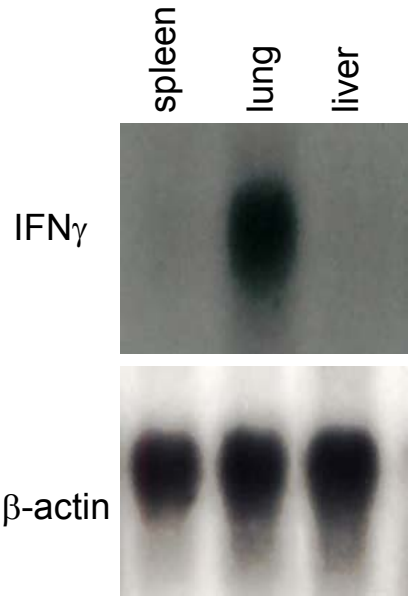

Figure 7: Northern blot analysis of RNA from spleen, lung and liver of a CC10-IFNγ-tg-IFNγ-KO mouse. Equal amounts (20 µg) of spleen, liver and lung total cellular RNA were loaded on a denaturing formaldehyde gel, transferred to a nylon membrane and hybridized with an IFNγ-specific, radiolabeled probe. Analysis was performed by phospho-imaging.

IP-10 and MHC class II is upregulated in the lungs of these mice (data not shown). Although low, the amount of IFNγ expressed in the lung of CC10-IFNγ-tg-IFNγ-KO animals is sufficient to partially protect them from *M. tuberculosis* infection, when compared to IFNγ-KO mice: 28 days after aerosol infection with *M. tuberculosis,* CC10-IFNγ-tg-IFNγ-KO mice have a significantly lower number of CFU in their lungs than IFNγ-KO mice. It is very likely due to the unregulated low expression of IFNγ and in contrast to the induced high levels of IFNγ in *M tuberculosis* infected C57BL/6 mice, that CFU in lungs of CC10-IFNγ-tg-IFNγ-KO are still higher than those of lungs of C57BL/6 mice (PhD thesis C. Reuter).

However, the low amount of IFNγ in the lungs of these mice makes them favorable for the analysis in a murine model of allergic airway inflammation. High levels of IFNγ in the lung are known to cause severe abnormalities like emphysema and a macrophage-, lymphocyte- and neutrophil-rich response (Wang et al., 2000). CC10-IFNγ-tg-IFNγ-KO mice do not show such symptoms at any age. The histologic appearance of their lungs and all other organs, their behavior, physical appearance and life span is identical to that of C57BL/6 and IFNγ-KO mice.

5.1.2 Establishment of an OVA sensitization and challenge protocol to induce eosinophilia in C57BL/6 mice

The majority of published experiments use BALB/c mice in models of allergic airway inflammation. BALB/c mice tend to react stronger than C57BL/6 mice in terms of levels of antigen-specific IgE, cytokine concentration in BALF, AHR and infiltration of eosinophils into the lung (Leong and Huston, 2001). Since the CC10-IFNγ-tg-IFNγ-KO mice are on C57BL/6 background, a protocol for the induction of allergic airway inflammation in C57BL/6 mice was established. Three different protocols were tested (A-C) (Figure 8). All three protocols include two sensitizations 14 days apart, each consisting of an intraperitoneal injection of 2 µg or 20 µg OVA in 100 µl Alum adjuvant. Animals in Group A and B received 2 µg OVA while animals in Group C

received 20 µg OVA. Challenge was performed at day 28 by intranasal application of 20 µg (A,B) or 100 µg (C) OVA in 25 µl PBS. Group A was challenged once with 20 µg OVA, while group B was challenged on three consecutive days with 20 µg OVA, and group C received 100 µg OVA on three consecutive days. One day after the last challenge, animals were analyzed for eosinophilia.

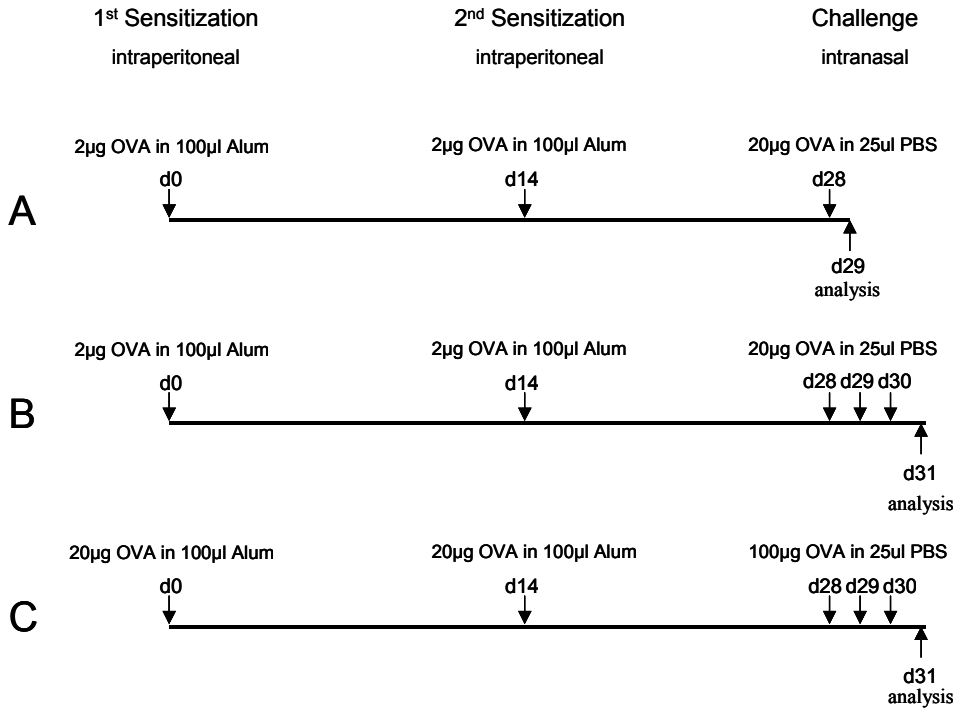

Figure 8: Three different sensitization and challenge protocols tested to determine the optimal induction of allergic airway inflammation in C57BL/6 mice.

A strong eosinophilia in the lung is one of the characteristic hallmarks of allergic airway inflammation. Indeed the number of eosinophils and especially of activated eosinophils has been correlated with severity of allergic airway inflammation in humans (Martin et al., 1996). In a highly allergic animal, eosinophilic infiltration of the lung leads to 50-80% percent eosinophils in bronchoalveolar lavage fluid (BALF). To determine the efficiency of the different sensitization and challenge protocols in induction of allergic airway inflammation, the percentage of eosinophils in BALF from animals in each group was determined (Figure 9). For this purpose the mice were sacrificed

and bronchoalveolar lavage (BAL) was performed 24 hours after the last challenge. The cells in the BALF were spun onto glass slides, stained with Hema-Schnellfaerbung and the percentage of eosinophils was determined microscopically using standard histologic criteria.

BALF from animals in group A did not show increased numbers of eosinophils when compared to BALF of untreated animals. In BALF of animals from groups B that had received the same challenge dose as group A but on three consecutive days increased but low numbers of eosinophils (18%) were counted. In contrast, high percentages of eosinophils were found in BALF from animals in group C. These mice were treated with ten times more OVA during sensitization and five times more OVA during three consecutive challenges. These results lead to the conclusion that only a high dose of OVA during sensitization and challenge and only three consecutive challenges were suitable to induce a strong allergic airway inflammation in C57BL/6 mice. Therefore all of the following experiments were performed using protocol C.

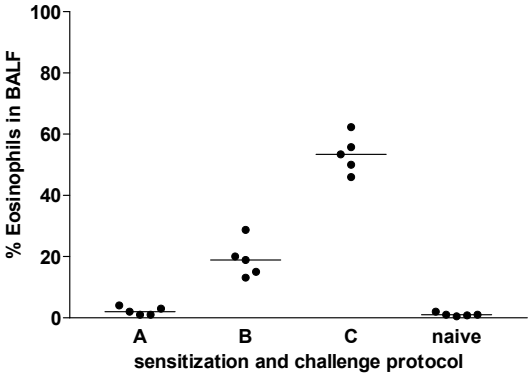

Figure 9: Percent eosinophils in BALF of mice treated with different sensitization and challenge protocols. Mice in group A received two i.p. sensitizations with 2 µg OVA in 100 µl Alum at day 0 and 14 and one i.n. challenge with 20 µg OVA in 25 µl PBS at day 28. Group B was sensitized and challenged similarly to group A but received three consecutive challenges at days 28-30. Group C received 20 µg OVA in 100 µl Alum at day 0 and 14 and was challenged three times on consecutive days using 100 µg OVA in 25 µl PBS at days 28-30. Animals were analyzed one day after the last challenge respectively. Naïve animals were untreated. One representative experiment of two is shown.

5.1.3 Characterization of C57BL/6, IFNγ-KO and CC10-IFNγ-tg-IFNγ-KO mice in a murine model of allergic airway inflammation

In order to analyze the effect of low but constitutive IFNγ expression in the lung of IFNγ-KO animals on the allergic response against OVA sensitization and challenge, groups of C57BL/6, IFNγ-KO and CC10-IFNγ-tg-IFNγ-KO animals were subjected to the sensitization and challenge protocol C, described above (see section 5.1.2).

5.1.3.1 Effects of IFNγ on OVA induced BALF eosinophilia

To asses the effect of locally produced IFNγ on the development of eosinophilia and cellular composition of BALF, cells in BALF from each animal were spun onto glass slides, stained and counted microscopically using standard histologic criteria (Figure 10). In naïve and sensitized animals, macrophages made up approximately 99% of all BALF cells. Eosinophils and neutrophils were virtually absent in BALF of naïve and sensitized animals with 0-2% and 0-1%, respectively. Therefore, lung-specific IFNγ expression alone did not induce eosinophilia in the absence of other stimulus. In all mice sensitized and subsequently challenged, a strong increase in cell numbers recovered from BALF was observed when compared to naïve or just sensitized animals (data not shown). After challenge, the number of macrophages only increased slightly, while the percentage and number of eosinophils and neutrophils within the BALF increased strongly in all three groups, demonstrating that despite of lung-specific IFNγ production, CC10-IFNγ-tg-IFNγ-KO animals were able to mount a allergic inflammatory response. Moreover, throughout all experiments, CC10-IFNγ-tg-IFNγ-KO mice showed a low but constitutive higher percentage and number of BALF eosinophils than INFγ-KO and wild-type controls. However, median percentages varied between experiments. Within the experiment represented in Figure 10-A, CC10-IFNγ-tg-IFNγ-KO mice showed a significantly higher percentage of eosinophils than C57BL/6 mice (p=0,07) and IFNγ-KO mice (p=0.015). The percentage and number of neutrophils in BALF of sensitized

and challenged mice did not differ significantly between the three analyzed groups (Figure 10-B). These data lead to the conclusion that lung-specific IFNγ expression in an IFNγ-KO animal leads to an increased airway inflammation in this model.

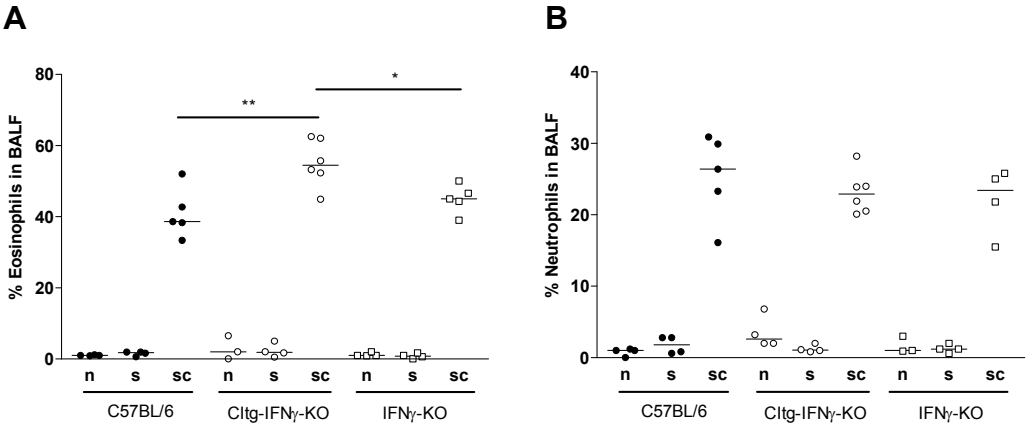

Figure 10: Percent eosinophils (A) and neutrophils (B) in BALF from naïve (n), sensitized (s) or sensitized and challenged (sc) C57BL/6, CC10-IFNγ-tg-IFNγ-KO and IFNγ-KO animals. Cells in BALF from individual animals were spun onto glass slides, stained with Hema-Schnellfaerbung and counted microscopically using standard histologic criteria. The data are represented as scatterplots with each spot representing one animal. Significant differences between medians of groups are indicated by asterisks. (** represents P=0.001-0.01; * represents P=0.05-0.01)

5.1.3.2 Histologic evaluation of lungs

To examine whether sensitization and challenge induced a characteristic lung pathology, lungs of all three groups were harvested 24 hours after the last challenge, frozen, sectioned and stained with H&E (Figure 11). The characteristic signs of asthma like lung pathology are visible in sections of all challenged groups of mice. High numbers of inflammatory cells throughout the whole lung and specifically in the peribronchovascular region were observed. Inflammation in the bronchial epithelial cells and a thickened epithelial layer were also detected. Although not proven by numbers, lungs of CC10-IFNγ-tg-IFNγ-KO looked less affected than those from the other two groups, possibly indicating a positive effect of IFNγ on lung pathology.

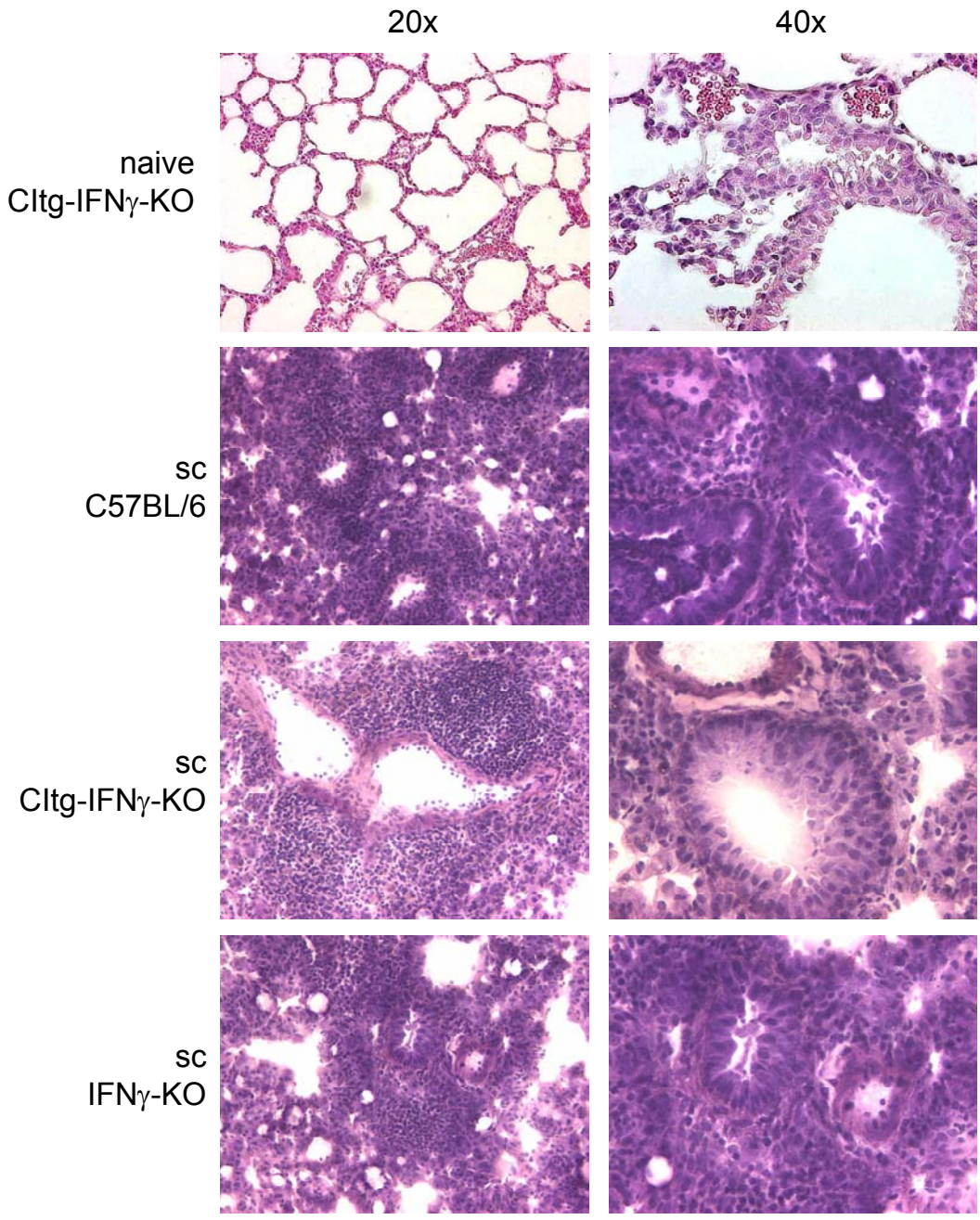

Figure 11: Lungs of naïve and challenged C57BL/6, CC10-IFNγ-tg-IFNγ-KO (CItg-IFNγ-KO) and IFNγ-KO mice. Lungs were harvested 24 hours after the last i.n. challenge, embedded in tissue-tek, frozen and sectioned. Sections were stained with H&E.

5.1.3.3 Effects of IFNγ on IgE in serum and lung-homogenates

During an allergic response the total and allergen-specific IgE levels increase dramatically. Although the exact role of IgE in the murine model of asthma is unknown, it is clear that IgE binds to high-affinity FcεI receptors on mast cells and granulocytes and sensitizes them. IgE also binds to the low affinity receptor FcεII (CD23), which is expressed on APCs and lymphocytes and thereby also modifies the adaptive immune response. However, IgE does not seem to be a prerequisite for asthma since airway inflammation and eosinophilia are not reduced even in the absence of IgE (Hogan et al., 1997).
To address the question whether IFNγ expression in the lung influences IgE emergence or expression level, total and OVA-specific IgE levels were measured in serum and lung-homogenates of OVA sensitized and challenged mice by ELISA (Figure 12). Interestingly, the average IgE levels in sera of sensitized as well as sensitized and challenged CC10-IFNγ-tg-IFNγ-KO animals were significantly lower than those of equally treated C57BL/6 and IFNγ-KO animals. No difference could be observed between the latter two groups (Figure 12-A). Only low to undetectable total IgE levels were observed in most naïve and only sensitized (or vehicle control challenged) animals.
In contrast to the significantly lower total IgE levels in sera of challenged CC10-IFNγ-tg-IFNγ-KO animals, the total IgE levels in lung-homogenates of these mice were significantly higher than those of C57BL/6 and IFNγ-KO animals (Figure 12-B). However, total IgE levels in lung-homogenates of naïve and sensitized animals did not display a significant difference between the three groups. Additionally, only a slight increase of total IgE in lung-homogenates was observed after sensitization in all three groups.

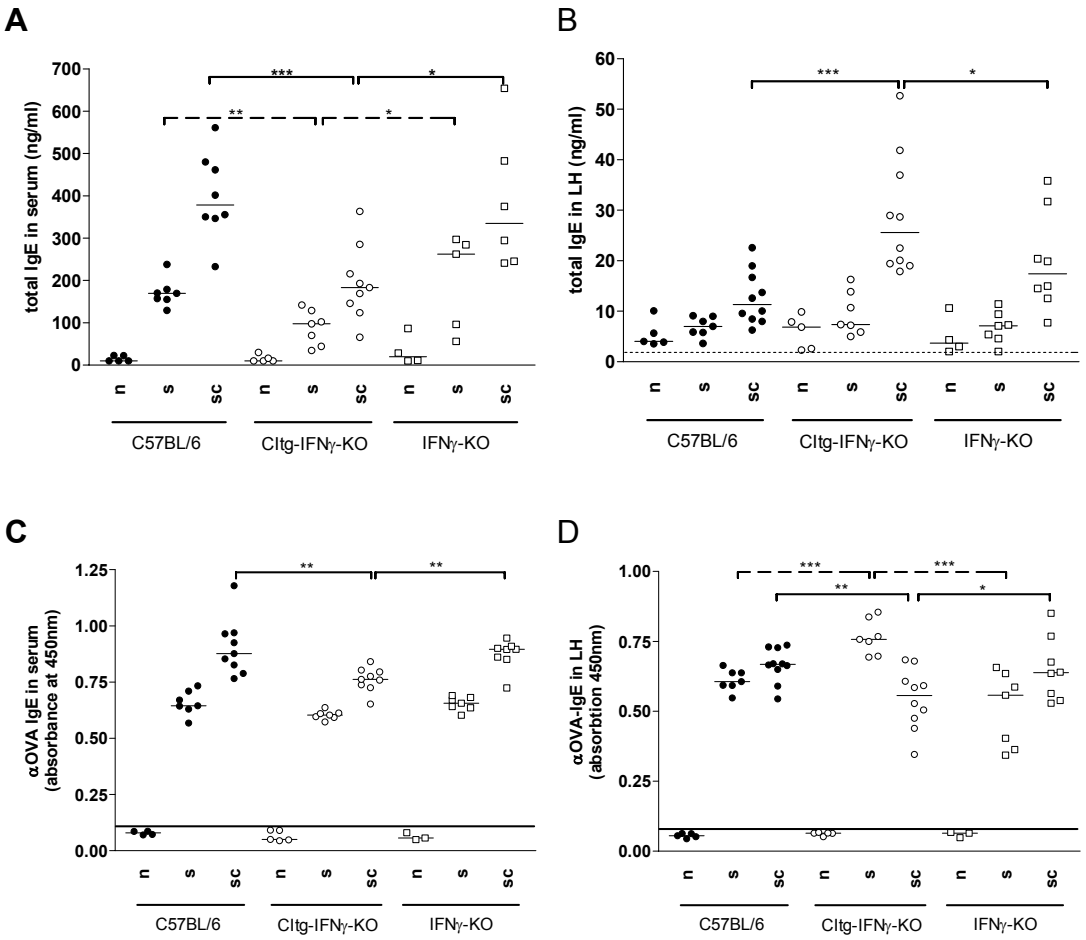

Figure 12: Total IgE levels in serum (A) and lung-homogenate (B) and OVA-specific IgE in serum (C) and lung-homogenates (D) of naïve (n), sensitized (s) and sensitized and challenged (sc) mice. Sera and lungs were collected 24hrs after the last i.n. challenge, lungs were homogenized, homogenate and sera were spun down and the supernatants were analyzed by ELISA. Concentrations of total IgE and absorbance of OVA-specific IgE are shown. In figures B, C and D vertical dotted lines represent the concentration or absorbance of a negative control. Significant differences between means are indicated with asterisks (*** represents P<0.001; ** represents P=0.001-0.01; * represents P=0.05-0.01).

As expected, αOVA-IgE was only detectable in sera and lung-homogenates after sensitization (Figure 12-C and D). Similar to the total IgE levels, αOVA-IgE levels were significantly lower in sera from challenged CC10-IFNγ-tg-IFNγ-KO animals than from equally treated C57BL/6 and IFNγ-KO animals. However, this was also observed for αOVA-IgE levels in lung-homogenates from the same animals and therefore contradicts the results of the total IgE levels. Moreover, αOVA-IgE levels in lung-homogenates from sensitized CC10-IFNγ-tg-IFNγ-KO mice were higher than those from sensitized and

challenged CC10-IFNγ-tg-IFNγ-KO animals, suggesting that IFNγ expression despite its spatial restriction influences total and OVA-specific IgE differentially during sensitization and challenge. While OVA-specific IgE serum concentrations after i.p. sensitization did not differ from those of the other two groups, OVA-specific IgE concentrations in lungs were increased. In contrast, OVA-specific IgE concentrations were reduced in serum as well as lung after intranasal challenge, always in comparison to those in C57BL/6 and IFNγ-KO animals.

5.1.3.4 Effects of IFNγ on cytokine and eotaxin mRNA levels in lungs

To investigate the underlying events that lead to the observed increased eosinophilia and different IgE levels in CC10-IFNγ-tg-IFNγ-KO animals, the expression levels of cytokines involved in this asthma model were measured. For this purpose lungs were taken from naïve animals, or 24hrs after the last i.n. challenge and RNA was extracted from each lung. RNA from animals of the same groups were pooled and reverse transcribed to cDNA. With this cDNA, a semiquantitative real-time PCR was performed, using primers for β-actin and GAPDH as controls for equal amounts of cDNA and intron-spanning primer pairs, specific for cytokine cDNA. Cytokine mRNA levels were always calculated relative to the expression level of the analyzed cytokine in naïve lungs of C57BL/6 mice (Figure 13).

IL-4 as one of the major cytokines responsible for the development of a Th2 immune response was strongly upregulated in lungs of all sensitized and subsequently challenged mice (Figure 13-A). However sensitized and challenged CC10-IFNγ-tg-IFNγ-KO animals showed the lowest levels of IL-4 mRNA while IFNγ-KO exhibited the highest. As IFNγ is known to counteract IL-4 and decrease its production, this result is possibly explained by the lung-specific IFNγ expression in CC10-IFNγ-tg-IFNγ-KO animals. Because IL-4 is responsible for the class switch in plasma cells this could also explain the lower total IgE concentration measured in sera of these mice.

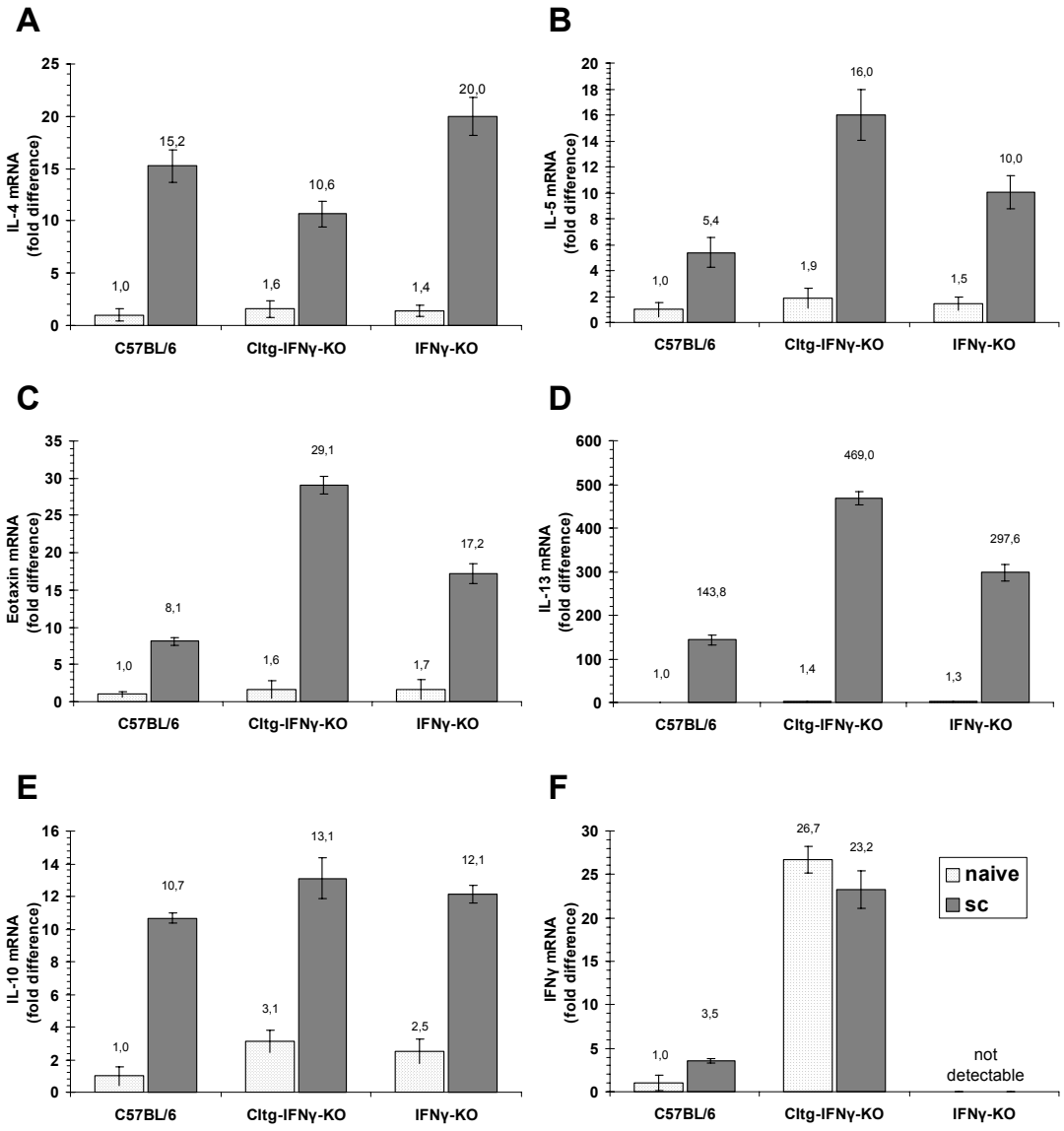

Figure 13: Relative levels of IL-4 (A), IL-5 (B), IL-13 (C), eotaxin (D), IL-10 (E) and IFNγ (F) mRNA in lungs of naïve or sensitized and challenged C57BL/6, CC10-IFNγ-tg-IFNγ-KO and IFNγ-KO animals. Quantification was performed by real-time RT-PCR. RNA was extracted from each lung and pooled with the RNA from animals within the same group. After reverse transcription to cDNA real-time PCR was performed using primers for β-actin and GAPDH simultaneously as controls and intron spanning cytokine-specific primers for quantification. Cytokine levels are represented as fold differences compared to the levels in lungs of naïve C57BL/6 mice. The error-bars represent the maximal differences between duplicates. One representative experiment of three is shown.

In contrast to IL-4 levels, IL-5 levels were highest in CC10-IFNγ-tg-IFNγ-KO animals, followed by those in IFNγ-KO animals (Figure 13-B). Of all sensitized and challenged groups, C57BL/6 mice showed the lowest levels of IL-5 mRNA. Although the IL-5 mRNA level was low, it was still higher than in the naïve or only sensitized control groups (data not shown). IL-5 cooperates

with the chemokine eotaxin, which is expressed by epithelial cells, T cells, fibroblasts and macrophages. As the main chemoattractant for eosinophils, eotaxin is mainly responsible for the recruitment of eosinophils to specific sites within the lung. Eotaxin expression in lungs of challenged mice corresponded to the IL-5 mRNA expression (Figure 13-C). It was the highest in CC10-IFNγ-tg-IFNγ-KO animals and the lowest in C57BL/6 animals, possibly explaining the high numbers of eosinophils observed in the BALF of CC10-IFNγ-tg-IFNγ-KO animals. However, so far there is no explanation for the increased IL-5 and eotaxin mRNA levels in the lungs of CC10-IFNγ-tg-IFNγ-KO animals.

As a proposed central mediator of murine asthma, IL-13 was virtually undetectable in lungs of naïve animals, but highly upregulated in those of sensitized and challenged animals (Figure 13-D). Despite the very high levels, the differences between the three groups of mice were almost similar to those measured for IL-5. CC10-IFNγ-tg-IFNγ-KO animals had almost twice as much IL-13 mRNA in their lungs than IFNγ-KO animals and three times more than C57BL/6 animals. This is surprising because IL-13 and IL-4 expression are known to correlate in this model. Therefore, it is likely that their induction is differentially regulated and IL-13 expression is not affected by IFNγ abundance. However, IL-13 and IL-4 have similar biological activities, which might explain the increased BALF eosinophilia observed in CC10-IFNγ-tg-IFNγ-KO animals.

Interestingly, IL-10, which has the potential to downregulate both Th1 and Th2 driven inflammatory processes, was upregulated in lungs of all sensitized and challenged animals (Figure 13-E). However, there was no significant difference between the three groups of mice. In contrast to the other cytokines analyzed, slightly elevated levels of IL-10 were observed in lungs of naïve CC10-IFNγ-tg-IFNγ-KO and IFNγ-KO animals, maybe reflecting a compensatory effect of unregulated IFNγ expression and/or total absence of IFNγ. Although this difference in IL-10 mRNA levels was not significant, the same tendency was observed in three independent experiments.

To study whether IFNγ levels in lungs of C57BL/6 mice change during allergic airway inflammation, real-time RT-PCR was also performed using IFNγ-specific primers. Surprisingly, IFNγ mRNA levels were upregulated in lungs of challenged C57BL/6 mice when compared to untreated naïve (Figure 13-F) and just sensitized controls (data not shown), suggesting an involvement of this Th1 cytokine in allergic airway inflammation. As expected, IFNγ levels did not differ between lungs of challenged or naïve control CC10-IFNγ-tg-IFNγ-KO mice, since IFNγ is produced by the constitutive expression of the transgene in these mice.

5.1.3.5 IL-4 and IL-5 production by stimulated splenocytes

To study the effect of lung-specific IFNγ expression on the spleen cell populations, Th2 cytokine expression of splenocytes from naïve, sensitized or sensitized and challenged animals were determined during sensitization and challenge with OVA. Single cell suspensions from spleens were cultured for 3 days. Cells were left untreated or were stimulated with 100 µg OVA, or anti-CD3 mAb and anti-CD28 mAb. Neither IL-4 nor IL-5 was detected in the supernatants from cells incubated with medium or OVA. Polyclonal stimulation with anti-CD3 mAb and anti-CD28 mAb lead to detectable levels of both IL-4 and IL-5 (Figure 14). Within these cultures, spleen cells from sensitized animals produced similar amounts of IL-4 and IL-5 compared to spleen cells from naïve mice. However, cultures from sensitized and challenged animals produced significantly higher levels of IL-4 and IL-5 than cultures from naïve animals.

Interestingly, levels of IL-5, produced by naïve, sensitized or sensitized and challenged C57BL/6 spleen cells were significantly lower than those of CC10-IFNγ-tg-IFNγ-KO and IFNγ-KO animals, suggesting that the lack of IFNγ leads to higher IL-5 production. Moreover, splenocytes of challenged CC10-IFNγ-tg-IFNγ-KO and IFNγ-KO mice produced similar levels of IL-5. However, IL-4 production was higher in challenged CC10-IFNγ-tg-IFNγ-KO mice than in challenged IFNγ-KO and C57BL/6 mice.

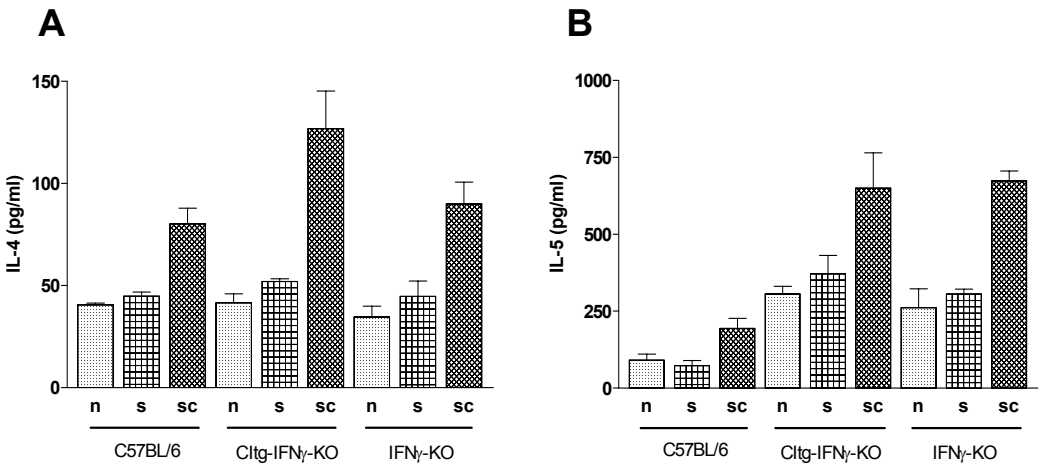

Figure 14: IL-4 (A) and IL-5 (B) produced by CD3/CD28 stimulated splenocytes isolated from naïve (n), sensitized (s) and sensitized and challenged (sc) C57BL/6, CC10-IFNγ-tg-IFNγ-KO or IFNγ-KO animals. Pooled single cell suspensions from spleens were incubated in triplicates with medium, 100 µg/ml OVA or 3 µg/ml anti-CD3 mAb and 5 µg/ml anti-CD28 mAb. After three days, supernatants were collected and analyzed by ELISA. Error-bars represent standard error between triplicates.

5.1.3.6 Effects of IFNγ on lymphocyte populations in the lung

To address the question whether the observed increase of eosinophilia and IL-5 in CC10-IFNγ-tg-IFNγ-KO animals was a consequence of increased numbers of Th2 lymphocytes or lower numbers of suppressor T cells in the lung, flow cytometric analysis was performed. To compare Th2 lymphocyte populations in each group, lung lymphocytes from individual animals were stained extracellularly for CD4 and intracellularly for IL-10 and IL-5. Numbers of CD4 positive, CD8 positive and regulatory / suppressive CD4 positive CD25 positive T cells were determined by staining with anti-CD4 mAb, anti-CD8 mAb and anti-CD25 mAb.

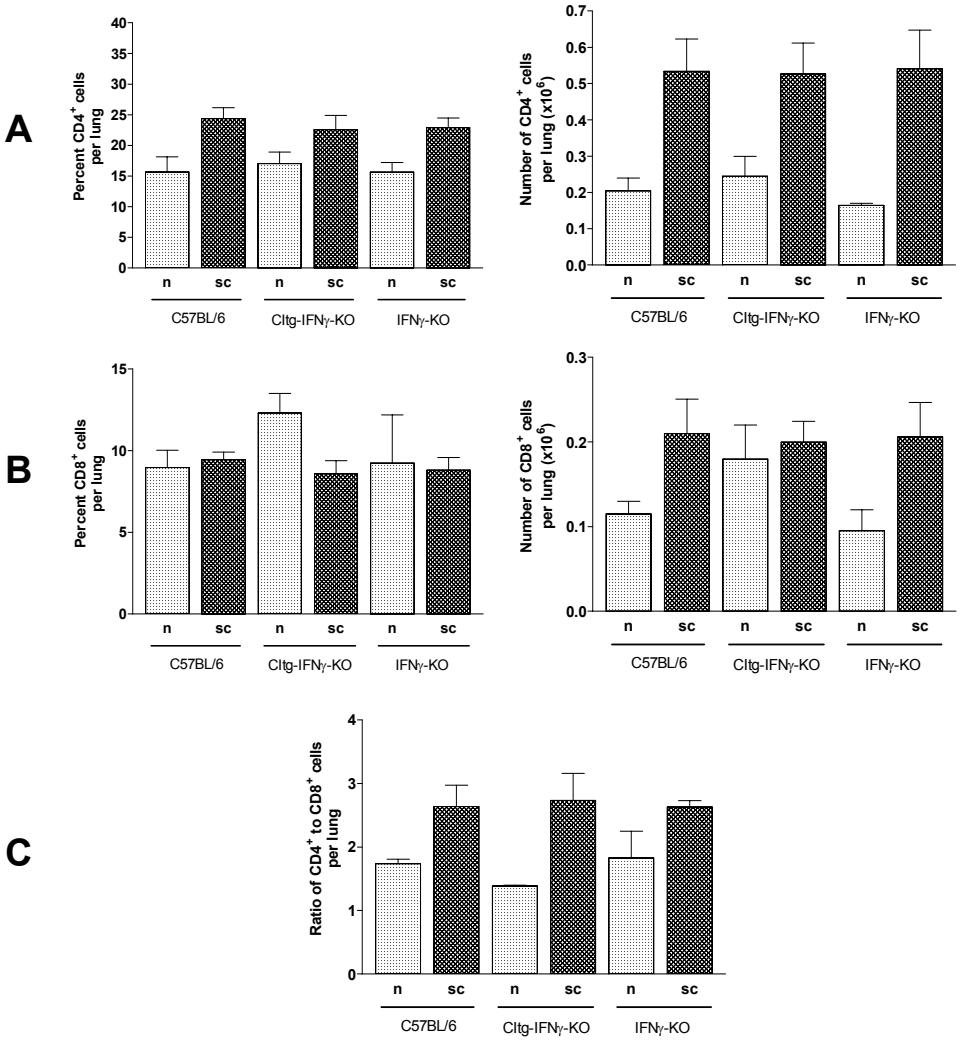

Figure 15: Frequencies and numbers of $CD4^+$ cells (A), $CD8^+$ cells (B) and ratio of $CD4^+$ to $CD8^+$ cells (C) in lungs of either naïve, or sensitized and challenged C57BL/6, CC10-IFNγ-tg-IFNγ-KO and IFNγ-KO animals determined by flow cytometric analysis as described in Methods (section 4.3.4). The arithmetic averages of at least three mice in each group are shown. Error-bars represent the standard error of the mean.

The frequency as well as the number of $CD4^+$ T cells was increased in lungs of sensitized and challenged animals as compared to those of naïve animals, indicating an ongoing inflammation (Figure 15-A). Moreover, the frequency and number of $CD8^+$ T cells was slightly higher in naïve CC10-IFNγ-tg-IFNγ-KO animals than in the other two naïve groups (Figure 15-B). Although the frequency of $CD8^+$ T cells was unchanged in sensitized and challenged mice when compared to naïve animals, the number of $CD8^+$ cells was increased. However, there was no difference in frequency and number of $CD4^+$ and $CD8^+$ cells within the three sensitized and challenged groups. Indicating that

IFNγ had no significant effect on the ratio and number of $CD4^+$ and $CD8^+$ cells during inflammation (Figure 15-C). We made the same observation with regards to the frequency and total number of $CD25^+$, IL-10^+ or IL-5^+ $CD4^+$ cells in lungs of sensitized and challenged animals (Figure 16).

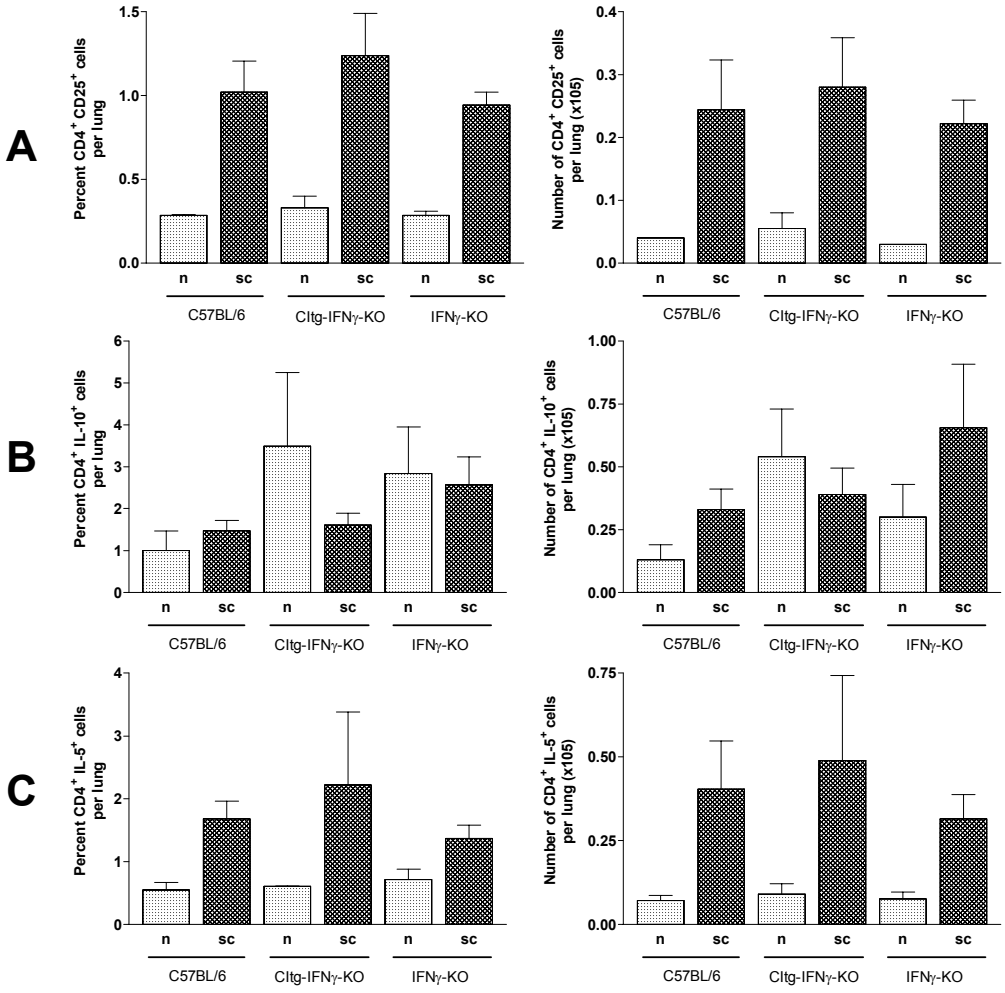

Figure 16: Frequencies and numbers of $CD4^+$ $CD25^+$ cells (A), IL-10^+ $CD4^+$ (B) and IL-5^+ $CD4^+$ positive cells (C) in lungs of either naïve, or sensitized and challenged C57BL/6, CC10-IFNγ-tg-IFNγ-KO and IFNγ-KO animals, determined by flow cytometric analysis as described in section 4.3.4. The arithmetic averages of at least three mice in each group are shown, with error-bars representing the standard error of the mean.

In accordance with our IL-10 mRNA findings, considerably higher frequencies and total numbers of IL-10^+ $CD4^+$ cells were detected in naïve CC10-IFNγ-tg-IFNγ-KO and IFNγ-KO mice in contrast to naïve C57BL/6 mice.

It is of note that in each analyzed mouse, there was no correlation between the total number or frequency of $CD25^+$ $CD4^+$ cells and percentage or number of eosinophils in BALF. Unexpectedly, this was also the case for the total number and frequency of IL-5^+ $CD4^+$ cells.

5.1.3.7 Effects of IFNγ on airway hyperresponsiveness

Airway hyperresponsiveness (AHR) is the major hallmark of human asthma and is also reflected in murine asthma. AHR is a function of an increased response to a given dose of bronchoconstrictor (hypersensitivity) and the ability to respond to a smaller dose of bronchoconstrictor (hyperactivity). In human asthma, a correlation between airway inflammation, eosinophilia and AHR is observed, although the direct mechanisms leading to AHR are yet unclear.

To study the effect of locally produced IFNγ on AHR, three animals of each group (C57BL/6, CC10-IFNγ-tg-IFNγ-KO and IFNγ-KO mice) were sensitized and challenged as described in section 4.5.3 and subjected to AHR measurement 24 hours after the last i.n. challenge. AHR measurement was performed in isolated perfused lungs as described in “Methods” (section 4.5.4). Briefly, mice were anesthetized, the trachea was cannulated and the lung was continuously perfused with fresh Krebs-Henseleit-hydroxyethyl-amylopectine buffer through the pulmonary artery while perfusate was collected from the left atrium. The lungs were negative pressure ventilated in a 37°C chamber and throughout the whole experiment chamber pressure, airflow velocity, tidal volume and arterial and venous pressure were monitored. Each experiment consisted of an initial period of baseline measurement and three treatments with increasing doses of the unspecific bronchoconstrictor methacholine,12 min apart to allow relaxation and recovery of bronchial musculature (Figure 17).

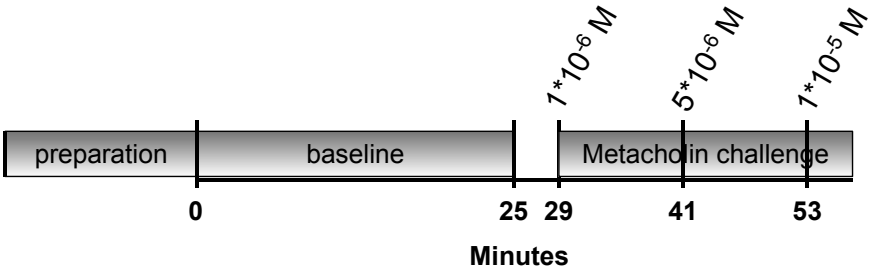

Figure 17: Protocol used for AHR measurement: During the preparation phase: mice were anesthetized, the trachea was cannulated and the lung was artificially ventilated. A cannula was placed into the left atrium, followed by insertion of an arterial cannula into the pulmonary artery through which lungs were perfused with Krebs-Henseleit-hydroxyethylamylopectine buffer in a non-recirculating manner. Finally, negative pressure ventilation was started and artificial thorax chamber, inhalation volume, airflow velocity and arterial and venous pressure were constantly monitored. After 25 min of baseline measurement, lungs were challenged with increasing does of methacholine. ($1*10^{-6}$ M, $5*10^{-6}$ M and $10*10^{-6}$ M) for one min, 12 min apart to allow the lung to recover.

From the data gathered during the baseline measurement airway resistance and dynamic compliance were calculated for each analyzed lung and to allow the comparison between lungs, the values were designated as 100% resistance or compliance for the analyzed lung. For each dose of methacholine, the resistance and compliance were calculated and put into relation to the baseline level. In this model, airway resistance reflects the reactivity of the large bronchiole and compliance reflects that of the peripheral bronchiole.

To estimate the degree of hypersensitivity induced by OVA sensitization and challenge, lungs of naïve and treated C57BL/6 animals were subjected to $1*10^{-5}$M, $5*10^{-5}$M and $1*10^{-4}$M methacholine and percent resistance was calculated from the obtained data (Figure 18). In sensitized and challenged mice, the reaction towards the lowest used dose was of such strength already, that in two out of five animals no measurement was possible due to extreme bronchoconstriction. In contrast, naïve lungs showed only a small reaction towards $1*10^{-5}$M methacholine challenge. At higher doses, none of the analyzed sensitized and challenged animals could be measured and thus no comparison was possible. These results indicate a high degree of hypersensitivity induced by OVA sensitization and challenge.

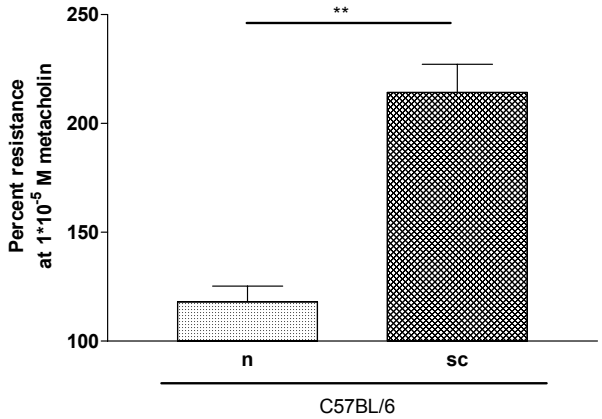

Figure 18: Percent resistance in lungs of naïve (n) and OVA sensitized and challenged (sc) C57BL/6 animals after treatment with $1*10^{-5}$ M methacholine. OVA sensitization / challenge and resistance measurement were performed as described in sections 4.5.3 and 4.5.4, respectively and in Figure 17. Resistance and compliance were calculated for each lung relative to that of baseline measurements without methacholine challenge. Arithmetic averages of at least three lungs of each group are shown, with error-bars representing the standard error of the mean. Significance of differences between means were calculated using ranks and Student-Newman-Keuls post-hoc test. Significances between means are indicated with asterisks (** represents P=0.001-0.01). Data for the sensitized and challenged group do not completely reflect the degree of hypersensitivity in this group, because extreme bronchoconstriction in two out of five animals prevented their measurement and thus only the data obtained for three animals are depicted.

To compare the degree of hyperactivity between sensitized and challenged C57BL/6, CC10-IFNγ-tg-IFNγ-KO and IFNγ-KO mice, lungs of five animals in each group were subjected to increasing doses of methacholine by the previously described protocol (Figure 19).

All animals reacted to doses as low as $1*10^{-6}$ M, indicating AHR in all three groups. Surprisingly, after challenge with $1*10^{-6}$ M methacholine, resistance was significantly lower and compliance significantly higher in CC10-IFNγ-tg-IFNγ-KO than in C57BL/6 and IFNγ-KO, indicating a lower AHR in these animals. At doses of $5*10^{-6}$ M methacholine this difference was similar although not significant any more. Due to extreme bronchoconstriction in most of the lungs of all three groups no measurement was possible at doses of $1*10^{-5}$ M methacholine. However, the less pronounced AHR in CC10-IFNγ-tg-IFNγ-KO indicates a positive effect of IFNγ on the lung-function in these animals, despite the higher numbers of eosinophils and the high levels of IL-5 and IL-13 mRNA. Nevertheless, local IFNγ expression in the lung was not able to completely abolish AHR.

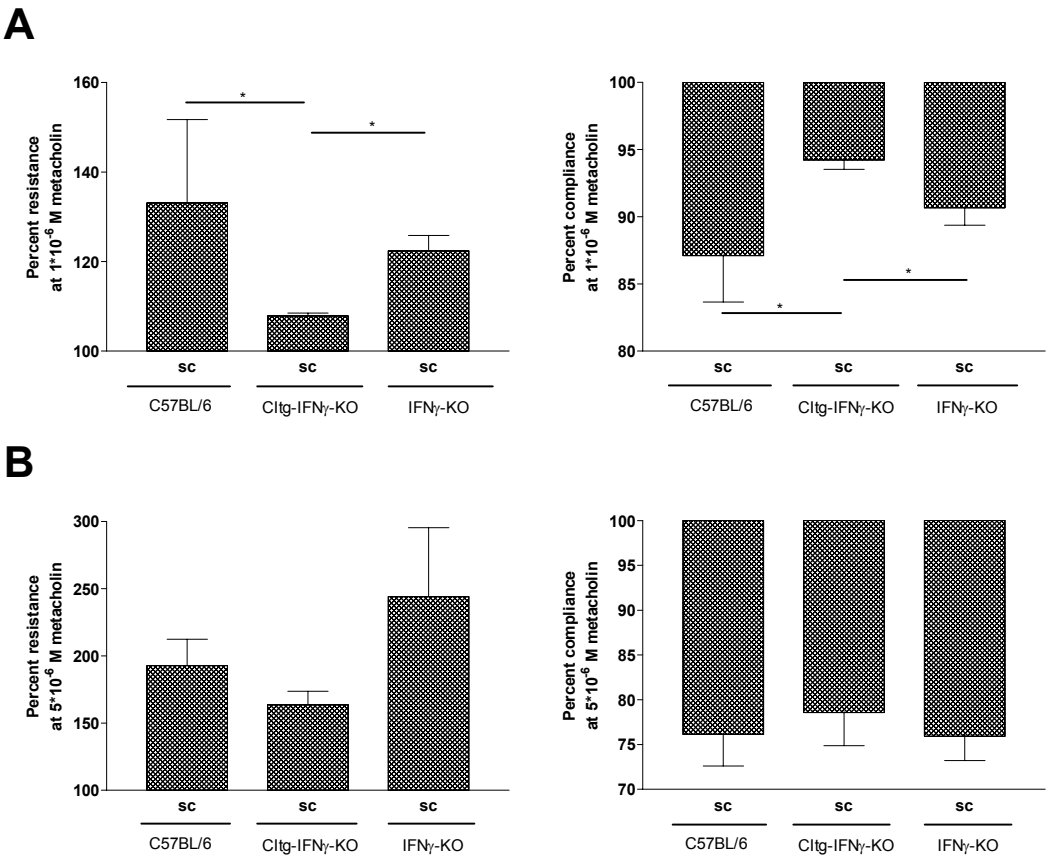

Figure 19: Resistance and compliance of lungs of sensitized and challenged (sc) C57BL/6, CC10-IFNγ-tg-IFNγ-KO and IFNγ-KO animals after treatment with $1*10^{-6}$M (A) or $5*10^{-6}$M (B) methacholine. OVA sensitization / challenge, compliance and resistance measurement were performed as described in sections 4.5.3 and 4.5.4, respectively and in Figure 17. Resistance and compliance were calculated for each lung relative to that of baseline measurements without methacholine challenge. Arithmetic averages of five animals in each group are shown, with error-bars representing the standard error of the mean. Significance of differences between means were calculated using ranks and Student-Newman-Keuls post-hoc test and significant differences are indicated by asterisks (* representing P = 0.05-0.01).

5.1.3.8 Effects of IFNγ on the transcriptome in lungs of sensitized and challenged animals

To further study the underlying mechanisms that led to increased eosinophilia, increased levels of IL-5, IL-13 and eotaxin-1 but lower AHR in CC10-IFNγ-tg-IFNγ-KO, RNA microarray analysis of sensitized and challenged versus only sensitized animals was performed. RNA was isolated from lungs of five animals of each group and was pooled with that of other animals of the same group. The RNA pools of sensitized or sensitized and challenged animals were labeled with Cy5 or Cy3, respectively and

hybridized to Agilent custom made microarrays, that contained oligonucleotide probes representing 8013 different genetic elements probably involved in immunologic processes. To exclude labeling effects and to minimize errors, the hybridization was repeated on a second array, but with swapped labeling colors. After measurement of spot-color and intensity on both arrays, data were analyzed using the Rosetta Inpharmatics Resolver software. Significantly up- and downregulated genes were selected for each group of animals by correlating the ratio between the two colors of each measured probe from one array with the ratio of the same probe in the colorswaped second array (Figure 20). Only anticorrelated genes were considered to be differentially regulated upon induction of asthma. For instance those genes that were Cy5 positive in the first and Cy3 positive with a similar intensity in the second array. The Resolver software calculates a probability value from a variety of internal controls, including the degree of anticorrelation for each measured ratio. This P value reflects the reliability of the measured data in the same way as P values for significances do.

In C57BL/6 animals 14.1% (231) of all measured mRNAs with P values smaller than 0.05 were expressed two fold less or higher in sensitized / challenged versus only sensitized lungs. In CC10-IFNγ-tg-IFNγ-KO and

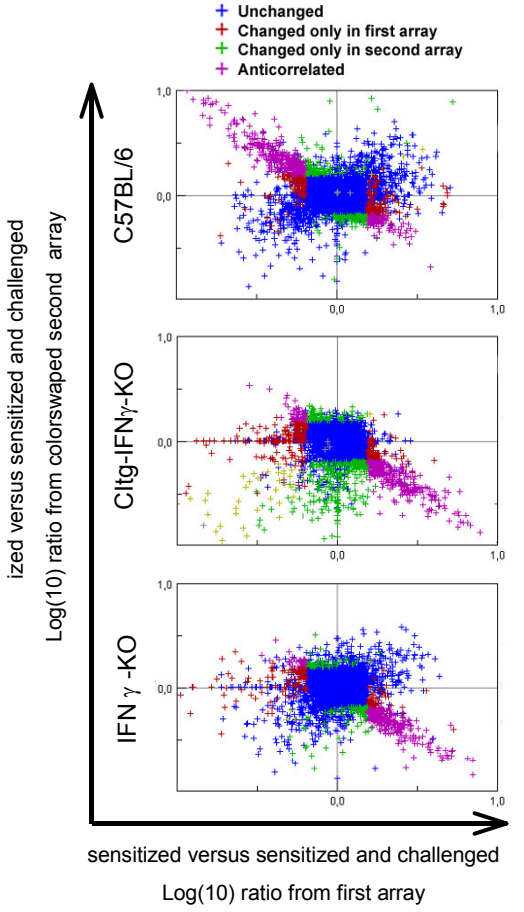

Figure 20: Correlation blots of Log(10) ratios deducted from two independent hybridizations of Cy5 and Cy3 labeled RNA isolated from lungs of only sensitized versus sensitized and challenged animals of each group. To exclude labeling effects and to reduce error, the second hybridization was performed using the same but reverse labeled RNA pools. Significantly different ratios were anticorrelating between the two hybridizations and are depicted in purple. Ratios depicted in blue were unchanged between both hybridizations and red or green ratios were only present in one of the two hybridizations.

IFNγ-KO animals we observed significant up- or downregulation upon challenge of 12.4% (190) and 10.6% (150) of the mRNAs respectively. Surprisingly, of all mRNAs derived from known genes (not ESTs), arginase-1 was the most upregulated gene in all three groups. However all three groups of mice had almost similar arginase-1 levels. Also highly upregulated in all groups, but with a 30% higher expression in CC10-IFNγ-tg-IFNγ-KO mice, was the tissue inhibitor of metalloproteinase-1 (TIMP-1). One of the corresponding targets of TIMP-1, the matrix metalloproteinase (MMP) 12, but not MMP-9, was also found to be upregulated in all three groups, although ca. 20% less in CC10-IFNγ-tg-IFNγ-KO mice compared to C57BL/6 and IFNγ-KO mice. Corresponding to the real-time RT-PCR data mRNA levels for IL-13, IL-5 and eotaxin-1 were significantly upregulated in all sensitized and challenged animals while IFNγ was only upregulated in C57BL/6 animals. However, in contrast to the real-time RT-PCR data the upregulation was only small and major differences between the groups were not detected.

Interestingly, most mRNAs found to be up- or downregulated upon challenge, were similarly regulated in all three groups, with the exception of genes, known to be induced by IFNγ (e.g. MIG, TGTP, IGTP), which were not regulated in IFNγ-KO and CC10-IFNγ-tg-IFNγ-KO animals. However, the degree of regulation was slightly different between the three groups: The correlation coefficients representing the amount of linear correlation of all reliably measured data between two groups, were 0.98 between C57BL/6 and IFNγ-KO mice, but 0.95 between CC10-IFNγ-tg-IFNγ-KO and C57BL/6 or IFNγ-KO mice. The difference indicates a modified response to challenge in lung-specific IFNγ expressing IFNγ-KO animals compared to C57BL/6 or IFNγ-KO animals. However, the general responses of all groups were similar, as indicated by the high correlation coefficients between all groups.

To identify genes that might be responsible for the observed differences of AHR between the three groups, we analyzed the data to find genes that were up- or downregulated, with differences between the groups comparative to the results obtained for AHR: C57BL/6 ≥ IFNγ-KO > CC10-IFNγ-tg-IFNγ-KO.

Interestingly, only 16 genes with P values smaller than 0.05 showed such a trend (Table 1). If all genes with P values smaller than 0.1 were taken into account, their number increased to 327. However, for most genes the differences were very small and most of these genes have not been specifically implicated in regulation of AHR or allergic inflammation. Moreover, most of the genes that were found to be regulated strongly different in lungs of challenged CC10-IFNγ-tg-IFNγ-KO compared to C57BL/6 and IFNγ-KO mice were ESTs (Table 2).

Fold difference between mRNA levels of sensitized versus sensitized and challenged mice			**Sequence name**	**NCBI Accession number**
C57BL/6	**IFNγ-KO**	**CItg-IFNγ-KO**		
1,95	2,34	2,64	Nfil3	NM_017373
1,90	1,91	2,48	Pdgfc	NM_019971
1,92	2,00	2,47	Pira6	NM_011093
1,52	2,24	2,46	F5	NM_007976
1,98	2,02	2,35	Pira5	U96686
1,35	1,50	2,30	Itgb2l	NM_008405
1,29	1,51	2,28	Spi2-rs1	NM_009253
1,30	1,35	2,27	AI464431	AI464431
1,70	1,82	2,23	BE851953	BE851953
1,37	1,44	2,06	BE630688	BE630688
-2,05	1,05	1,21	Fshr	NM_013523
-2,27	-1,16	1,02	AI550301	AI550301
-2,10	-1,34	-1,05	NM_029813	NM_029813
-2,04	-1,26	-1,21	AV002728	AV002728
-2,63	-2,57	-1,21	Slc7a11	NM_011990
-2,16	-1,81	-1,45	AI849305	AI849305
-2,05	-1,75	-1,59	Pgrmc	NM_016783

Table 1: Genes that were up- or downregulated upon challenge, with differences between the groups comparative to the results obtained for AHR. Shown genes were up- or downregulated in C57BL/6 mice less or equal than in IFNγ-KO and less than in CC10-IFNγ-tg-IFNγ-KO mice. Data were obtained by microarray analysis as described in section 4.1.13. Depicted are fold differences between only sensitized and sensitized / challenged animals of each group, name of the gene and NCBI accession number. Only genes with P values smaller than 0.05 are shown.

Fold difference between mRNA levels of sensitized versus sensitized and challenged mice			Sequence name	NCBI Accession number
C57BL/6	IFNγ-KO	CItg-IFNγ-KO		
12,81	11,9	5,31	AV373372	AV373372
1,15	-1,06	-4,39	AV373559	AV373559
2,69	1,33	5,23	AI875606	AI875606
-1,15	-2,61	3,34	AV373244	AV373244
-1,49	-1,80	2,95	AI666358	AI666358
3,34	1,88	-2,32	AV045376	AV045376
-2,89	-4,05	1,21	AV080959	AV080959
-1,23	-1,18	2,25	AV366460	AV366460
-1,32	-1,33	2,00	AI662100	AI662100
-1,62	-1,23	2,05	BE691458	BE691458
1,82	1,99	2,94	BE994964	BE994964
1,58	1,23	2,51	AW824687	AW824687
1,30	1,35	2,27	AI464431	AI464431
2,63	1,78	3,54	BE457883	BE457883

Table 2: Messenger-RNAs which show the strongest difference of up- or downregulation in CC10-IFNγ-tg-IFNγ-KO mice compared to C57BL/6 and IFNγ-KO mice. These are all ESTs of unknown function. Data were obtained by microarray analysis as described in section 4.1.13. Depicted are fold differences between only sensitized and sensitized / challenged animals of each group, name of the gene and NCBI accession number. Only genes with P values smaller than 0.05 are shown.

It is possible that genes, which are involved in the development of AHR and that must be differentially expressed in CC10-IFNγ-tg-IFNγ-KO mice compared to C57BL/6 and IFNγ-KO mice, were not up- or downregulated upon challenge, but were constitutively expressed or suppressed in CC10-IFNγ-tg-IFNγ-KO mice. To identify these genes, mRNA from sensitized and challenged lungs of IFNγ-KO was hybridized against lung mRNA from equally treated CC10-IFNγ-tg-IFNγ-KO animals.

Surprisingly, only 6.9% (63) of all reliably measured mRNAs were differentially expressed in lungs of challenged CC10-IFNγ-tg-IFNγ-KO mice compared to IFNγ-KO mice. Among these were 35 ESTs and several genes known to be induced by IFNγ (e.g. IGTP, IIGP, TGTP, Mag2), but also TIMP-1, CXCL13 and IL-18 binding protein, which were all upregulated in CC10-IFNγ-tg-IFNγ-KO mice. However, the differences were small and none of the other genes could be assigned to modification of lung-function or inflammation.

In conclusion, within the examined selection of genes, that were present on the microarray, we detected only very few genes that may be involved in the development of AHR and airway inflammation and that were differentially regulated between CC10-IFNγ-tg-IFNγ-KO mice and C57BL/6 or IFNγ-KO mice. Moreover, for none of these genes the difference between CC10-IFNγ-tg-IFNγ-KO mice and C57BL/6 or IFNγ-KO mice was large enough to explain the observed differences of AHR and airway inflammation of CC10-IFNγ-tg-IFNγ-KO mice. The lack of strongly different regulated genes could either be due to the lack of such genes within the examined subpopulation of the transcriptome or the large number of subtle differences observed was causing the described effects.

5.2 Transgenic mice with tissue-specific expression of IFNγ

5.2.1 Generation of transgenic mice with tissue-specific, constitutive IFNγ expression in the gut

To study the effects of locally expressed IFNγ on the physiologic homeostasis of intestinal immunity, chronic inflammatory processes and infection, we aimed to generate mice carrying a transgene composed of a gut-specific promoter and IFNγ cDNA. To be able to analyze the effects of IFNγ only expressed in this strictly defined region, the IFNγ expressing constructs were introduced into IFNγ-KO animals, making the transgene the only source of IFNγ in these animals. The use of wild-type mice would not enable this analysis because of the spatially unrestricted and inconsistent expression of endogenous IFNγ, which largely depends on the immune status of the animal.

5.2.1.1 The transgene cassettes

The constant renewal of the epithelium of the intestinal mucosa is a major difficulty when targeting IFNγ expression to the intestine. To ensure sufficient expression of IFNγ, three transgene cassettes with different promoters were constructed, each promoter normally activated in a different cell type. Although not previously used to generate transgenic animals, the Intestinal Trefoil Factor (ITF) promoter was chosen because of its highly restricted expression in goblet cells of the small and large intestine (Suemori et al., 1991). A 1.8kb region upstream of the rat ITF gene was used to construct the transgene cassette because *in vitro* studies had shown that this region is sufficient to express a transgene only in goblet like cells (Sands et al., 1995). The endogenous villin promoter is active in epithelial cells that develop a brush border, like those embedded in the villi of the large and small intestine but also in the kidney (Boller et al., 1988; Robine et al., 1985). Using a transgenic mouse model, Pinto and colleges showed that the DNA sequence 9kb upstream of the villin coding sequence is able to direct expression of a

transgene to all proliferating epithelial cells along the crypt villus axis, throughout the small and large intestine, but also at a low level in the kidney (Pinto et al., 1999). This 9kb promoter sequence was kindly provided to us by the authors. The third promoter used, the liver fatty acid binding protein promoter (lfabp), has been extensively studied in various transgenic animals (Kim et al., 1993; Saam and Gordon, 1999; Simon et al., 1997; Simon et al., 1993). While the complete promoter is active in the liver, Gordon and colleagues showed that a short form of it, consisting of nucleotides –596 to +21, is specifically active in proliferating and non-proliferating epithelial cells, Paneth cells and goblet cells along the crypt villus axis in all areas of the small intestine.

To construct the three transgene cassettes, IFNγ cDNA was isolated by RT-PCR from C57BL/6 spleen cDNA and cloned into the sequencing vector pCR-Scrip-Amp. After verification of the inserted IFNγ sequence, this plasmid was used as the template for further PCRs with primers containing restriction sites for further cloning. All restriction sites added during further PCR amplifications were immediately upstream of the start codon or downstream of the stop codon, to exclude any influence of non-coding IFNγ cDNA on expression. The villin-IFNγ-BGHpA cassette was constructed by amplifying the IFNγ cDNA with primers containing an AatII restriction site upstream and a NotI restriction site downstream of the coding sequence. The resulting PCR product was digested appropriately and cloned into the vector p9kb-aatII, which contained the 9kb villin promoter fragment upstream of an AatII site. After verifying the amplified IFNγ cDNA sequence, the villin promoter together with the IFNγ cDNA was cloned into the vector pcDNA3.1-Zeo-ΔCMV using the KpnI and NotI restriction sites. The vector pcDNA3.1-Zeo-ΔCMV is based on the plasmid pcDNA3.1-Zeo, but lacks the CMV promoter. It contains a bovine growth hormone polyadenylation (BGHpA) signal sequence downstream of a multicloning site and it additionally harbors a Zeocin resistance cassette. The pcDNA3.1-Zeo-ΔCMV backbone was also used to construct the ITF-IFNγ-BGHpA cassette. For the latter, the IFNγ cDNA was amplified using primers containing XhoI and ApaI restriction sites.

The PCR product was inserted into the pcDNA3.1-Zeo-ΔCMV vector by restriction digest with XhoI and ApaI and subsequent ligation with equally digested vector. The ITF promoter was inserted using the EcoRI and XhoI restriction sites adjacent to the ITF promoter sequence and still present in multicloning site of the vector, 5´ of the IFNγ sequence. The final construct pcDNA3.1-Zeo-ΔCMV-ITF-IFNγ was verified by sequencing.

The lfabp-IFNγ-BGHpA cassette was constructed by introducing PCR amplified IFNγ cDNA, containing XhoI and ApaI restriction sites, into the complete pcDNA3.1-Zeo vector, yielding a positive control vector for transfection studies, due to the CMV promoter in front of the IFNγ sequence (pcDNA3.1-Zeo-CMV-IFNγ-BGHpA). To introduce the lfabp promoter and delete the CMV promoter, the lfabp promoter sequence was PCR amplified using primers that introduced a BamHI restriction site upstream and a NotI restriction site downstream of the promoter sequence. The resulting PCR product was cloned into the IFNγ containing pcDNA3.1-Zeo vector using the appropriate restriction enzymes, leading to the replacement of the CMV promoter with the lfabp promoter. Before further use, the whole sequence of the transgene cassette was verified.

5.2.1.2 *In vitro* testing of the transgene cassettes

Prior to the generation of transgenic animals, all three constructs were tested *in vitro* by stable transfection of CaCo2 cells. This cell line has multiple properties of small intestinal enterocytes (Rousset, 1986), which might lead to activity of the promoters. After transfection and subsequent selection for Zeocin resistance, multiple transgenic single cell clones were expanded from each transfection. $5*10^6$ cells generated from each clone were cultured for three days, before supernatants were collected and analyzed by ELISA for IFNγ. Low amounts of IFNγ were detectable in supernatants of only few transgenic clones. However, all cassettes lead to at least one clone with IFNγ expression, demonstrating the functionality of all three transgene cassettes (Table 3).

CaCo2 cells transfected with:	Clone #	IFNγ (U/ml)
pcDNA3.1-Zeo-ΔCMV-lfabp-IFNγ	A01	12 +/- 4
	A02	<4
	B04	<4
	C03	10 +/- 3
pcDNA3.1-Zeo-ΔCMV-ITF-IFNγ	A05	<4
	D05	<4
	D06	<4
	E08	14 +/- 4
pcDNA3.1-Zeo-ΔCMV-villin-IFNγ	A10	<4
	A12	<4
	B09	16 +/- 6
pcDNA3.1-Zeo-IFNγ	A04	50 +/- 9
	A09	70 +/- 6
pcDNA3.1-Zeo-null	E01	<4
	E03	<4

Table 3: IFNγ in supernatants from stably transfected CaCo2 cells. CaCo2 cells were transfected with the different transgene cassettes and positive and negative control vectors, subsequently selected for Zeomycin resistance and single resistant cells were expanded. For IFNγ expression analysis $5*10^6$ cells from each clone were plated on $25cm^2$ dishes in triplicates and after 72 hours supernatants were analyzed by ELISA. The intermediate construct pcDNA3.1-Zeo-IFNγ with IFNγ under the control of the CMV promoter was used as a positive control and the empty backbone pcDNA3.1-Zeo-null as a negative control. Values are IFNγ U/ml and +/- values indicate the standard deviation between triplicate assays.

5.2.1.3 Generation of ITF- and lfabp-IFNγ transgenic mice

Since all constructs showed functional activity *in vitro* we used all of them to generate transgenic animals. Each transgene cassette was excised from the backbone by restriction digest and purified on ethidum bromide free agarose gels. The linearized cassettes were microinjected into the male pronucleus of eggs from IFNγ-KO female mice fertilized by IFNγ-KO males. One day after microinjection, viable 2-cell embryos were reimplanted into oviducts of pseudopregnant CD1 foster mothers and resulting cubs were analyzed by Southern blot and PCR genotyping for transgene integration. After 31 rounds of microinjection and analysis of 347 live born cubs, we obtained only one ITF-IFNγ-BGHpA transgenic female and three lfabp-IFNγ-BGHpA transgenic male founder animals (named tgII#4, tgLI#23 and tgLI#31) (e.g. Figure 21). Despite many attempts, we were not successful in generating villin-IFNγ-BGHpA transgenic animals. Moreover, the ITF-IFNγ-BGHpA transgenic

female did not transmit the transgene to its offspring when mated with IFNγ-KO or C57BL/6 males. Therefore, no mouse line could be generated from this animal. However, each of the three lfabp-IFNγ-BGHpA transgenic male founders produced at least four transgenic offspring when mated with IFNγ-KO females, even though the tgLI#4 and tgLI#31 did not transmit the transgene according to the Mendelian rule. It is likely that the transgene in these founder animals had integrated in a mosaic pattern, i.e. less than half of the sperm carried the transgene. This is not surprising, because according to Hogan and colleagues 20% of founder animals carry the transgene in a mosaic pattern and therefore transmit the transgene at a frequency of only 5-10% (Hogan et al., 1986). All F1-animals originating from founders tgLI#23 and tgLI#31 transmitted the transgene according to the Mendelian rule in all further generations, while tgLI#4 animals did not. Nevertheless, mice originating from each founder were bred separately with IFNγ-KO animals for at least three generations, leading to three lfabp-IFNγ-BGHpA transgenic mouse lines (tgLI#4, tgLI#23 and tgLI#31).

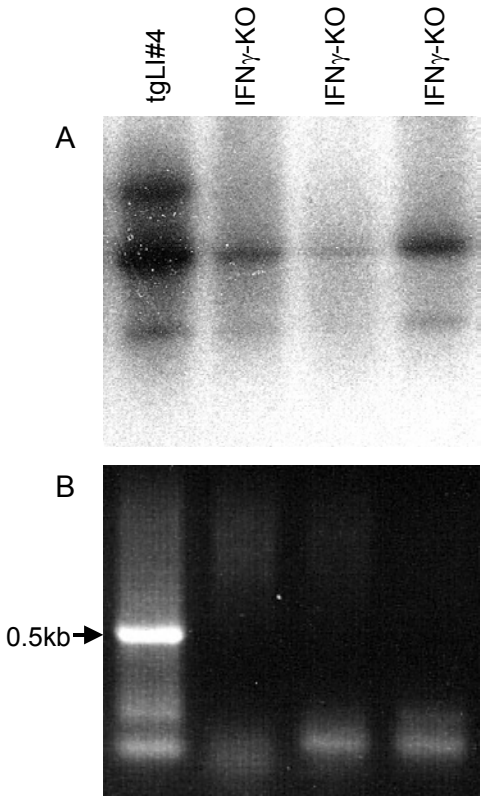

Figure 21: (A) Southern blot analysis of potential lfabp-IFNγ-BGHpA transgenic (tgLI) founder animals using an IFNγ cDNA probe. (B) Genotype PCR analysis of the same animals using a transgene-specific primer pair (lfabp-forward and IFNγ-exon-3-reverse).

5.2.1.4 Verification of the endogenous IFNγ genotype

Prior to the phenotypic characterization of the three lfabp-IFNγ-BGHpA (tgLI) lines, animals were tested for the presence of two targeted alleles of the IFNγ-locus. A genotyping PCR was designed that amplified the transgenic IFNγ gene and the endogenous IFNγ gene (Figure 22-A). Since the transgenic IFNγ gene lacks the introns, it can be distinguished from the endogenous IFNγ gene by size difference. Together with a second PCR, using primers specific for the neomycin resistance cassette and the adjacent IFNγ sequence of the targeted IFNγ-locus (Figure 22-B), we were able to differentiate between all possible genotypes regarding IFNγ. Moreover, the analysis confirmed the endogenous IFNγ-KO genotype of all animals from the three initial transgenic lines. This PCR analysis was also used in all further generations and when animals from the tgLI#4 line were crossed to C57BL/6 or CD1 background.

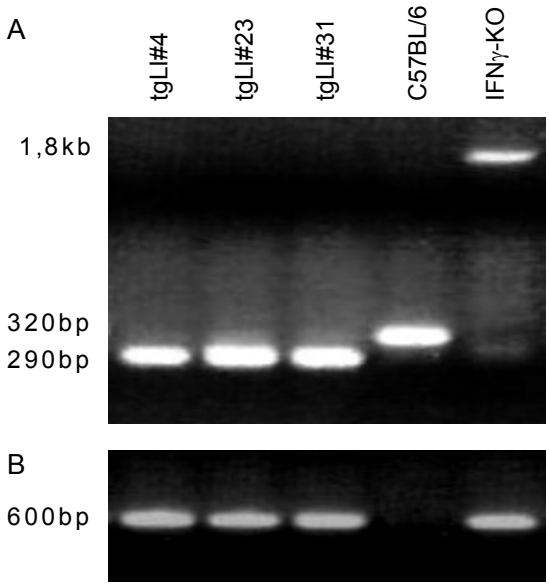

Figure 22: PCR detection of transgenic and endogenous IFNγ (A) or neomycin-resistance-gene integration into the IFNγ-locus (B). PCR results for the three tgLI lines, a C57BL/6 and a IFNγ-KO animal are shown. To amplify transgenic or endogenous IFNγ, primers specific for exon-2 and exon-3 of the IFNγ gene were used. The presence of a neomycin-resistance cassette in the end of exon-2 of the endogenous IFNγ gene was verified using primers specific for the end of the neomycin-resistance gene and exon-3 of IFNγ.

5.2.2 Analysis of the lfabp-IFNγ transgenic mouse lines

5.2.2.1 Analysis of IFNγ expression in the lfabp-IFNγ-BGHpA transgenic mouse lines tgLI#23, tgLI#31 and tgLI#4

To investigate whether the transgenic IFNγ is expressed in the small intestine of the tgLI animals we performed conventional semi quantitative RT-PCR. Therefore, RNA was isolated from spleen, liver, duodenum, ileum and proximal colon of C57BL/6 mice and IFNγ-KO mice and from animals of each tgLI line. RNA was reverse transcribed to cDNA and PCR was performed with primers specific for IFNγ and β–actin. Non reverse transcribed RNA was used as control for genomic DNA contamination.

IFNγ mRNA was only detected in duodenum, ileum and proximal colon of tgLI#4 animals and in spleen, duodenum, ileum and proximal colon of C57BL/6 animals (Figure 23). However, in all 10-week old tgLI#4 animals analyzed, IFNγ expression levels in small intestine and colon were only

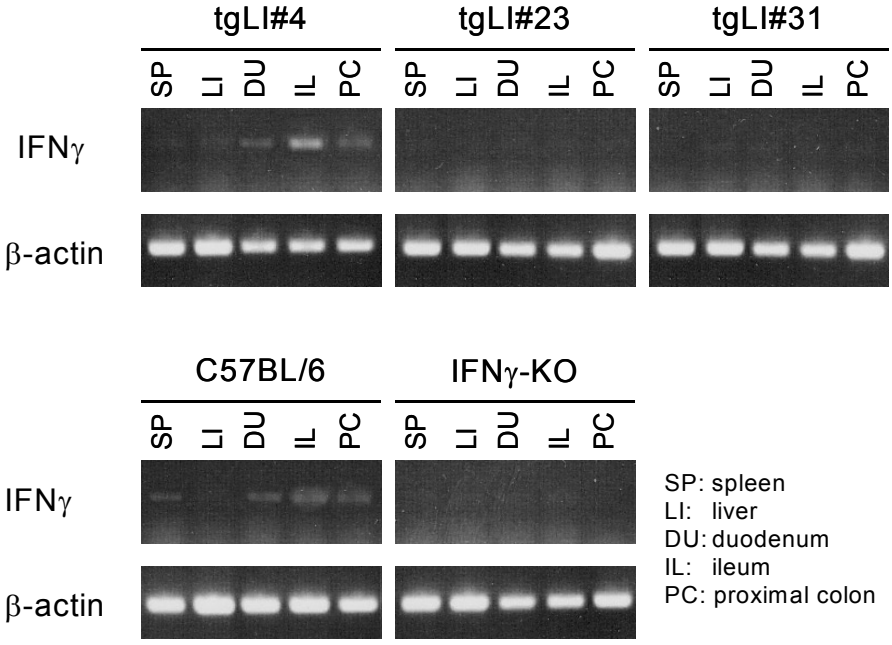

Figure 23: IFNγ and β-actin RT-PCRs of RNA isolated from different tissues of 10-week old tgLI#4, tgLI#23, tgLI#31, C57BL/6 and IFNγ-KO mice. The cDNA in each sample was derived from total cellular RNA by reverse transcription and was diluted to the approximately same concentration of β-actin cDNA, which is considered to be equally expressed in all samples. PCRs were negative in all samples when non-reverse transcribed RNA was used as PCR template. One representative experiment of three is shown.

slightly higher than IFNγ levels in naïve C57BL/6 animals. IFNγ expression was not detected in any tissue of tgLI#23, tgLI#31 and IFNγ-KO animals.

To analyze whether the IFNγ-mRNA produced from the transgene was translated into protein, ileum from 10-week old tgLI#4, IFNγ-KO and C57BL/6 mice was harvested, frozen, sectioned and stained with anti-IFNγ mAb. Surprisingly, we observed no difference between sections from tgLI#4 and IFNγ-KO, and neither between sections from IFNγ-KO and C57BL/6 mice (data not shown). The latter indicated that IFNγ expression levels in naïve C57BL/6 and tgLI#4 animals were below the detection limit of this assay.

In the tgLI#4 line, IFNγ is supposed to be expressed by villus epithelial cells in the small intestine. Therefore, intestinal epithelial cells (IEC) were isolated from tgLI#4, C57BL/6 and IFNγ-KO mice and used for direct western blotting or cultivation *in vitro* for 48 hours prior to IFNγ ELISA of their supernatants. IFNγ protein could not be detected in protein extracts from IEC by anti-IFNγ western blotting or IEC culture supernatants using anti-IFNγ ELISA. Since the amount of IFNγ protein was too low to be detected by western blotting, we used dot blot analysis, which enabled us to analyze the whole supernatant from cultured IEC and therefore enrich the amount of IFNγ protein on the blot membrane. Using this method we were able to detected IFNγ protein in the IEC supernatants of tgLI#4 and C57BL/6 mice (Figure 24). However, the amount of IFNγ protein in these two supernatants was only slightly above the detection limit.

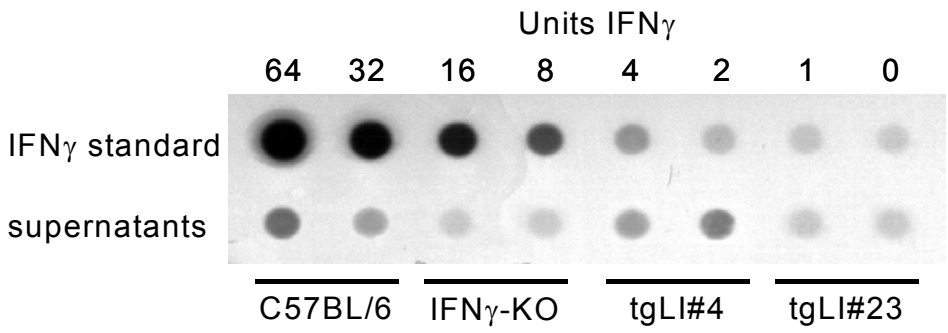

Figure 24: IFNγ dot blot analysis of supernatants from IEC cultures. IEC were isolated and $2x10^6$ cells were incubated for 48 hours in 500µl medium. Supernatants were sucked through nitrocellulose membrane and IFNγ bound to the membrane was detected by anti-IFNγ mAb. Duplicates represent supernatants from two IEC cultures of the same animal.

Since IEC from C57BL/6 mice do not produce any IFNγ, it is likely that the detected IFNγ-protein in these supernatants was produced by contaminating intraepithelial lymphocytes (IEL) and lamina propria lymphocytes (LPL). However, IEL and LPL from tgLI#4 mice do not have this capacity, indicating that the transgenic IFNγ mRNA was translated into protein.

To examine whether this IFNγ protein was functional, semi quantitative RT-PCR was performed to estimate the expression level of the IFNγ inducible protein 10 (IP-10/CXCL10). While IP-10 mRNA was not detectable in duodenum, ileum and proximal colon of tgLI#23 and IFNγ-KO mice, low amounts of IP-10 mRNA were observed in these tissues of tgLI#4 mice and C57BL/6 mice (Figure 25). Although IP-10 mRNA levels in the intestine of tgLI#4 animals were similar to those in C57BL/6 animals, the detection of IP-10 indicated the expression of functional transgenic IFNγ throughout the whole intestine of tgLI#4 mice.

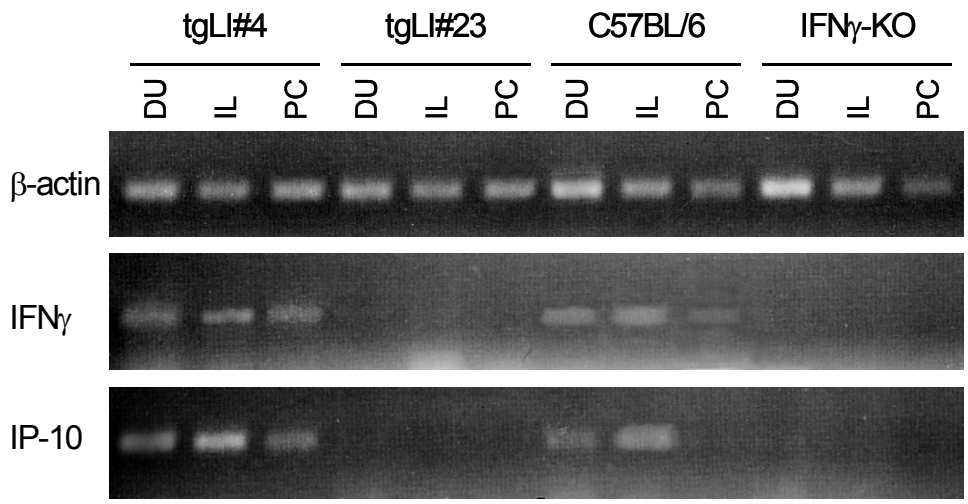

Figure 25: IP-10, IFNγ and β-actin RT-PCRs of RNA isolated from the duodenum (DU), ileum (IL) and proximal colon (PC) of 10-week old tgLI#4, tgLI#23, C57BL/6 and IFNγ-KO mice. The cDNA in each sample was derived from total cellular RNA by reverse transcription and was diluted to the approximately same concentration of β-actin cDNA, which is considered to be equally expressed in all samples. One representative experiment of two is shown.

To confirm the lack of IFNγ expression in animals from the transgenic lines tgLI#23 and tgLI#31, multiple animals from different generations and of different age were repeatedly analyzed for transgene expression. While all animals from line tgLI#31 were negative, more sensitive real-time RT-PCR analysis revealed that animals from line tgLI#23 did express very low levels of IFNγ (data not shown). However, further analysis of tgLI#23 mice by flow cytometric analysis of IEL and LPL composition and oral *Salmonella typhimurium* infection did not reveal significant differences between IFNγ-KO animals and tgLI#23 animals (data not shown).

5.2.2.2 Characterization of the Ifabp-IFNγ-BGHpA transgenic mouse line tgLI#4

As indicated above, the transmission of the transgene in the tgLI#4 line did not obey the Mendelian rule. On average, we got one transgenic mouse out of eight offspring rather than one out of two as expected when crossing heterozygous tgLI#4 animals to IFNγ-KO or C57BL/6 animals. Moreover, we got one out of seven rather than three out of four, when crossing two heterozygous animals (data not shown). In fact, only two homozygous transgenic animals were obtained throughout two years of breeding. The unexpectedly low transgene transmission in the tgLI#4 line lead to the problem that only very few animals of this line were available for analysis. Thus, experiments like infection studies, requiring many animals of at least similar age were impossible and most analyses had to be performed using those animals that were too old for breeding. However, in contrast to animals from the tgLI#23 and tgLI#31 lines, animals from the tgLI#4 line showed multiple phenotypic differences compared to non-transgenic littermates, IFNγ-KO and C57BL/6 animals.

5.2.2.2.1 Lower weight of tgLI#4 mice compared to IFNγ-KO and C57BL/6 mice

In addition to the unusual low rate of transgene transmission, heterozygous transgenic animals were noted to be approximately 30% lighter in weight and smaller in size than IFNγ-KO and C57BL/6 animals of the same age, while the size of non-transgenic littermates was consistently comparable to IFNγ-KO animals (Figure 26). Moreover, the two homozygous tgLI#4 animals were extremely small compared to non-transgenic littermates (Figure 27). Interestingly, one of them died five weeks after birth. The average life span of heterozygous tgLI#4 animals could also not be determined. Since the number of transgenic animals that were obtained was limited, we were forced to use all available animals for further analyses before their natural death.

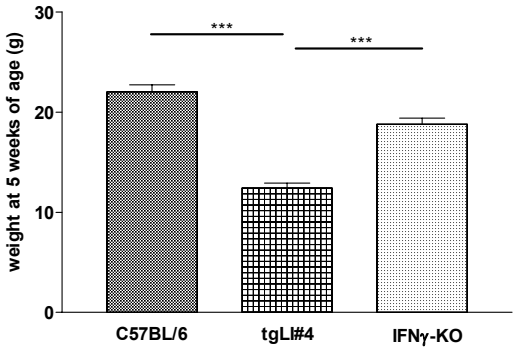

Figure 26: Average weight of tgLI#4 animals at five weeks of age compared to that of non-transgenic littermates (IFNγ-KO) and C57BL/6 animals. Arithmetic averages of five animals are shown. Error-bars indicate standard deviation and asterisks indicate significant differences between means, calculated with an unpaired t-test. (*** represents P<0.001)

Figure 27: Pictures of a 6-week old homozygous tgLI#4 female mouse (on the right and bottom respectively) together with a non-transgenic littermate.

5.2.2.2.2 Excessive water consumption and presence of erythrocytes within the urine of tgLI#4 mice

Overnight single housing in metabolism cages showed that tgLI#4 animals consumed five times more water than age and sex matched C57BL/6 and IFNγ-KO animals (Figure 28). Roche Combur urine test strips, although designed for humans, revealed that in contrast to age matched C57BL/6 and IFNγ-KO animals, all of the five analyzed 4-6 month old tgLI#4 animals had ca. 50-200 erythrocytes per milliliter in their urine and a slightly lower urine pH (pH 5 instead of pH 6; data not shown). However, no difference in numbers of leukocytes (ca. 10-25 per ml) and similar levels of glucose (less than 2.2 mM), acetone (less than 7 mM), bilirubin (less than 9 µM), protein (ca. 300 mg/l) and nitrit (less than 11 µM) were observed in the urine of all three groups (data not shown).

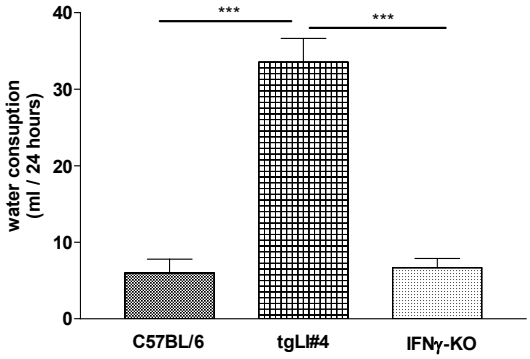

Figure 28: Water consumption of 5-month old tgLI#4, C57BL/6 and IFNγ-KO mice per day and animal. Mice were kept separate in metabolism cages for 48 hours and water consumption was determined after 24 and 48 hours, measured by differential weighing of supplied water bottles. Arithmetic averages of five animals in each group are shown. Error-bars indicate standard deviation and asterisks indicate significant differences between means, calculated with an unpaired t-test. (*** represents P<0.001)

5.2.2.2.3 Interstitial nephritis, tubulitis and perirenal inflammation in aged tgLI#4 animals.

Since we observed high water consumption and erythrocytes within the urine of tgLI#4 mice, we analyzed the organs to determine whether the liver, spleen, intestine or kidneys of tgLI#4 mice were phenotypically different compared to those from non-transgenic littermates, IFNγ-KO or C57BL/6 animals. For phenotypic and histologic analyses 6-week old and 8-month old animals were sacrificed, organs frozen, sectioned and stained with H&E. All analyzed organs of 6-week old tgLI#4 mice were phenotypically similar to

those from non-transgenic littermates or age matched C57BL/6 and IFNγ-KO mice. However, kidneys from 8-month old tgLI#4 mice were enlarged, pale and contained a vacuole filled with clear liquid, which disintegrated upon removal of the kidneys from the animals (Figure 29).

Figure 29: Pictures of 8-month old tgLI#4 mice with opened peritoneum. Kidneys are indicated by arrows.

The histologic analyses of H&E stained sections from duodenum, ileum, colon and kidney revealed no differences between 6-week old tgLI#4, IFNγ-KO, and C57BL/6 animals (data not shown). However, kidney sections from 8-month old tgLI#4 animals showed infiltration of the interstitium (interstitial nephritis) (Figure 30-B, C and D), local infiltration of glomeruli (focal glomerulonephritis) (Figure 30-D) and infiltration of tubular epithelium (tubulitis) (Figure 30-C), accompanied by dilated tubuli (tubular extasie) (Figure 30-B and D). High numbers of inflammatory cells were also detected around the kidney (perirenale nephritis) (Figure 30-A).

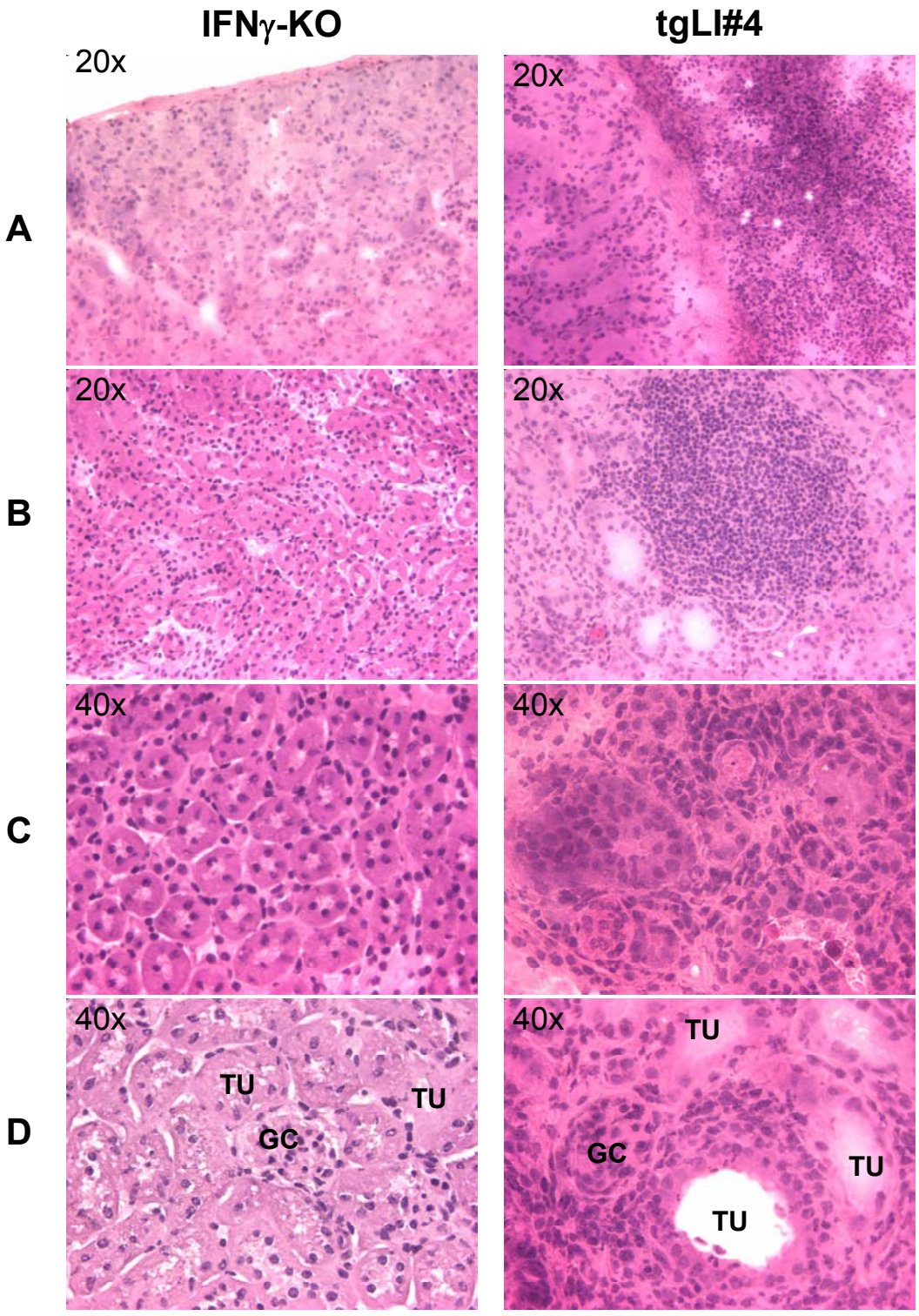

Figure 30: Kidney sections of 8-month old IFNγ-KO (left) and tgLI#4 (right) animals. Low magnification pictures of the outer kidney area with perirenal area (A) and inner kidney area (B) and high magnification (C and D) of tubuli (TU) and glomeruli (GC) are shown. Kidneys were removed, frozen, sectioned and stained with H&E.

5.2.2.2.4 High levels of IFNγ in kidneys of aged tgLI#4 mice

Since the lfabp promoter, which was used to generate the tgLI#4 line, was previously shown to be active in the kidney of a few transgenic animals (Simon et al., 1993), we next examined whether transgenic IFNγ was possibly overexpressed in the kidneys of old tgLI#4 mice. The IFNγ expression was measured in spleen, ileum, kidney, liver, lung, uterus and skin of two 8-month old tgLI#4 animals using real-time RT-PCR.

Small amounts of IFNγ mRNA were detected in the ileum of tgLI#4 mice, but not in the spleen, liver, lung, uterus, or skin of these mice (Figure 31-A and data not shown). However, detected levels were low and as previously observed for 10-week old tgLI#4 animals, not different from the IFNγ levels in ileum of naïve C57BL/6 mice. Nevertheless, high amounts of IFNγ mRNA were observed in kidneys from both analyzed 8-month old tgLI#4 mice, while IFNγ mRNA was not detectable in kidneys from C57BL/6 and IFNγ-KO animals (Figure 31-A). Because both analyzed tgLI#4 animals were on an IFNγ-KO background, the IFNγ must have been expressed from the transgene. This was verified by additional real-time RT-PCR, using primers specific for IFNγ cDNA expressed from the transgene (data not shown).

To examine whether the detected IFNγ mRNA was translated to protein, kidney sections from both tgLI#4 mice and IFNγ-KO control mice were stained with anti-IFNγ mAb. IFNγ protein expression was detectable in kidney sections from both analyzed 8-month old tgLI#4 mice but not in kidney sections from IFNγ-KO mice (Figure 32).The IFNγ protein was mostly located in the interstitium and adjacent to tubuli, indicating that it was possibly produced by epithelial cells within these tissues.

The biological functionality of the detected IFNγ protein was evaluated by further real-time RT-PCR with primers specific for IP-10 cDNA (Figure 31-B). Interestingly, high levels of IP-10 mRNA were present in the kidneys from both analyzed tgLI#4 mice, while no or only low IP-10 mRNA levels were detected in kidneys of C57BL/6 and IFNγ-KO mice. IP-10 mRNA levels in spleen, liver, lung, uterus and skin from tgLI#4 mice were not different from

IP-10 mRNA levels in the respective organs of IFNγ-KO mice (Figure 31-B and data not shown). As IP-10 is strongly induced by functional IFNγ protein, this result was a clear indication of high amounts of functional transgenically produced IFNγ protein in the kidneys of tgLI#4 mice.

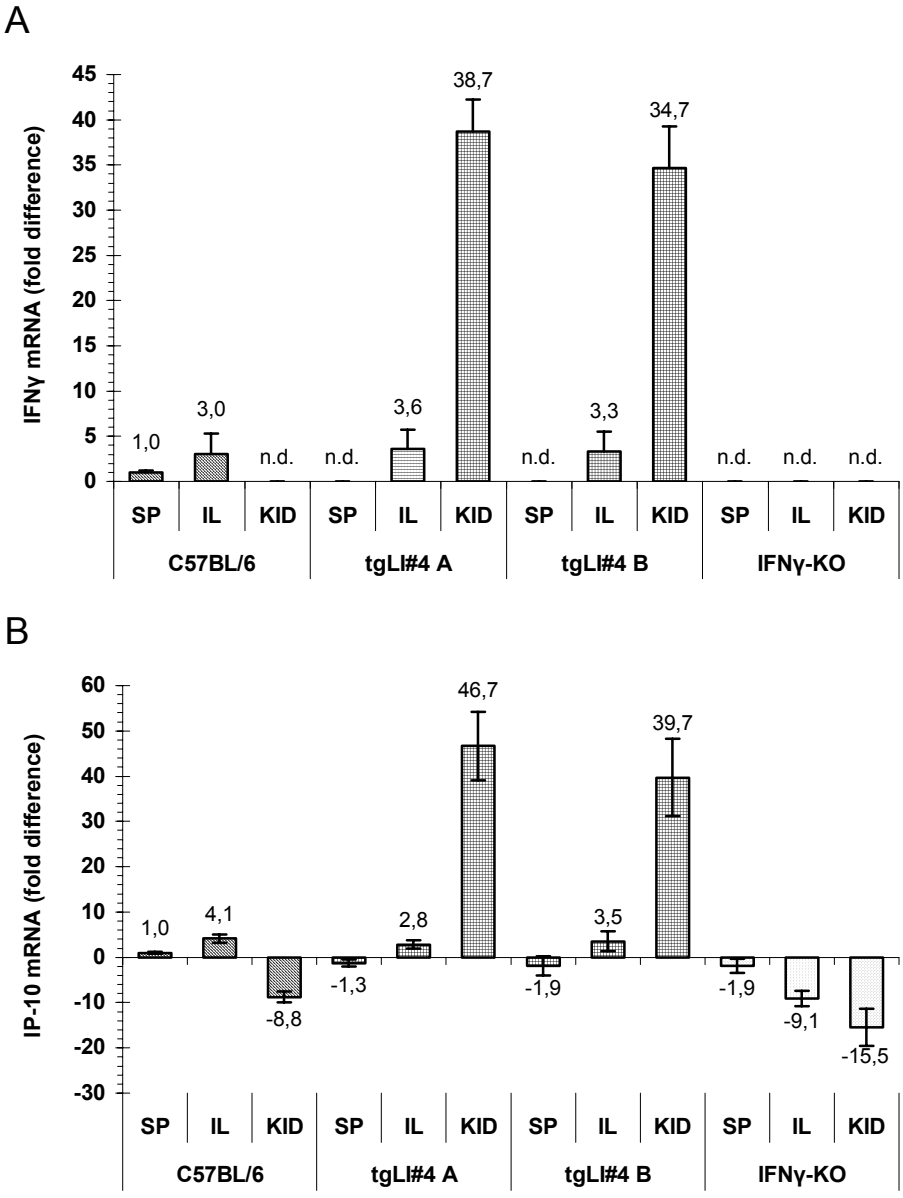

Figure 31: Relative IFNγ mRNA levels (A) and IP-10 mRNA levels (B) in spleen (SP), ileum (IL) and kidney (KID) of C57BL/6, IFNγ-KO and of two 8-month old tgLI#4 mice. IFNγ and IP-10 mRNA levels are represented as fold difference compared to the levels in spleen of naïve C57BL/6 mice. RNA was extracted from each organ and in case of C57BL/6 and IFNγ-KO animals, the RNA from the same organs were pooled. After reverse transcription to cDNA semiquantitative real-time PCR was performed using primers for β-actin and GAPDH as controls for the amount of cDNA and IFNγ or IP-10-specific primers for quantification. The bars represent the maximal differences between two real-time RT-PCRs with independently generated cDNA. Not detectable levels of IFNγ are indicated by n.d.

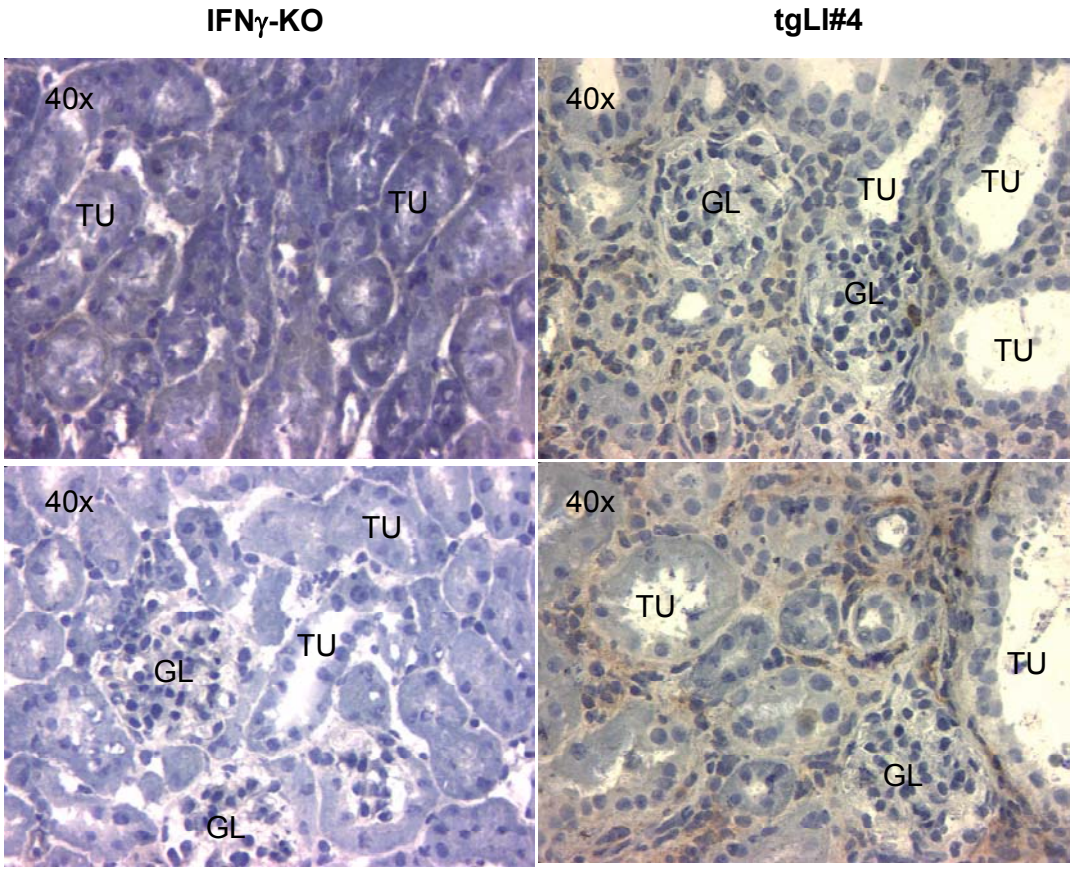

Figure 32: Anti-IFNγ stained kidney sections of IFNγ-KO and 8-month old tgLI#4 mice. High magnification (40x) of inner kidney structure with glomeruli (GL), tubuli (TU) and interstitium are shown. Kidneys were removed, frozen, sectioned and stained with immunoperoxidase staining. Primary anti-IFNγ mAb was detected using a goat anti-rat peroxidase coupled secondary antibody, followed by detection of the peroxidase with AEC as substrate and chromogen.

5.2.2.2.5 In tgLI#4 mice the transgene integrated into the AMACO gene

Transgenes integrate randomly into the host genome. Integration of a foreign sequence into a gene can lead to phenotypic changes, which are not related to the transgene but rather to a changed expression of the host gene. To examine, whether the phenotypic aberrations observed in tgLI#4 mice might be a result of integration into an important gene for kidney function, the location of the transgene was mapped. Genomic DNA from homozygous and heterozygous tgLI#4 animals was digested with multiple restriction enzymes and sizes of transgene containing DNA fragments were estimated using Southern blot analysis (data not shown). The DNA from digests that

contained small transgene containing fragments, was purified and then ligated to specially designed linkers obtained from *Clontech*. Using nested PCR, DNA fragments spanning from the transgene to the linker were amplified and sequenced. Sequence comparison with Celera and NCBI mouse genome databases revealed that the transgene had integrated as a single copy into chromosome 19 at 19D2. Further PCRs and subsequent sequencing of the amplified DNA, showed that the integration site was located in the intron-1 of the hypothetical gene “similar to matrilin 4 isoform 2” (sm4i2) (hypothesized by Celera from hypothetical protein NP_766428.1). Personal communication with Raimund Wagener (University of Cologne, Germany) identified this hypothetical “sm4i2” gene to be part of the AMACO gene, the gene of a newly identified extracellular matrix protein. The AMACO gene is 38kb long and consists of 14 exons with a non-coding exon-0. The lfabp-IFNγ-BGHpA cassette together with a 500bp rest of the pcDNA3.1/Zeo backbone had integrated in the 11kb long intron-1, with its reading frame in opposite direction to that of the AMACO reading frame (Figure 33).

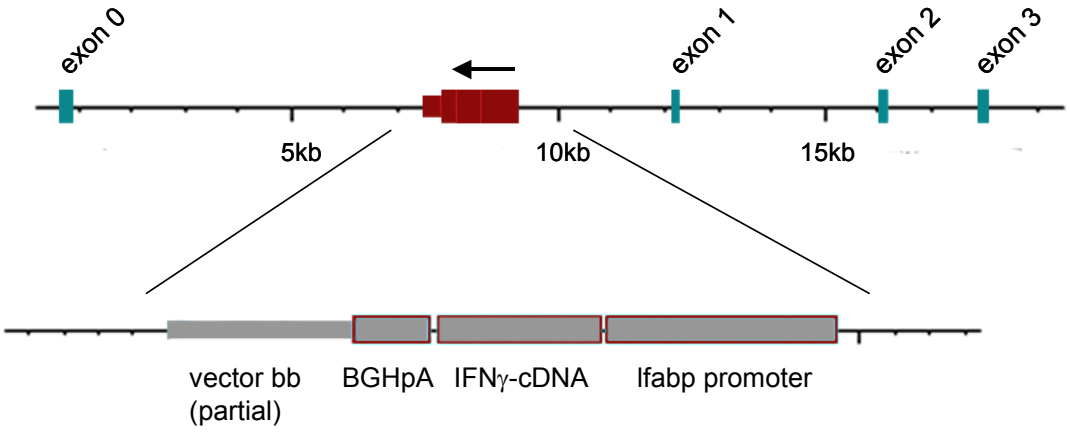

Figure 33: Map of the integration site of the lfabp-IFNγ-BGHpA transgene in tgLI#4 mice. In the upper panel the exon and intron structure of the first 20kb of the AMACO gene are shown. A more detailed representation of the transgene sequence is shown in the lower panel. The lfabp-promoter, the IFNγ-cDNA, the BGHpA sequence and the 500bp pcDNA3.1/Zeo vector backbone (vector bb) are indicated.

5.2.2.2.6 AMACO

Raimund Wagener and colleagues identified AMACO and analyzed its expression profile (personal communication): The 791 amino acids long AMACO protein consists of a signal peptide sequence, a N-terminal Von Willebrand Factor A (VWA) like domain connected to two additional, tandem VWA-like domains by a cysteine-rich sequence and an epidermal growth factor (EGF) like domain. The C-terminus is made up of another EGF-like domain followed by a unique sequence (Figure 34).

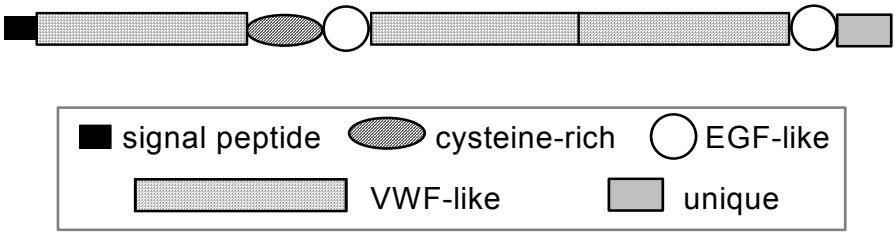

Figure 34: Domain structure of AMACO.

Northern blot analysis and RT-PCR by Raimund Wagener and colleagues showed that AMACO is expressed in most tissues of newborn mice, but not in adult mice. In adult mice, AMACO is strongly expressed in the kidney, the skin and the uterus, but can also be detected in the intestine and the lung. In the kidney of adult mice, in contrast to kidney of newborns, only a 5` truncated mRNA was detected by northern blot, probably transcribed by a second promoter, located in intron-4 of the AMACO gene. This truncated mRNA (exons 5-14) lacks an early start codon and can therefore not be translated (ncRNA). Immunohistochemistry using affinity-purified antibodies against AMACO on paraffin sections of kidney, lung, skin and uterus confirmed the lack of AMACO protein in the kidney. The cells that express AMACO are chondrocytes, lung and uterine epithelial cells and keratinocytes. The protein is deposited in the extracellular matrix surrounding these cells and appears to be particularly concentrated in and around the basement membranes that underlie epithelial cells. This suggests that AMACO is a structural component of some basement membranes or functions in joining basement membranes to the underlying stroma.

5.2.2.2.7 AMACO overexpression in the kidneys of tgLI#4 mice

Because the IFNγ transgene integrated into intron-1 of the AMACO gene, AMACO expression could be affected. Therefore, AMACO mRNA expression was analyzed in two 8-month old tgLI#4 animals that showed phenotypic changes and inflammation in their kidneys. Firstly, northern blot analysis was performed using a probe consisting of exon-7 to exon-11 of the AMACO cDNA (Figure 35).

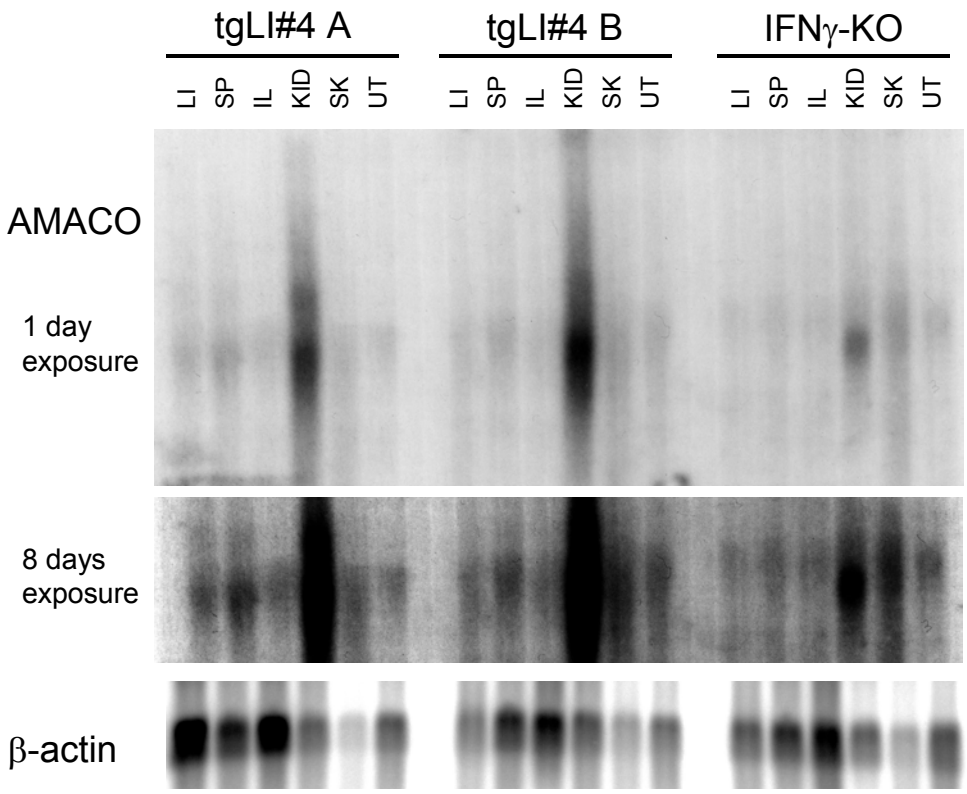

Figure 35: Northern blot analysis of RNA isolated from liver (LI), spleen (SP), ileum (IL), kidney (KID), skin (SK) and uterus (UT) of two 8-month old tgLI#4 mice and a pool from three 8-month old IFNγ-KO mice. Isolated RNA was separated by size, transferred to nylon membrane and hybridized with a radiolabeled AMACO probe (upper two panels) or a β-actin probe (lower panel). The probe consisted of exons 7 to 11 of the AMACO cDNA and detects the full length as well as the 5` truncated form of the AMACO mRNA.

Full length as well as the 5` truncated form of AMACO, should have been detectable by the used probe. Probably as a result of insufficient size differentiation, only one band was detected in all analyzed tissues from tgLI#4 as well as IFNγ-KO mice. In all mice analyzed, AMACO mRNA expression was strongest in kidneys. However, AMACO expression in

kidneys of tgLI#4 mice was significantly stronger than that in kidneys of IFNγ-KO mice, indicating an altered regulation of AMACO in the tgLI#4 animals.
To further analyze the AMACO expression in tgLI#4 mice, real-time RT-PCR was performed. Four exon spanning primer pairs were used to detect either the 5` region (primers A-0/A-1 and B-3/B-4) or the 3` region (C-7/C-8 and D-10/D-11) of the AMACO cDNA (Figure 36).

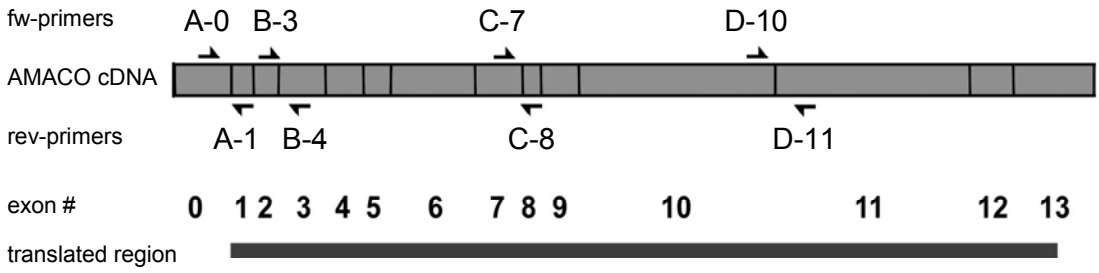

Figure 36: AMACO cDNA structure with annealing sites of forward (fw) and reverse (rev) primers used for real-time RT-PCR measurement of the 3` and 5` parts of AMACO mRNA. Exon numbers and the translated region of AMACO mRNA are indicated below. Primer names contain the exon number to which they anneal to.

The relative amount of the 5` and 3` region of AMACO mRNA was measured in the isolated RNA from ileum, kidney, uterus, spleen and lung of two 8-month old tgLI#4 and IFNγ-KO mice (Figure 37). Both regions of AMACO mRNA were detected in all of these organs and additional expression was observed in the skin and liver of these animals (data not shown). However, highest amounts of 3` AMACO mRNA were detected in the kidneys of tgLI#4 mice. Though it was also high in kidneys of IFNγ-KO mice, 3` AMACO mRNA levels were three to four fold lower than in tgLI#4 mice, which was similar to differences seen in northern blot analysis. Nevertheless, amounts of the 5` region were also very high in kidneys of tgLI#4 mice, whereas they were very low but still detectable in kidneys of IFNγ-KO mice. In kidneys of IFNγ-KO mice, 33 fold more 3` AMACO mRNA than 5` AMACO mRNA was observed. In contrast, the difference between amounts of 3` and 5` AMACO mRNA in kidneys of tgLI#4 animals was only 1.33 to 2 fold, indicating a different regulation of AMACO in the kidney of tgLI#4 animals. Yet, the difference of AMACO mRNA amounts between ileum of tgLI#4 mice and ileum of IFNγ-KO

was small. Moreover, strong differences of AMACO mRNA amounts were also observed in uterus, spleen and lung of tgLI#4 compared to IFNγ-KO mice, but transcription levels of the 5` and 3` regions of AMACO mRNA were similar in these organs. Taken together, this indicates that it was not the transcription of the transgene that lead to a different AMACO transcription, but probably its sole presence in intron-1.

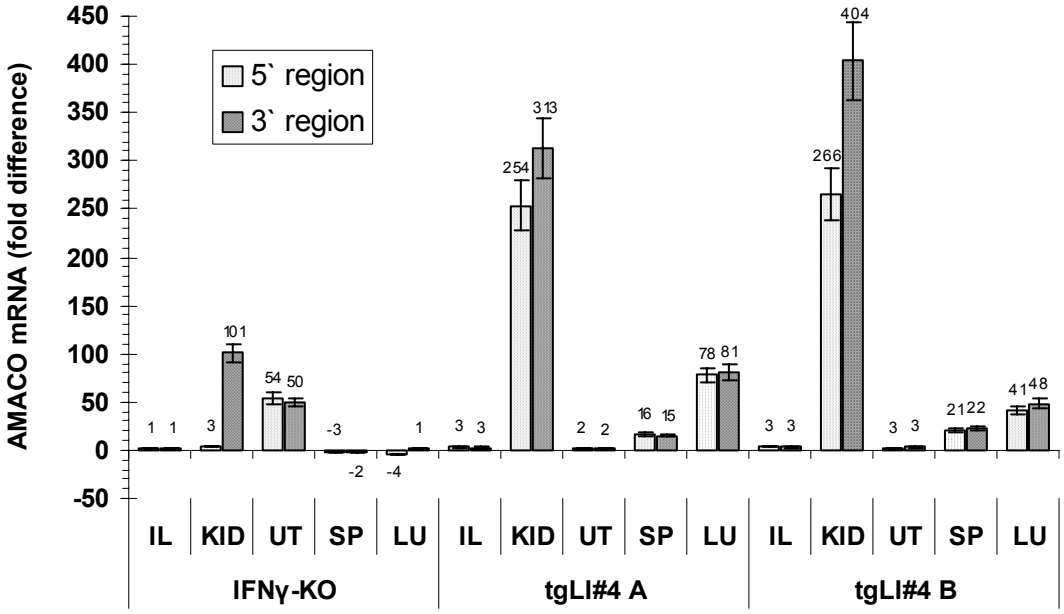

Figure 37: Relative levels of 5` (light bars) and 3` (dark bars) AMACO mRNA in ileum (IL), kidney (KID), uterus (UT), spleen (SP) and lung (LU) of 8-month old IFNγ-KO and two 8-month old tgLI#4 mice. 5` and 3` AMACO mRNA levels are represented as fold difference compared to the levels in ileum of naive IFNγ-KO mice, assuming that within ileum of IFNγ-KO mice, 3`and 5` mRNA levels are equal. RNA was extracted from different organs and in case of IFNγ-KO animals, the RNA from the same organs were pooled. After reverse transcription to cDNA semiquantitative real-time PCR was performed using primers for β-actin and GAPDH as controls for the amount of cDNA and AMACO primer pairs A, B, C and D for quantification. The relative AMACO mRNA amounts shown were calculated from at least two independent measurements of each organ using all primer pairs. Error-bars indicate the standard error of means.

The real-time RT-PCR results imply that in kidneys of tgLI#4 mice, AMACO is primarily transcribed as full length mRNA, in contrast to the AMCO transcription in kidneys of IFNγ-KO mice, where mostly but not exclusively 3` mRNA was found. To exclude the possibility that the detected 5` and 3` AMACO transcription in kidneys of tgLI#4 mice was caused by two independent transcriptions of an incomplete mRNA of the 5` part and a 3` part, leading to similar levels of both parts, but not full length mRNA, further

northern blot analyses were performed. RNA from kidneys of two tgLI#4 animals and a pool of RNA from kidneys of IFNγ-KO mice was separated on a high percentage formaldehyde gel, transferred to nylon membrane and probed with either a radiolabeled 3` or a radiolabeled 5` probe (Figure 38). Although real-time RT-PCR results indicated that small amounts of the 5` part of AMACO mRNA are also transcribed in kidney of IFNγ-KO mice, no band was detected in IFNγ-KO mice, when blots were hybridized with a probe directed against the 5` region of AMACO cDNA, indicating that its expression is probably below the detection limit. In contrast, strong signals of 5` AMACO mRNA were detected in the tgLI#4 animals. 3` AMACO mRNA was detected in kidneys from tgLI#4 and IFNγ-KO mice, although transcription level differences between tgLI#4 and IFNγ-KO mice were not as strong as previously observed by northern blot analysis and real-time RT-PCR. Interestingly, two additional bands were detected with both probes in tgLI#4 mice, possibly indicating unusual splicing caused by the transgene integration.

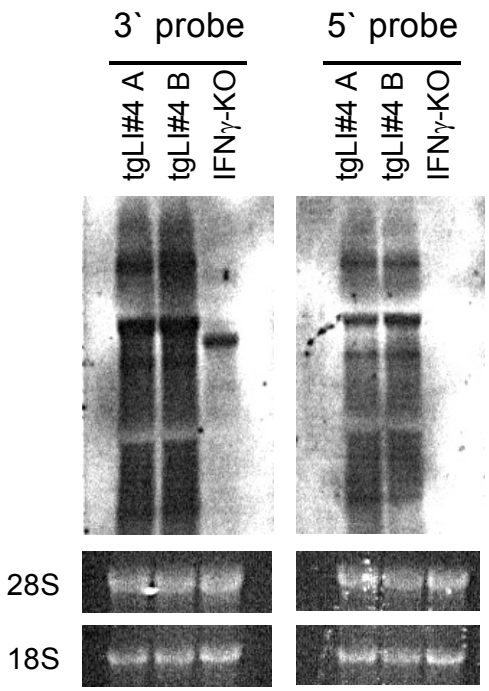

Figure 38: Northern blot analysis of kidney of two tgLI#4 and IFNγ-KO mice. RNA from kidneys of two 8-month old tgLI#4 animals and a pool of RNA from kidneys of IFNγ-KO mice was separated on a high percentage formaldehyde gel, transferred to nylon membrane and probed with a radiolabeled probe either from the 3` end (left) or from the 5` end (right) of AMACO cDNA. Below the ethidium bromide-stained ribosomal 18S and 28S RNAs are shown.

6 Discussion

The major aim of this study was the analysis of the effects of local IFNγ on the development of inflammation-associated diseases in mucosal tissue. The cytokine IFNγ is an important mediator of inflammation during infections with intracellular pathogens, but also effects inflammatory processes during allergic responses and the homeostasis of the mucosal immune system. In the first part of the study, we aimed at investigating the influence of IFNγ in local inflammatory processes in the lung during an allergic response. Therefore, a previously established transgenic mouse line with constitutive, lung-specific IFNγ expression was analyzed in a murine model of asthma. Due to a targeted deletion of the endogenous IFNγ-gene in these mice, IFNγ is exclusively expressed by the transgene, allowing the analysis of a strictly defined spatial and temporal expression of IFNγ, without interference from highly inducible endogenous IFNγ.

To further study the effects of IFNγ on (i) the homeostasis of the intestinal immunity, on (ii) chronic inflammatory processes in the gut, and (iii) to investigate the role of intestinal IFNγ expression, during an oral infection with intracellular bacteria like S*almonella typhimurium* or *Listeria monocytogenes*, we intended to generate a transgenic mouse line with gutspecific IFNγ expression. In the second part, the generation of such a mouse line, and its unexpected phenotype is described.

6.1 Effect of lung-specific IFNγ expression in a murine model of allergic airway inflammation

To elucidate the *in vivo* effector functions of IFNγ in the lung during a Th2 dominated inflammatory process, we compared the response of CC10-IFNγ-tg-IFNγ-KO mice, IFNγ-KO mice and C57BL/6 mice to sensitization and subsequent intranasal challenge with the allergen OVA.

We observed that C57BL/6 and IFNγ-KO mice developed similar levels of airway hyperresponsiveness, infiltration of eosinophils in the BALF and OVA-specific IgE. Similarities in the reaction of C57BL/6 and IFNγ-KO mice are not surprising, considering that the inflammatory response in this model is Th2 mediated. However, these results are in contrast with previous reports that observed a stronger response of IFNγ-KO or IFNγ-R-KO mice, at least in some of the characteristic asthma like reactions. IFNγ-R-KO and IFNγ-KO mice were shown to develop a significantly stronger anti-OVA IgE response, an increased BALF eosinophilia and enhanced airway hyperresponsiveness (AHR) (Coyle et al., 1996; Hofstra et al., 1998; Wild et al., 2000). The exact reasons for the different findings remain unclear, but a possible explanation for this discrepancy might lie in the different protocols used for sensitization, challenge and analysis. Many of these studies included more or longer intervals between sensitizations or analyzed the animals at later time points after challenge.

However, in our model lung-specific IFNγ expression was found to have inhibitory but also intensifying effects on the asthma-like reaction induced by OVA sensitization and challenge. This is demonstrated by the finding that the two major hallmarks of allergic asthma, BALF eosinophilia and AHR are oppositely affected. While OVA induced BALF eosinophilia is significantly higher, airway responsiveness to the unspecific bronchoconstrictor methacholine is significantly lower in CC10-IFNγ-tg-IFNγ-KO mice, when compared to control C57BL/6 and IFNγ-KO mice. This observation is in

contrast to previous findings, which describe a decrease of all asthma-like reactions, including eosinophilia, when animals were treated with IFNγ (Iwamoto et al., 1993; Lack et al., 1996; Li et al., 1996). IFNγ was demonstrated to suppress Th2 cell dependent allergic responses (Erb et al., 1999; Yoshida et al., 2002), and low levels of IFNγ were reported to have anti-inflammatory effects through inhibition of the migration of naïve T cells and Th2 cells (Flaishon et al., 2002). The exact reason for the contrasting findings remains unclear, however, all these models used treatment with IFNγ during the sensitization phase and/or during, or immediately before, challenge. Hence it is likely that these results cannot be compared to a transgenic animal with constitutive low IFNγ expression in the lung. Moreover, several reports have indicated that IFNγ or at least IFNγ expressing Th1 cells do not always lead to reduced eosinophilia in sensitized and challenged mice. In some cases they even increase the allergic airway inflammation. For example, Hansen and colleagues have shown that adoptive transfer of allergen-specific Th1 cells into naïve recipients increased airway inflammation after sensitization and challenge, instead of counter balancing the Th2 response as hypothesized by the “hygiene theory”, which hypothesized that Th1 cells generated in the course of infections, are mainly responsible for decreased allergic responses (Hansen et al., 1999). Kumano and colleagues observed that administration of recombinant IL-18 to sensitized mice enhanced IFNγ and TNFα production and, unexpectedly, also increased BALF eosinophilia and IL-5 production without affecting AHR (Kumano et al., 1999). However, when only given during challenge, IL-18 still increased IFNγ levels, but decreased BALF eosinophilia and AHR (Wild et al., 2000). Moreover, human asthma is associated with the production of IFNγ, which appears to contribute to disease pathologenesis (Chandrasekaran and Gordon, 1993; Corrigan and Kay, 1990). Interestingly, we also found an increase of IFNγ in sensitized and challenged, compared to naïve C57BL/6 mice, indicating similar mechanisms in human asthma and our murine model of asthma. Additional studies have shown that AHR could not be induced in OVA challenged BALB/c mice treated with anti-IFNγ

antibodies prior to the challenge period (Hessel et al., 1997). In line with previous studies regarding the effects of IFNγ, which are supportive of our findings, Hofstra and colleagues demonstrated that parental IFNγ treatment of C57BL/6 mice downregulated OVA-specific IgE, BALF eosinophilia and AHR while aerosolized IFNγ treatment only suppressed AHR (Hofstra et al., 1998). Other studies, dissecting the role of IP-10 (CXCL10) in allergic asthma support of our observations as well. IP-10 is strongly induced by IFNγ (Ohmori and Hamilton, 1993), and is also upregulated in CC10-IFNγ-tg-IFNγ-KO mice. Medoff and colleagues showed that IP-10 strongly induces eosinophilia in a transgene model, although accompanied by increased AHR (Medoff et al., 2002). However, treatment of wild-type mice with exogenous IP-10 at the time of allergen challenge also increases eosinophilia, but decreases the AHR for 24hours after the last challenge (Thomas et al., 2002). Overall, these data suggest that IFNγ has a dual role in the development of allergic asthma. IFNγ appears to have both proinflammatory and anti-inflammatory activities, depending on the local concentration and timing of expression or application within the immune response.

The discrepancy between eosinophilia and AHR that we observed in challenged CC10-IFNγ-tg-IFNγ-KO mice is in contrast to many previous findings, which describe a correlation between the degree of eosinophilia in BALF and severity of AHR in mouse and human (Busse and Sedgwick, 1992; Kay, 1991; Martin et al., 2001). Currently, it is hypothesized that activated eosinophils damage the respiratory epithelium, and thereby expose the underlying sensory nerves to nonspecific bronchoconstrictors, resulting in increased sensitivity (Gleich et al., 1988). Nevertheless, attempts to establish a causative link between eosinophil effector proteins and AHR have failed (Denzler et al., 2000). So far, the direct mechanisms leading to AHR remain unclear and it is therefore likely that the correlation between eosinophilia and AHR might be a coincidence, rather than a causative relationship.

The diverse effects of constitutive lung-specific IFNγ expression in the used asthma model are also represented by cytokine and eotaxin mRNA levels and IgE levels in lungs of challenged CC10-IFNγ-tg-IFNγ-KO mice. Eotaxin, IL-5 and IL-13 mRNA are increased in the lung, while IL-4 mRNA and anti-OVA IgE are decreased, when compared to their level in lungs of equally treated C57BL/6 and IFNγ-KO mice. The observation of increased BALF eosinophilia in the challenged CC10-IFNγ-tg-IFNγ-KO mice is therefore not surprising. Eotaxin, is expressed by epithelial cells, T cells, fibroblasts and macrophages and is mainly responsible for the recruitment of eosinophils to specific sites within the lung (Ganzalo et al., 1996). IL-5 also functions as an eosinophil chemoattractant, but additionally promotes maturation, proliferation and immortalization of eosinophils (Sanderson, 1992). However, high levels of IL-5 in the lung have been shown to induce AHR accompanied by high BALF eosinophilia even in the absence of IL-4 or IgE, (Hamelmann et al., 2000; Shi et al., 1998). Additionally, IL-5-KO mice do not develop airway eosinophilia but also no AHR (Foster et al., 1996). These findings are in contrast to our observations that IL-5 and eotaxin mRNA are increased but AHR is decreased in CC10-IFNγ-tg-IFNγ-KO mice, compared to C57BL/6 and IFNγ-KO control mice. However, other models of airway inflammation have shown that eosinophilia and modulation of airway responsiveness can occur independent of each other (Corry et al., 1996; Coyle et al., 1998; Lefort et al., 1996). Corry and colleagues for example, showed that anti-IL-4 antibody treatment reduces AHR, without affecting airway eosinophilia, whereas anti-IL-5 antibody treatment did not alter AHR, but reduced airway eosinophilia. This indicates that in some models AHR is strongly dependent on IL-4 levels, but independent of IL-5 expression (Corry et al., 1996).

It is likely that we are dealing with similar mechanisms in our model. Considering the low IL-4 mRNA levels in lungs of challenged CC10-IFNγ-tg-IFNγ-KO mice this could explain the lower AHR in these mice, in spite of the increased IL-5 levels. Since IL-4 is responsible for the class switch in plasma cells, lower levels of IL-4 mRNA are possibly responsible for the decreased anti-OVA IgE levels in sera and lung-homogenates of the transgenic mice

(Zhou et al., 1997). Low anti-OVA IgE concentrations could be a factor that leads to the observed lower AHR. IgE binds to high-affinity FcεI receptors on granulocytes and mast cells, leading to the discharge of proinflammatory mediators such as histamine and leukotriens that can cause AHR (Holgate et al., 1986). Although IgE binding to its low affinity receptor CD23 contributes to eosinophilic infiltration (Heusser et al., 1997), it also acts as a negative regulatory signal in allergic airway inflammation (Payet and Conrad, 1999). Interestingly, treatment of C57BL/6 mice with aerosolized IFNγ did not lead to lower anti-OVA IgE levels, as we observed, but only to lower AHR (Hofstra et al., 1998). It is possible that the level of IFNγ expression in the lungs of CC10-IFNγ-tg-IFNγ-KO mice is strong enough to reach the draining lymph nodes, where IgE synthesis takes place after challenge (Chvatchko et al., 1996), while aerosolized IFNγ treatment does not. The same holds true for the observed IL-4 levels in lungs of CC10-IFNγ-tg-IFNγ-KO mice. The lung-specific IFNγ expression could have inhibited the Th2-cell proliferation or mast cell proliferation and development, Th2 cells and mast cells are the main sources of IL-4 (Bradding et al., 1994; Elser et al., 2002; Huang et al., 2001; Mosmann and Coffman, 1989).

It is surprising however that IL-13 mRNA levels were increased in challenged CC10-IFNγ-tg-IFNγ-KO animals, compared to equally treated C57BL/6 and IFNγ-KO control mice. Previous reports have shown that IL-13 and IL-4 expression correlate in this model of allergic asthma, and IL-13 is also expressed by Th2-cells (Kips, 2001; Wynn, 2003). Therefore, it is likely that their expression is differentially regulated and IL-13 expression is not affected by IFNγ abundance. However, IL-13 and IL-4 have similar biological activities, which is partially reflected in the structure of their receptors, which share the IL-4Rα chain and also use the same signaling pathway (Callard et al., 1996). The abundance of IL-13 in lungs of challenged CC10-IFNγ-tg-IFNγ-KO mice is even more surprising, because IL-13 was shown to induce AHR. Although the mechanism by which IL-13 induces AHR remains unclear, Kuperman and colleagues, for example, observed a direct effect of IL-13 on

AHR via epithelial cells (Kuperman et al., 2002). Moreover, targeted deletion of IL-13 completely abolishes AHR (Walter et al., 2001), while transgenic overexpression severely induces it (Zhu et al., 1999). However, recent studies have shown that a second IL-13 receptor (IL-13Rα2), which does not share the IL-4Rα chain but strongly binds IL-13 as well, has the potential to downregulate the IL-13 effects. Wood and colleagues showed that mice with a targeted deletion of this receptor exhibit enhanced IL-13 responsiveness (Wood et al., 2003). Although it is speculative, it is possible that the high levels of IL-13 measured in the lungs of CC10-IFNγ-tg-IFNγ-KO mice, do not lead to increased AHR because of high amounts of this scavenger receptor. Nevertheless, it is to bear in mind that AHR in challenged CC10-IFNγ-tg-IFNγ-KO mice is not abolished. These mice are still more sensitive to small doses of methacholine than naïve controls, indicating a possible induction of AHR by IL-13.

One theory to explain the enhanced eosinophilia and increased IL-5 and IL-13 levels experienced in the CC10-IFNγ-tg-IFNγ-KO mice would be that regulatory T-cells only differentiate in absence of IFNγ, as shown for regulatory IL-10 producing $CD4^+$ $CD25^+$ T cells (Barrat et al., 2002). Thus, the constitutive presence of IFNγ could inhibit the differentiation of a regulatory T-cell subset in the CC10-IFNγ-tg-IFNγ-KO mouse line and be the reason for the enhanced production of IL-5 and IL-13 seen in the transgenic mice. However, the percentage and number of $CD4^+$ $CD25^+$ T-cells was slightly but insignificantly higher in lungs of challenged CC10-IFNγ-tg-IFNγ-KO mice, compared to C57BL/6 and IFNγ-KO mice, indicating that their development is not impaired in the presence of locally produced IFNγ. Moreover, the number of IL-10 producing T cells is even increased in naïve, but not different in challenged CC10-IFNγ-tg-IFNγ-KO mice, compared to C57BL/6 mice. Nevertheless, in spite of the slightly higher levels of regulatory T cells, the development and activity of Th2 cells seems rather enhanced, reflected by the slightly higher number and percentage of IL-5 producing T cells and higher levels of IL-5 mRNA.

To further understand the influence of IFNγ in this murine model of asthma, we have carried out DNA microarray profile analysis of CC10-IFNγ-tg-IFNγ-KO mice undergoing experimental asthma and compared our findings to results obtained for equally treated IFNγ-KO and C57BL/6 mice. Our data show that approximately 10% of the tested genome was dysregulated during induction of experimental asthma. However, the majority of induced genes were similarly regulated between the three allergen-challenged groups of mice, implicating an only minor effect of low levels of locally expressed IFNγ in this model. It was surprising that the gene for arginase I was the strongest allergen-induced gene in all three groups. Interestingly, arginine is a regulator of diverse pathways, including production of nitric oxide (NO), polyamines, and proline. Because these molecules regulate critical processes associated with asthma, including airway tone, cell hyperplasia, and collagen deposition (Mills, 2001; Morris, 2002), it is likely that arginase I is specifically involved in regulating airway inflammation. Moreover, increased arginase I activity has been found to underlie allergen-induced deficiency of NO and AHR development in a guinea pig model of allergic asthma (Meurs et al., 2002). Only recently, the L-arginine metabolism has been implicated in the pathogenesis of asthma. (Vercelli, 2003; Zimmermann et al., 2003). Zimmerman and colleagues demonstrated that arginase I expression is induced by IL-4 and IL-13 in a STAT6-dependent manner, and arginase I is highly expressed in airway epithelial cells of human and mouse asthmatic lungs, while none of the NO synthases (NOS) are differentially regulated. Our results are in agreement with these findings, as we could not detect differential expression of NOS. Nevertheless, if the arginine metabolism and thus arginase I expression is one of the major mechanisms that lead to AHR as indicated by the authors, one could not explain the lower AHR in CC10-IFNγ-tg-IFNγ-KO mice, since arginase I expression is similar in all three groups of mice. Other pathways that are influenced by IFNγ expression must also be involved. One of the pathways that seems to be differentially influenced during allergic airway inflammation in CC10-IFNγ-tg-IFNγ-KO mice compared to C57BL/6 and IFNγ-KO mice, could be those leading to

basement membrane injury, which is associated with allergic inflammation and possibly leads to AHR. During acute allergic airway inflammation, tissue injury in the epithelial basement membrane is at least in part mediated by matrix metalloproteinases, which are capable of degrading almost all of the extracellular matrix components (Chiappara et al., 2001; Kumagai et al., 2002). In a knockout mouse model, Cataldo and colleagues could show that matrix metalloproteinase 9 (MMP9) deficiency impairs cellular infiltration and AHR in the OVA induced murine model of asthma (Cataldo et al., 2002). In this context, the slightly higher expression level of tissue inhibitor of matrix metalloproteinases-1 (TIMP1), which we observed in CC10-IFNγ-tg-IFNγ-KO mice compared to C57BL/6 and IFNγ-KO mice, is a possible indication of differentially regulated tissue injury in the IFNγ expressing mice. Since MMPs are necessary for transmigration of lymphocytes, macrophages, DC and neutrophils through the membrane, this could also explain the slightly lower infiltration seen in the lungs of CC10-IFNγ-tg-IFNγ-KO mice. However, it remains unclear, how the increased BALF eosinophilia could develop if MMP activity is partially inhibited, considering that MMP activity is also necessary for the migration of eosinophils.

Nevertheless, it is so far not clear how AHR develops, and although we analyzed the possible influence of 8000 genes, it remains unclear how exactly the low expression of IFNγ in the lung influences AHR. It also remains to be elucidated, how IFNγ expression in the lung can lead to increased eotaxin, IL-5 and IL-13 levels, but slightly decreased IL-4 levels. A possible explanation might be that the used protocol induces an overly intensive inflammatory response, possibly concealing the subtle changes that lead to the observed differences. Further analysis of lymphocyte populations from lung and draining lymph nodes should shed light on the possible role of Th1 and Th2 cells in the development of the allergic response in CC10-IFNγ-tg-IFNγ-KO mice, as this has not been analyzed sufficiently yet. Furthermore, the role of the IFNγ-KO background of the CC10-IFNγ transgenic animals also needs to be analyzed by crossing them back to C57BL/6 background.

In conclusion, more studies need to be performed, to elucidate the exact proinflammatory and anti-inflammatory actions of lung-specific IFNγ in the development of allergic asthma.

However, the results of this study clearly demonstrate pleiotropic actions of constitutive lung-specific IFNγ expression in the model of OVA induced allergic asthma. While eosinophilia is increased, the other major hallmark of allergic asthma, airway hyperresponsiveness to unspecific broncho-constrictors, is reduced.

6.2 Transgenic mice with tissue-specific expression of IFNγ

To analyze the effects of IFNγ on the homeostasis of mucosal immunity and chronic inflammatory processes in the gut, and to investigate the role of intestinal IFNγ expression, during an oral infection with intracellular bacteria like S*almonella typhimurium* or *Listeria monocytogenes*, we aimed at generating a transgenic mouse line with gutspecific IFNγ expression.

The constant renewal of the epithelium of the intestinal mucosa is a major obstacle when targeting IFNγ expression to the intestine. To ensure sufficient expression of IFNγ, three transgene cassettes with different promoters were constructed. The Intestinal Trefoil Factor (ITF) promoter was chosen because of its potentially high restriction to goblet cells of the small and large intestine (Sands et al., 1995; Suemori et al., 1991), although it has not been used previously to generate transgenic animals. The second promoter chosen, was a 9kb fragment of the villin promoter that was shown to direct expression of a transgene to all proliferating epithelial cells along the crypt villus axis throughout the small and large intestine, with only low expression in kidney (Pinto et al., 1999). The liver fatty acid binding protein promoter (lfabp), has been extensively studied in various transgenic animals (Kim et al., 1993; Saam and Gordon, 1999; Simon et al., 1997; Simon et al., 1993). In contrast to the intestinal fatty acid binding protein promoter (ifabp), which showed considerable activity in kidney, Gordon and colleagues showed that a shorted form of lfabp is exclusively active in proliferating and non-proliferating epithelial cells, Paneth cells and goblet cells along the crypt villus axis throughout the small intestine, with only residual activity in kidney detected in only few transgenic animals.

We cloned the IFNγ cDNA immediately behind the promoters. Multiple reports have shown that 3` and 5` untranslated regions of mRNA can influence translation efficiency. Particularly, cytokine mRNAs often contain

sequences that destabilize or stabilize the mRNA by themselves or act as targets for other destabilizing or stabilizing factors e.g. AU-rich element clusters (Brown et al., 1996; Clark, 2000; Kishore et al., 1999). Hence only the translated region of the IFNγ cDNA was used for all three transgene cassettes.

After verification of the transgene cassettes in stably transfected CaCo2 cells, all cassettes were injected separately into the pronuclei of oocytes from IFNγ-KO mice. All together 31 injections of approximately 40 oocytes each were performed, leading to 347 potential founders, and only three lfabp-IFNγ transgenic IFNγ-KO mouse lines.

Although it is technically more demanding and not as efficient, we used IFNγ-KO mice of a pure C57BL/6 background (Dalton et al., 1993) to generate the transgenic animals, instead of commonly used hybrid strains, like e.g. the 129Sv/J strain. In comparison to mice of the C57BL/6 genetic background, 129Sv/J mice for example, carry different alleles of immunologically important genes that might lead to different phenotypes in infection experiments. Examples of such genes in the 129Sv/J strain include the different MHC alleles and a functional version of the Solute carrier 11a1 (Slc11A1 / NrampI), which is a ion transporter in the phagosome membrane linked to natural resistance to the intracellular pathogens *Salmonella typhimurium*, *Leishmania major* and *Mycobacterium bovis BCG* (Atkinson et al., 1997; North and Medina, 1998; Pinner et al., 1997; Vidal et al., 1995).

In order to directly compare the generated transgenic mice with IFNγ-KO or C57BL/6 mice, and to be able to clearly distinguish the effect of the transgene from effects caused by the genetic background, the use of 129Sv/J oocytes would have made several backcrosses with C57BL/6 mice necessary. However, this is time consuming and not as reliable as the generation of the transgenic line directly on a C57BL/6 genetic background. It might happen that even after several backcrosses immunological important but different genes remain. An example of such problems is the IL-10-KO mouse, which was generated on a 129Sv/J genetic background and backcrossed at least nine times onto the C57BL/6 genetic background, but

still contains the functional Nramp1 gene of 129Sv/J mice (personal observation). The reason for this is the close proximity of the IL-10 gene and the Nramp1 gene, which would be inherited separately only in the rare event of a crossover in between the two locuses.

On the other hand, the use of IFNγ-KO mice of a C57BL/6 genetic background is technically more demanding, because the yield of oocytes per superovulated IFNγ-KO female is much lower than per 129Sv/J female and additionally, the oocytes and the pronuclei of IFNγ-KO females are less resistant to physical damage. This problem is partially demonstrated by the high number of oocyte injections performed, but the subsequent relatively low number of live born cubs and the low rate of successful transgene integration.

However, the very low number of transgenic founder animals achieved, could also be due to the transgene itself. All used promoters were shown to become active in embryonic development already. The used lfabp promoter fragment, for example, is active in all epithelial cells in the intervillus and nascent villus epithelium of a transgenic embryo, latest by day 13 after conception (E13) (Roth et al., 1992). Although we have not analyzed this issue, it is likely that by the time the lfabp promoter is activated and dependent on the integration site of the transgene, high IFNγ levels are present throughout the whole small intestine of the developing lfabp-IFNγ transgenic embryo. Previous studies of transgenic IFNγ expression in fetal pancreas or IFNγ treatment of fetal livers have shown that dependent on the IFNγ levels, strong inflammations develop in the respective organs. Dependent on the IFNγ levels, this lead to organ failure and early death (Lee and Sarvetnick, 1997; Sarvetnick et al., 1988). It is therefore possible that some of the transgenic animals, namely those with high levels of IFNγ expression early in embryonic development, were never born, but rather died in uterus. The effects of high IFNγ expression could also explain why two out of the three lfabp-IFNγ transgenic lines generated do not have considerable IFNγ expression, and why one line only shows low IFNγ expression in the small intestine.

Nevertheless, we achieved one lfabp-IFNγ transgenic IFNγ-KO line (tgLI#4) that shows low expression of IFNγ protein in the small intestine of young animals. The expressed IFNγ protein is likely secreted and functional, because mRNA levels of the chemokine interferon-gamma-inducible 10-kd protein (IP-10 / CXCL10) were slightly upregulated in the small intestine of such animals. It has been shown that IP-10 is transcribed upon STAT1 signaling, which is strongly induced by the binding of IFNγ to its receptor (Ohmori and Hamilton, 1995; Ohmori and Hamilton, 2001). Nevertheless, IP-10 upregulation can not be considered an absolute proof of presence of functional IFNγ protein, because STAT1 signaling can also be induced by type I interferons (i.e. IFNα and IFNβ), which are rapidly induced by virus infections but also by lipopolysaccharides (LPS) (Meraz et al., 1996; Toshchakov et al., 2002). Since LPS is not a very strong IP-10 inducer in the absence of IFNγ, it is unlikely though possible that the slight upregulation of IP-10 in the small intestine of tgLI#4 animals was caused by a higher LPS content, e.g. from *E. coli* present in the small intestine of these animals.

It was surprising to find strong IFNγ expression from the transgene, accompanied by IP-10 expression, in the kidneys of old tgLI#4 animals. Although the lfabp promoter was shown to have some residual activity in kidney epithelium (Simon et al., 1997), we did not expect that the promoter activity would be 10 to 20 times higher in kidney than in the small intestine. However, after discovering the integration site of the transgene, this finding can be partially explained. The transgene has integrated into intron-1 of the not yet described AMACO gene. In agreement with Wagener and colleagues (personal communication) our real-time RT-PCR results show that even in IFNγ-KO control animals, AMACO is strongly expressed in the kidney, which is not the case in most other organs including the small intestine (100 fold more). Since locus accessibility could be one major factor in regulation of gene expression as described for many genes of the immune system (Mostoslavsky et al., 2003), the probably high accessibility of the AMACO locus in the kidney results in the observed overexpression of the thereby equally high accessibility of the transgene, in spite of a lower activity of the

promoter in this tissue. Similarly, the only low expression of the transgene observed in the small intestine can be explained by the possibly less accessible locus in this organ.

Interestingly, tgLI#4 mice develop a partial kidney failure, indicated by their excessive water consumption and the presence of erythrocytes in their urine (hematuria). At least in the analyzed 8-month old tgLI#4 animals the partial kidney failure was accompanied by phenotypic changes of the kidney and histologically evident nephritis. The kidneys showed typical symptoms of polycystic kidney disease. They were pale-yellow, severely enlarged and filled with clear liquid. Histologic analysis of the kidneys revealed perirenal infiltration, infiltration of the interstitium and local infiltration of glomeruli and tubular epithelium with lymphocytes, macrophages, neutrophils and some eosinophils. These findings are indicative of chronic tubulointerstitial nephritis (TIN). The causes of TIN are various and include allergic reactions to drugs, autoimmune reactions, and bacterial or viral infections of the kidney (pyelonephritis). Multiple reports have shown that the development of TIN caused by pyelonephritis but also the development of TIN caused by autoimmune reactions often involves cellular rather than humoral immunity (Meeus et al., 1993; Wuthrich and Sibalic, 1998). Since one important aspect of cellular immunity is the IFNγ production by $CD4^+$ and $CD8^+$ T-cells, this might indicate that the high overexpression of IFNγ in the kidneys of tgLI#4 mice plays a crucial role in the development of TIN in these mice. This hypothesis is supported by previous observations made in transgenic animal models with tissue-specific IFNγ overexpression in the liver or the lung of adult animals, and the previously mentioned study characterizing pancreas-specific overexpression of IFNγ in embryos. Toyonaga and colleagues, for example, showed that liver-specific overexpression of IFNγ leads to strong inflammation in this organ, similar to human chronic active hepatitis (Toyonaga et al., 1994). Moreover, Wang and colleagues demonstrated in an inducible transgenic system that IFNγ overexpression in the lung leads to pulmonary emphysema similar to human chronic obstructive pulmonary disease (COPD) (Wang et al., 2000). In both models, the degree of

inflammation was dependent on the expression level of IFNγ and always involved infiltration by macrophages, neutrophils and T cells.

Although the mechanisms of IFNγ induced inflammation in the absence of an infection remain unclear, several hypotheses can be made. The infiltration of leukocytes and granulocytes could be a direct effect of IFNγ overexpression, because IFNγ leads to the expression of several chemokines e.g. IL-8, Mig (CXCL9), IP-10 (CXCL10), I-TAC (CXCL11). Many of these chemokines, are involved in the recruitment of leukocytes and granulocytes (Dufour et al., 2002; Narumi et al., 1997). IP-10 e.g., which we found to be highly upregulated in the infiltrated kidneys, binds to and activates CXCR3, which is expressed on activated T cells, macrophages, neutrophils and eosinophils (Garcia-Lopez et al., 2001; Jinquan et al., 2000), and promotes infiltration of these cells into tissues with high IP-10 expression (Boztug et al., 2002). IFNγ also acts as an activator of macrophages and eosinophils (Ochiai et al., 1999), and thereby not only leads to the recruitment of these cells, but also induces their effector functions, which could then lead to damage of tubuli and glomeruli. Indications for such a mechanism were previously observed in a model of systemic lupus erythematosus (SLE) (Carvalho-Pinto et al., 2002). In an adaptive transfer model, Carvalho-Pinto and colleagues showed that IFNγ expression by macrophages is mainly responsible for the recruitment of macrophages to the kidney and also necessary to induce glomeronephritis. An additional possible mechanism of IFNγ induced inflammation, is the activation of normally quiescent autoreactive T cells. Since IFNγ leads to an upregulation of MHC class II molecules on various cells, the high amount of self antigen possibly presented in the kidney of tgLI#4 mice and the ability of infiltrated neutrophils to activate T cells, could break tolerance. Supportive of this concept is the report by Sarvetnick and colleagues (Sarvetnick et al., 1988). They constructed two transgenic lines with IFNγ or MHC class II overexpression in islets of Langerhans. The observed inflammatory destruction of the islets, was similar in both transgenic lines, and depended on infiltrating lymphocytes.

However, we cannot exclude that the integration of the transgene into the intron-1 of the AMACO gene contributes to the observed changes of the kidneys, and their inflammation. Although the exact function of AMACO is unknown, findings by Wagener and colleagues indicate that it is probably a structural component of the basement membrane (personal communication). The AMACO expression in kidneys of tgLI#4 mice is different from that in IFNγ control mice. AMACO expression is not only higher in kidney of tgLI#4 mice, but in contrast to the normally truncated AMACO mRNA transcription in IFNγ-KO mice, full length AMACO mRNA is mainly transcribed, indicating that the predominant use of the second promoter within the intron-4 of the AMACO gene is abolished by the transgene integration. However, in case the AMACO mRNA in kidney of tgLI#4 mice is translated, it is possible that the presence of higher levels of AMACO protein lead to changes in extracellular matrix (ECM) structures. These changes could increase the permeability of membranes within the nephron, e.g. the glomerate membrane, and therefore lead to the extreme water consumption, cysts, inflammation and finally kidney failure. Supportive of such an involvement of unnatural AMACO expression are findings regarding the role of other extracellular matrix proteins like collagens in some cases of human hereditary nephritis (Hudson et al., 2003; Lemmink et al., 1997; Turner and Rees, 1996). Alport syndrome e.g. is frequently caused by mutations within type IV collagen genes (Turner and Rees, 1996). The exact mechanisms of disease development in Alport syndrome patients are unknown, but interestingly Alport syndrome is also characterized by hematuria, infiltration of the interstitium and by local infiltration of glomeruli. Nevertheless, it is usually accompanied by proteinuria and easily detectable ocular problems. Although further analysis is necessary, changes in the glomerate membrane or other components of the filter structure, and membrane changes that would allow the efflux of erythrocytes, are unlikely in the kidney of tgLI#4 mice, because they are usually associated with proteinuria (Jalanko et al., 2001), which was not different in these animals from that found in C57BL/6 and IFNγ-KO control mice.

However, the unusual expression level of AMACO protein could break tolerance to this protein and induce a cellular or humoral response that leads to the partial destruction of basal membranes.

Because a break of tolerance, could also be induced by IFNγ overexpression, as described above, it is not possible to clearly distinguish between effects resulting from AMACO expression or those resulting from IFNγ expression. To find out, whether the chronic tubulointerstitial nephritis observed in tgLI#4 mice is caused by possible integration effects, leading to AMACO overexpression, or caused by the expression of the transgene, IFNγ, the tgLI#4 line needs to be crossed to the IFNγ-receptor knockout line, as this will eliminate all IFNγ induced changes. Moreover, further analysis of the mechanisms that lead to the chronic tubulointerstitial nephritis and the phenotypic changes of the kidneys will be necessary. Primarily this should include the characterization of the infiltrate and possible structural changes in the basal membrane. The characterization of the timing of disease development and analysis of kidney function also requires further investigation.

Since we were not able to generate a transgenic mouse line with exclusive IFNγ overexpression in the intestine, despite of numerous attempts, we must consider the possibility that the constitutive gut-specific expression of IFNγ early in embryonic development interferes with the creation of such a mouse line. We will need to use a system, in which IFNγ expression is absent until induction from the outside. The tet-on system has been shown to fulfill these requirements in a previous study involving IFNγ overexpression (Wang et al., 2000). In this system, the reverse tetracycline transactivator (rtTA) is placed under the control of a tissue-specific promoter and the tetracycline-responsive promoter drives IFNγ gene expression. Tissue-specific expression of IFNγ is then induced by the oral application of doxycyclin, which binds to rtTA and enables it to bind to the tetracycline-responsive promoter and thereby activate it (Gossen and Bujard, 1992).

However, this inducible system has disadvantages in experimental infection studies in mice because the antibiotic effect of doxycyclin adds a further variable to the system.

Due to the low rate of transgene transmission in the one line that shows IFNγ expression in the gut, and the resulting limited number of transgenic animals, we were not able to asses the role of IFNγ overexpression in the development of inflammatory bowel disease and the control of food borne pathogens. Nevertheless, the here generated mouse line tgLI#4 represents a novel *in vivo* model, which allows new insights into the development of possibly autoimmune chronic tubulointerstitial nephritis, either caused by the overexpression of a newly described extracellular matrix component, AMACO, or the exclusive overexpression of IFNγ in the kidney.

7 Summary

Overexpression or underrepresentation of IFNγ has been found in many dysregulated inflammatory responses. Inflammatory bowel disease (IBD) e.g. is associated with increased IFNγ expression, and conversely, asthma is thought to develop partially due to a lack of IFNγ expression. However, the role of local IFNγ presence in these diseases has not been completely elucidated. It is not clear what role local, mucosal IFNγ expression plays in the homeostasis of the intestinal immune system, the development of IBD and the protection from food born pathogens like *Salmonella* and *Listeria*.

The goal of this work, was to analyze the effects of tissue-specific IFNγ expression in two models of inflammation-associated diseases.

In the first part, we aimed at studying the influence of IFNγ in local inflammatory processes in the lung during an asthma like allergic response. To restrict our analysis to IFNγ expression in the lung and to exclude influences of endogenous IFNγ-production, we used a previously established transgenic mouse line with constitutive, lung-specific IFNγ expression and a targeted deletion of the IFNγ-gene (the CC10-IFNγ-tg-IFNγ-KO mouse line) and compared the asthma-like reaction of these mice with that of wild-type C57BL/6 and IFNγ-KO mice.

Analysis of cytokine and anti OVA-IgE levels in the lungs of asthmatic mice revealed that local IFNγ expression increases the expression of IL-5 and IL-13, rather than decreases their expression, as previously described for intranasal IFNγ treatment. Consistent with the increased IL-5 and IL-13 levels, we found significantly increased eosinophilia in BALF of CC10-IFNγ-tg-IFNγ-KO mice, indicating that this hallmark of asthma is enhanced by local IFNγ expression. In contrast, the other major feature of allergic asthma, airway hyperresponsiveness (AHR), was reduced by local IFNγ expression. Whether this reduction was caused by lower levels of IL-4 and anti-OVA IgE, which we also observed in CC10-IFNγ-tg-IFNγ-KO mice, is not clear. Transcriptome analysis of asthmatic CC10-IFNγ-tg-IFNγ-KO mice, and comparison of the results to those obtained for asthmatic C57BL/6 and IFNγ-

KO mice revealed no individual gene that could be responsible for the lower AHR. However, we found a slightly elevated expression of TIMP-1, indicating a possible reduction of tissue remodeling and tissue damage in lung-specific IFNγ expressing mice. The general comparison of asthma induced or downregulated genes from all three groups revealed a similar transcriptome responses in wild-type (C57BL/6) and IFNγ-KO mice. In contrast, subtle differences in the transcriptome response between C57BL/6 and IFNγ-KO compared to CC10-IFNγ-tg-IFNγ-KO were observed, further indicating a broad action of IFNγ expression on the development of asthma.

In conclusion, our results clearly demonstrate pleiotropic actions of constitutive lung-specific IFNγ expression in this model of allergic asthma. More studies need to be performed, to elucidate the exact proinflammatory and anti-inflammatory actions of lung-specific IFNγ in the development of allergic asthma.

In the second model we aimed to develop an IBD model, by generating mice that express IFNγ exclusively in the gut, thus allowing the analysis of the effects of IFNγ on the homeostasis of the mucosal immune system and the induction of IBD. We also planned to analyze the effects of local gut-specific IFNγ expression on infection with food borne pathogens.

We constructed three transgene cassettes with different promoters, each of them active in a different cell type of the gut epithelium. After verification in stably transfected cells, we performed numerous injections in oocytes, that resulted in only four transgenic animals. While one of the four possible founder animals did not transmit the transgene, three transgenic lines were generated from the other three founder animals. Animals of one of these lines, the tgLI#4 line, did not transmit the transgene according to the Mendelian rule and interestingly, this line was also the only line of the three that showed IFNγ expression in the gut. Since all promoters used in the transgene constructs become active during embryonic development, it is possible that the unusual low number transgenic founder animals and also the unusual low rate of transgene transmission of the tgLI#4 line was due to the interference of IFNγ expression with the development of the embryo.

Older mice of the tgLI#4 line showed symptoms of partial kidney failure, they drank excessive amounts of water and developed hematuria. Analysis of these mice revealed cysts within the kidneys and tubulointerstitial and perirenal nephritis. Unexpectedly, we found high IFNγ expression from the transgene in these kidneys, which could be a reason for the development of inflammation.

To exclude integration effects, we mapped the integration site of the transgene and found that the transgene had integrated into intron-1 of a gene coding for a not yet described extracellular matrix component, AMACO. Analysis of AMACO expression in the kidney of the tgLI#4 mice revealed that the transgene integration led to the overexpression of full length instead of a normally truncated and untranslated form of the AMACO mRNA. As changes in extracellular matrix composition could also account for many of the observed symptoms, it remains elusive, if the phenotypic changes in the kidneys and the symptoms of partial kidney failure on tgLI#4 mice were caused by IFNγ overexpression or by the overexpression of full length AMACO in this organ. To shed light on this question, we will backcross this line onto an IFNγ-receptor deficient background, in which possible IFNγ induced effects are excluded. Nevertheless, the here generated mouse line tgLI#4 represents a novel *in vivo* model, which allows new insights into the development of autoimmune chronic tubulointerstitial nephritis.

Since the only line that shows IFNγ expression in the gut did not generate enough offspring and also developed symptoms of kidney failure accompanied by high IFNγ expression in the kidney, we were not able to asses the role of local gut-specific IFNγ in the development of IBD or in the control of infections with food borne pathogens. Yet we might have generated a novel *in vivo* model of IFNγ induced chronic inflammation of the kidney, allowing further analysis of the mechanisms by which IFNγ mediates these effects.

8 Literature

Abbas, A. K., Lichtman, A. H., and Pober, J. S. (2000). Cellular and molecular immunology, 4th edn (Philadelphia, Saunders).

Agnello, D., Lankford, C. S., Bream, J., Morinobu, A., Gadina, M., O'Shea, J. J., and Frucht, D. M. (2003). Cytokines and transcription factors that regulate T helper cell differentiation: new players and new insights. J Clin Immunol *23*, 147-161.

Akira, S., Takeda, K., and Kaisho, T. (2001). Toll-like receptors: critical proteins linking innate and acquired immunity. Nat Immunol *2*, 675-680.

Annacker, O., Pimenta-Araujo, R., Burlen-Defranoux, O., Barbosa, T. C., Cumano, A., and Bandeira, A. (2001). CD25+ CD4+ T cells regulate the expansion of peripheral CD4 T cells through the production of IL-10. J Immunol *166*, 3008-3018.

Atkinson, P. G., Blackwell, J. M., and Barton, C. H. (1997). Nramp1 locus encodes a 65 kDa interferon-gamma-inducible protein in murine macrophages. Biochem J *325 (Pt 3)*, 779-786.

Ball, T. M., Castro-Rodriguez, J. A., Griffith, K. A., Holberg, C. J., Martinez, F. D., and Wright, A. L. (2000). Siblings, day-care attendance, and the risk of asthma and wheezing during childhood. N Engl J Med *343*, 538-543.

Banchereau, J., and Steinman, R. M. (1998). Dendritic cells and the control of immunity. Nature *392*, 245-252.

Barrat, F. J., Cua, D. J., Boonstra, A., Richards, D. F., Crain, C., Savelkoul, H. F., de Waal-Malefyt, R., Coffman, R. L., Hawrylowicz, C. M., and O'Garra, A. (2002). In vitro generation of interleukin 10-producing regulatory CD4(+) T cells is induced by immunosuppressive drugs and inhibited by T helper type 1 (Th1)- and Th2-inducing cytokines. J Exp Med *195*, 603-616.

Bauer, S., Kirschning, C. J., Hacker, H., Redecke, V., Hausmann, S., Akira, S., Wagner, H., and Lipford, G. B. (2001). Human TLR9 confers responsiveness to bacterial DNA via species-specific CpG motif recognition. Proc Natl Acad Sci U S A *98*, 9237-9242.

Beutler, B. (2002). TLR4 as the mammalian endotoxin sensor. Curr Top Microbiol Immunol *270*, 109-120.

Birnboim, H. C., and Doly, J. (1979). A rapid alkaline extraction procedure for screening recombinant plasmid DNA. Nucleic Acids Res *7*, 1513-1523.

Bluestone, J. A., Khattri, R., Sciammas, R., and Sperling, A. I. (1995). TCR gamma delta cells: a specialized T-cell subset in the immune system. Annu Rev Cell Dev Biol *11*, 307-353.

Boehm, U., Klamp, T., Groot, M., and Howard, J. C. (1997). Cellular responses to interferon-gamma. Annu Rev Immunol *15*, 749-795.

Bogdan, C., Rollinghoff, M., and Diefenbach, A. (2000). Reactive oxygen and reactive nitrogen intermediates in innate and specific immunity. Curr Opin Immunol *12*, 64-76.

Boller, K., Arpin, M., Pringault, E., Mangeat, P., and Reggio, H. (1988). Differential distribution of villin and villin MRNA in mouse intestinal epithelial cells. Differentiation *39*, 51-57.

Bonhagen, K., Thoma, S., Bland, P., Bregenholt, S., Rudolphi, A., Claesson, M. H., and Reimann, J. (1996). Cytotoxic reactivity of gut lamina propria CD4+ alpha beta T cells in SCID mice with colitis. Eur J Immunol *26*, 3074-3083.

Boyce, J. A. (2003). Mast cells: beyond IgE. J Allergy Clin Immunol *111*, 24-32; quiz 33.

Boztug, K., Carson, M. J., Pham-Mitchell, N., Asensio, V. C., DeMartino, J., and Campbell, I. L. (2002). Leukocyte infiltration, but not neurodegeneration, in the CNS of transgenic mice with astrocyte production of the CXC chemokine ligand 10. J Immunol *169*, 1505-1515.

Bradding, P., Roberts, J. A., Britten, K. M., Montefort, S., Djukanovic, R., Mueller, R., Heusser, C. H., Howarth, P. H., and Holgate, S. T. (1994). Interleukin-4, -5, and -6 and tumor necrosis factor-alpha in normal and asthmatic airways: evidence for the human mast cell as a source of these cytokines. Am J Respir Cell Mol Biol *10*, 471-480.

Brandeis, J. M., Sayegh, M. H., Gallon, L., Blumberg, R. S., and Carpenter, C. B. (1994). Rat intestinal epithelial cells present major histocompatibility complex allopeptides to primed T cells. Gastroenterology *107*, 1537-1542.

Bretscher, P. (1992). The two-signal model of lymphocyte activation twenty-one years later. Immunol Today *13*, 74-76.

Bretscher, P. A. (1975). The two signal model for b cell induction. Transplant Rev *23*, 37-48.

Brown, C. Y., Lagnado, C. A., and Goodall, G. J. (1996). A cytokine mRNA-destabilizing element that is structurally and functionally distinct from A+U-rich elements. Proc Natl Acad Sci U S A *93*, 13721-13725.

Brusselle, G., Kips, J., Joos, G., Bluethmann, H., and Pauwels, R. (1995). Allergen-induced airway inflammation and bronchial responsiveness in wild-type and interleukin-4-deficient mice. Am J Respir Cell Mol Biol *12*, 254-259.

Busse, W. W., and Sedgwick, J. B. (1992). Eosinophils in asthma. Ann Allergy *68*, 286-290.

Callard, R. E., Matthews, D. J., and Hibbert, L. (1996). IL-4 and IL-13 receptors: are they one and the same? Immunol Today *17*, 108-110.

Carlow, D. A., Teh, S. J., and Teh, H. S. (1998). Specific antiviral activity demonstrated by TGTP, a member of a new family of interferon-induced GTPases. J Immunol *161*, 2348-2355.

Carvalho-Pinto, C. E., Garcia, M. I., Mellado, M., Rodriguez-Frade, J. M., Martin-Caballero, J., Flores, J., Martinez, A. C., and Balomenos, D. (2002). Autocrine production of IFN-gamma by macrophages controls their recruitment to kidney and the development of glomerulonephritis in MRL/lpr mice. J Immunol *169*, 1058-1067.

Cataldo, D. D., Tournoy, K. G., Vermaelen, K., Munaut, C., Foidart, J. M., Louis, R., Noel, A., and Pauwels, R. A. (2002). Matrix metalloproteinase-9 deficiency impairs cellular infiltration and bronchial hyperresponsiveness during allergen-induced airway inflammation. Am J Pathol *161*, 491-498.

Cerf-Bensussan, N., and Guy-Grand, D. (1991). Intestinal intraepithelial lymphocytes. Gastroenterol Clin North Am *20*, 549-576.

Chandrasekaran, C., and Gordon, J. I. (1993). Cell lineage-specific and differentiation-dependent patterns of CCAAT/enhancer binding protein alpha expression in the gut epithelium of normal and transgenic mice. Proc Natl Acad Sci U S A *90*, 8871-8875.

Chawla-Sarkar, M., Lindner, D. J., Liu, Y. F., Williams, B. R., Sen, G. C., Silverman, R. H., and Borden, E. C. (2003). Apoptosis and interferons: role of interferon-stimulated genes as mediators of apoptosis. Apoptosis *8*, 237-249.

Chen, Y., Kuchroo, V. K., Inobe, J., Hafler, D. A., and Weiner, H. L. (1994). Regulatory T cell clones induced by oral tolerance: suppression of autoimmune encephalomyelitis. Science *265*, 1237-1240.

Chiappara, G., Gagliardo, R., Siena, A., Bonsignore, M. R., Bousquet, J., Bonsignore, G., and Vignola, A. M. (2001). Airway remodelling in the pathogenesis of asthma. Curr Opin Allergy Clin Immunol *1*, 85-93.

Chvatchko, Y., Kosco-Vilbois, M. H., Herren, S., Lefort, J., and Bonnefoy, J. Y. (1996). Germinal center formation and local immunoglobulin E (IgE) production in the lung after an airway antigenic challenge. J Exp Med *184*, 2353-2360.

Clark, A. (2000). Post-transcriptional regulation of pro-inflammatory gene expression. Arthritis Res *2*, 172-174.

Collazo, C. M., Yap, G. S., Sempowski, G. D., Lusby, K. C., Tessarollo, L., Woude, G. F., Sher, A., and Taylor, G. A. (2001). Inactivation of LRG-47 and IRG-47 reveals a family of interferon gamma-inducible genes with essential, pathogen-specific roles in resistance to infection. J Exp Med *194*, 181-188.

Cookson, W. (1999). The alliance of genes and environment in asthma and allergy. Nature *402*, B5-11.

Cooper, A. M., Dalton, D. K., Stewart, T. A., Griffin, J. P., Russell, D. G., and Orme, I. M. (1993). Disseminated tuberculosis in interferon gamma gene-disrupted mice. J Exp Med *178*, 2243-2247.

Corrigan, C. J., and Kay, A. B. (1990). CD4 T-lymphocyte activation in acute severe asthma. Relationship to disease severity and atopic status. Am Rev Respir Dis *141*, 970-977.

Corry, D., Kulkarni, P., and Lipscomb, M. F. (1984). The migration of bronchoalveolar macrophages into hilar lymph nodes. Am J Pathol *115*, 321-328.

Corry, D. B., Folkesson, H. G., Warnock, M. L., Erle, D. J., Matthay, M. A., Wiener-Kronish, J. P., and Locksley, R. M. (1996). Interleukin 4, but not interleukin 5 or eosinophils, is required in a murine model of acute airway hyperreactivity. J Exp Med *183*, 109-117.

Coyle, A. J., Kohler, G., Tsuyuki, S., Brombacher, F., and Kopf, M. (1998). Eosinophils are not required to induce airway hyperresponsiveness after nematode infection. Eur J Immunol *28*, 2640-2647.

Coyle, A. J., Tsuyuki, S., Bertrand, C., Huang, S., Aguet, M., Alkan, S. S., and Anderson, G. P. (1996). Mice lacking the IFN-gamma receptor have impaired ability to resolve a lung eosinophilic inflammatory response associated with a prolonged capacity of T cells to exhibit a Th2 cytokine profile. J Immunol *156*, 2680-2685.

Curotto de Lafaille, M. A., and Lafaille, J. J. (2002). CD4(+) regulatory T cells in autoimmunity and allergy. Curr Opin Immunol *14*, 771-778.

Dalton, D. K., Pitts-Meek, S., Keshav, S., Figari, I. S., Bradley, A., and Stewart, T. A. (1993). Multiple defects of immune cell function in mice with disrupted interferon-gamma genes. Science *259*, 1739-1742.

de Jong, Y. P., Abadia-Molina, A. C., Satoskar, A. R., Clarke, K., Rietdijk, S. T., Faubion, W. A., Mizoguchi, E., Metz, C. N., Alsahli, M., ten Hove, T.*, et al.* (2001). Development of chronic colitis is dependent on the cytokine MIF. Nat Immunol *2*, 1061-1066.

de Veer, M. J., Holko, M., Frevel, M., Walker, E., Der, S., Paranjape, J. M., Silverman, R. H., and Williams, B. R. (2001). Functional classification of interferon-stimulated genes identified using microarrays. J Leukoc Biol *69*, 912-920.

Denzler, K. L., Farmer, S. C., Crosby, J. R., Borchers, M., Cieslewicz, G., Larson, K. A., Cormier-Regard, S., Lee, N. A., and Lee, J. J. (2000). Eosinophil major basic protein-1 does not contribute to allergen-induced airway pathologies in mouse models of asthma. J Immunol *165*, 5509-5517.

Di Marzio, P., Puddu, P., Conti, L., Belardelli, F., and Gessani, S. (1994). Interferon gamma upregulates its own gene expression in mouse peritoneal macrophages. J Exp Med *179*, 1731-1736.

Dufour, J. H., Dziejman, M., Liu, M. T., Leung, J. H., Lane, T. E., and Luster, A. D. (2002). IFN-gamma-inducible protein 10 (IP-10; CXCL10)-deficient mice reveal a role for IP-10 in effector T cell generation and trafficking. J Immunol *168*, 3195-3204.

Elser, B., Lohoff, M., Kock, S., Giaisi, M., Kirchhoff, S., Krammer, P. H., and Li-Weber, M. (2002). IFN-gamma represses IL-4 expression via IRF-1 and IRF-2. Immunity *17*, 703-712.

Erb, K. J., Holloway, J. W., Sobeck, A., Moll, H., and Le Gros, G. (1998). Infection of mice with Mycobacterium bovis-Bacillus Calmette-Guerin (BCG) suppresses allergen-induced airway eosinophilia. J Exp Med *187*, 561-569.

Erb, K. J., Kirman, J., Delahunt, B., Moll, H., and Le Gros, G. (1999). Infection of mice with Mycobacterium bovis-BCG induces both Th1 and Th2 immune responses in the absence of interferon-gamma signalling. Eur Cytokine Netw *10*, 147-154.

Fahy, J. V., Corry, D. B., and Boushey, H. A. (2000). Airway inflammation and remodeling in asthma. Curr Opin Pulm Med *6*, 15-20.

Farrar, J. D., Asnagli, H., and Murphy, K. M. (2002). T helper subset development: roles of instruction, selection, and transcription. J Clin Invest *109*, 431-435.

Fearon, D. T., and Locksley, R. M. (1996). The instructive role of innate immunity in the acquired immune response. Science *272*, 50-53.

Finkelman, F. D., Katona, I. M., Urban, J. F., Jr., Holmes, J., Ohara, J., Tung, A. S., Sample, J. V., and Paul, W. E. (1988). IL-4 is required to generate and sustain in vivo IgE responses. J Immunol *141*, 2335-2341.

Finkelman, F. D., and Urban, J. F., Jr. (2001). The other side of the coin: the protective role of the TH2 cytokines. J Allergy Clin Immunol *107*, 772-780.

Flaishon, L., Topilski, I., Shoseyov, D., Hershkoviz, R., Fireman, E., Levo, Y., Marmor, S., and Shachar, I. (2002). Cutting edge: anti-inflammatory properties of low levels of IFN-gamma. J Immunol *168*, 3707-3711.

Flynn, J. L., Chan, J., Triebold, K. J., Dalton, D. K., Stewart, T. A., and Bloom, B. R. (1993). An essential role for interferon gamma in resistance to Mycobacterium tuberculosis infection. J Exp Med *178*, 2249-2254.

Foster, P. S., Hogan, S. P., Ramsay, A. J., Matthaei, K. I., and Young, I. G. (1996). Interleukin 5 deficiency abolishes eosinophilia, airways hyperreactivity, and lung damage in a mouse asthma model. J Exp Med *183*, 195-201.

Fournier, M., Lebargy, F., Le Roy Ladurie, F., Lenormand, E., and Pariente, R. (1989). Intraepithelial T-lymphocyte subsets in the airways of normal subjects and of patients with chronic bronchitis. Am Rev Respir Dis *140*, 737-742.

Foxwell, B. M., Barrett, K., and Feldmann, M. (1992). Cytokine receptors: structure and signal transduction. Clin Exp Immunol *90*, 161-169.

Fruh, K., and Yang, Y. (1999). Antigen presentation by MHC class I and its regulation by interferon gamma. Curr Opin Immunol *11*, 76-81.

Fuss, I. J., Neurath, M., Boirivant, M., Klein, J. S., de la Motte, C., Strong, S. A., Fiocchi, C., and Strober, W. (1996). Disparate CD4+ lamina propria (LP) lymphokine secretion profiles in inflammatory bowel disease. Crohn's disease LP cells manifest increased secretion of IFN-gamma, whereas ulcerative colitis LP cells manifest increased secretion of IL-5. J Immunol *157*, 1261-1270.

Ganzalo, J. A., Jia, G. Q., Aguirre, V., Friend, D., Coyle, A. J., Jenkins, N. A., Lin, G. S., Katz, H., Lichtman, A., Copeland, N.*, et al.* (1996). Mouse Eotaxin expression parallels eosinophil accumulation during lung allergic inflammation but it is not restricted to a Th2-type response. Immunity *4*, 1-14.

Garcia-Lopez, M. A., Sanchez-Madrid, F., Rodriguez-Frade, J. M., Mellado, M., Acevedo, A., Garcia, M. I., Albar, J. P., Martinez, C., and Marazuela, M. (2001). CXCR3 chemokine receptor distribution in normal and inflamed tissues: expression on activated lymphocytes, endothelial cells, and dendritic cells. Lab Invest *81*, 409-418.

Gebert, A. (1995). Identification of M-cells in the rabbit tonsil by vimentin immunohistochemistry and in vivo protein transport. Histochem Cell Biol *104*, 211-220.

Gerblich, A. A., Salik, H., and Schuyler, M. R. (1991). Dynamic T-cell changes in peripheral blood and bronchoalveolar lavage after antigen bronchoprovocation in asthmatics. Am Rev Respir Dis *143*, 533-537.

Gleich, G. J., Flavahan, N. A., Fujisawa, T., and Vanhoutte, P. M. (1988). The eosinophil as a mediator of damage to respiratory epithelium: a model for bronchial hyperreactivity. J Allergy Clin Immunol *81*, 776-781.

Gossen, M., and Bujard, H. (1992). Tight control of gene expression in mammalian cells by tetracycline-responsive promoters. Proc Natl Acad Sci U S A *89*, 5547-5551.

Goto, E., Kohrogi, H., Hirata, N., Tsumori, K., Hirosako, S., Hamamoto, J., Fujii, K., Kawano, O., and Ando, M. (2000). Human bronchial intraepithelial T lymphocytes as a distinct T-cell subset: their long-term survival in SCID-Hu chimeras. Am J Respir Cell Mol Biol *22*, 405-411.

Hahn, H., and Kaufmann, S. H. (1981). The role of cell-mediated immunity in bacterial infections. Rev Infect Dis *3*, 1221-1250.

Hamelmann, E., Takeda, K., Haczku, A., Cieslewicz, G., Shultz, L., Hamid, Q., Xing, Z., Gauldie, J., and Gelfand, E. W. (2000). Interleukin (IL)-5 but not immunoglobulin E reconstitutes airway inflammation and airway hyperresponsiveness in IL-4-deficient mice. Am J Respir Cell Mol Biol *23*, 327-334.

Hansen, G., Berry, G., DeKruyff, R. H., and Umetsu, D. T. (1999). Allergen-specific Th1 cells fail to counterbalance Th2 cell-induced airway hyperreactivity but cause severe airway inflammation. J Clin Invest *103*, 175-183.

Hara, M., Kingsley, C. I., Niimi, M., Read, S., Turvey, S. E., Bushell, A. R., Morris, P. J., Powrie, F., and Wood, K. J. (2001). IL-10 is required for regulatory T cells to mediate tolerance to alloantigens in vivo. J Immunol *166*, 3789-3796.

Hardy, K. J., and Sawada, T. (1989). Human gamma interferon strongly upregulates its own gene expression in peripheral blood lymphocytes. J Exp Med *170*, 1021-1026.

Harmsen, A. G., Muggenburg, B. A., Snipes, M. B., and Bice, D. E. (1985). The role of macrophages in particle translocation from lungs to lymph nodes. Science *230*, 1277-1280.

Harty, J. T., and Bevan, M. J. (1995). Specific immunity to Listeria monocytogenes in the absence of IFN gamma. Immunity *3*, 109-117.

Herz, U., Gerhold, K., Gruber, C., Braun, A., Wahn, U., Renz, H., and Paul, K. (1998). BCG infection suppresses allergic sensitization and development of increased airway reactivity in an animal model. J Allergy Clin Immunol *102*, 867-874.

Hess, J., Ladel, C., Miko, D., and Kaufmann, S. H. (1996). Salmonella typhimurium aroA- infection in gene-targeted immunodeficient mice: major role of CD4+ TCR-alpha beta cells and IFN-gamma in bacterial clearance independent of intracellular location. J Immunol *156*, 3321-3326.

Hessel, E. M., Van Oosterhout, A. J., Van Ark, I., Van Esch, B., Hofman, G., Van Loveren, H., Savelkoul, H. F., and Nijkamp, F. P. (1997). Development of airway hyperresponsiveness is dependent on interferon-gamma and independent of eosinophil infiltration. Am J Respir Cell Mol Biol *16*, 325-334.

Heusser, C. H., Wagner, K., Bews, J. P., Coyle, A., Bertrand, C., Einsle, K., Kips, J., Eum, S. Y., Lefort, J., and Vargaftig, B. B. (1997). Demonstration of the therapeutic potential of non-anaphylactogenic anti-IgE antibodies in murine models of skin reaction, lung function and inflammation. Int Arch Allergy Immunol *113*, 231-235.

Hofstra, C. L., Van Ark, I., Hofman, G., Nijkamp, F. P., Jardieu, P. M., and Van Oosterhout, A. J. (1998). Differential effects of endogenous and exogenous interferon-gamma on immunoglobulin E, cellular infiltration, and airway responsiveness in a murine model of allergic asthma. Am J Respir Cell Mol Biol *19*, 826-835.

Hogan, B., Costantini, F., and Lacy, E. (1986). Manipulating the mouse embryo : a laboratory manual (Cold Spring Harbor, NY, Cold Spring Harbor Laboratory).

Hogan, S. P., Mould, A., Kikutani, H., Ramsay, A. J., and Foster, P. S. (1997). Aeroallergen-induced eosinophilic inflammation, lung damage, and airways hyperreactivity in mice can occur independently of IL-4 and allergen-specific immunoglobulins. J Clin Invest *99*, 1329-1339.

Holgate, S. T., Hardy, C., Robinson, C., Agius, R. M., and Howarth, P. H. (1986). The mast cell as a primary effector cell in the pathogenesis of asthma. J Allergy Clin Immunol *77*, 274-282.

Holt, P. G., Schon-Hegrad, M. A., Phillips, M. J., and McMenamin, P. G. (1989). Ia-positive dendritic cells form a tightly meshed network within the human airway epithelium. Clin Exp Allergy *19*, 597-601.

Hooper, L. V., and Gordon, J. I. (2001). Commensal host-bacterial relationships in the gut. Science *292*, 1115-1118.

Huang, T. J., MacAry, P. A., Eynott, P., Moussavi, A., Daniel, K. C., Askenase, P. W., Kemeny, D. M., and Chung, K. F. (2001). Allergen-specific Th1 cells counteract efferent Th2 cell-dependent bronchial hyperresponsiveness and eosinophilic inflammation partly via IFN-gamma. J Immunol *166*, 207-217.

Hudson, B. G., Tryggvason, K., Sundaramoorthy, M., and Neilson, E. G. (2003). Alport's syndrome, Goodpasture's syndrome, and type IV collagen. N Engl J Med *348*, 2543-2556.

Iqbal, N., Oliver, J. R., Wagner, F. H., Lazenby, A. S., Elson, C. O., and Weaver, C. T. (2002). T helper 1 and T helper 2 cells are pathogenic in an antigen-specific model of colitis. J Exp Med *195*, 71-84.

Iwamoto, I., Nakajima, H., Endo, H., and Yoshida, S. (1993). Interferon gamma regulates antigen-induced eosinophil recruitment into the mouse airways by inhibiting the infiltration of CD4+ T cells. J Exp Med *177*, 573-576.

Jacobs, H., and Bross, L. (2001). Towards an understanding of somatic hypermutation. Curr Opin Immunol *13*, 208-218.

Jalanko, H., Patrakka, J., Tryggvason, K., and Holmberg, C. (2001). Genetic kidney diseases disclose the pathogenesis of proteinuria. Ann Med *33*, 526-533.

James, S. P., Fiocchi, C., Graeff, A. S., and Strober, W. (1986). Phenotypic analysis of lamina propria lymphocytes. Predominance of helper-inducer and cytolytic T-cell phenotypes and deficiency of suppressor-inducer phenotypes in Crohn's disease and control patients. Gastroenterology *91*, 1483-1489.

Janeway, C. A., Jr., and Medzhitov, R. (2002). Innate immune recognition. Annu Rev Immunol *20*, 197-216.

Jankovic, D., Liu, Z., and Gause, W. C. (2001). Th1- and Th2-cell commitment during infectious disease: asymmetry in divergent pathways. Trends Immunol *22*, 450-457.

Jinquan, T., Jing, C., Jacobi, H. H., Reimert, C. M., Millner, A., Quan, S., Hansen, J. B., Dissing, S., Malling, H. J., Skov, P. S., and Poulsen, L. K. (2000). CXCR3 expression and activation of eosinophils: role of IFN-gamma-inducible protein-10 and monokine induced by IFN-gamma. J Immunol *165*, 1548-1556.

Jones, B. D., Ghori, N., and Falkow, S. (1994). Salmonella typhimurium initiates murine infection by penetrating and destroying the specialized epithelial M cells of the Peyer's patches. J Exp Med *180*, 15-23.

Jouanguy, E., Altare, F., Lamhamedi-Cherradi, S., and Casanova, J. L. (1997). Infections in IFNGR-1-deficient children. J Interferon Cytokine Res *17*, 583-587.

Kaisho, T., and Akira, S. (2001). Toll-like receptors and their signaling mechanism in innate immunity. Acta Odontol Scand *59*, 124-130.

Kaufmann, S. H. (1993). Immunity to intracellular bacteria. Annu Rev Immunol *11*, 129-163.

Kaufmann, S. H. (1996). gamma/delta and other unconventional T lymphocytes: what do they see and what do they do? Proc Natl Acad Sci U S A *93*, 2272-2279.

Kay, A. B. (1989). Inflammatory cells in bronchial asthma. J Asthma *26*, 335-344.

Kay, A. B. (1991). Eosinophils and asthma. N Engl J Med *324*, 1514-1515.

Kelsall, B. L., and Strober, W. (1996). Distinct populations of dendritic cells are present in the subepithelial dome and T cell regions of the murine Peyer's patch. J Exp Med *183*, 237-247.

Kiderlen, A. F., Kaufmann, S. H., and Lohmann-Matthes, M. L. (1984). Protection of mice against the intracellular bacterium Listeria monocytogenes by recombinant immune interferon. Eur J Immunol *14*, 964-967.

Kim, S. H., Roth, K. A., Moser, A. R., and Gordon, J. I. (1993). Transgenic mouse models that explore the multistep hypothesis of intestinal neoplasia. J Cell Biol *123*, 877-893.

Kips, J. C. (2001). Cytokines in asthma. Eur Respir J Suppl *34*, 24s-33s.

Kishore, R., Tebo, J. M., Kolosov, M., and Hamilton, T. A. (1999). Cutting edge: clustered AU-rich elements are the target of IL-10-mediated mRNA destabilization in mouse macrophages. J Immunol *162*, 2457-2461.

Kuhn, R., Lohler, J., Rennick, D., Rajewsky, K., and Muller, W. (1993). Interleukin-10-deficient mice develop chronic enterocolitis. Cell *75*, 263-274.

Kumagai, K., Ohno, I., Imai, K., Nawata, J., Hayashi, K., Okada, S., Senoo, H., Hattori, T., and Shirato, K. (2002). The involvement of matrix metalloproteinases in basement membrane injury in a murine model of acute allergic airway inflammation. Clin Exp Allergy *32*, 1527-1534.

Kumano, K., Nakao, A., Nakajima, H., Hayashi, F., Kurimoto, M., Okamura, H., Saito, Y., and Iwamoto, I. (1999). Interleukin-18 enhances antigen-induced eosinophil recruitment into the mouse airways. Am J Respir Crit Care Med *160*, 873-878.

Kuperman, D. A., Huang, X., Koth, L. L., Chang, G. H., Dolganov, G. M., Zhu, Z., Elias, J. A., Sheppard, D., and Erle, D. J. (2002). Direct effects of interleukin-13 on epithelial cells cause airway hyperreactivity and mucus overproduction in asthma. Nat Med *8*, 885-889.

Kvale, D., Krajci, P., and Brandtzaeg, P. (1992). Expression and regulation of adhesion molecules ICAM-1 (CD54) and LFA-3 (CD58) in human intestinal epithelial cell lines. Scand J Immunol *35*, 669-676.

Lack, G., Bradley, K. L., Hamelmann, E., Renz, H., Loader, J., Leung, D. Y., Larsen, G., and Gelfand, E. W. (1996). Nebulized IFN-gamma inhibits the development of secondary allergic responses in mice. J Immunol *157*, 1432-1439.

Laemmli, U. K. (1970). Cleavage of structural proteins during the assembly of the head of bacteriophage T4. Nature *227*, 680-685.

Lanzavecchia, A., and Sallusto, F. (2001). Antigen decoding by T lymphocytes: from synapses to fate determination. Nat Immunol *2*, 487-492.

Lee, M. S., and Sarvetnick, N. (1997). Fetal exposure to interferon-gamma leads to induction of antigen-presenting molecules and leukocyte recruitment. Autoimmunity *25*, 147-155.

Lefort, J., Bachelet, C. M., Leduc, D., and Vargaftig, B. B. (1996). Effect of antigen provocation of IL-5 transgenic mice on eosinophil mobilization and bronchial hyperresponsiveness. J Allergy Clin Immunol *97*, 788-799.

Lefrancois, L. (1991). Intraepithelial lymphocytes of the intestinal mucosa: curiouser and curiouser. Semin Immunol *3*, 99-108.

Lemmink, H. H., Schroder, C. H., Monnens, L. A., and Smeets, H. J. (1997). The clinical spectrum of type IV collagen mutations. Hum Mutat *9*, 477-499.

Leong, K. P., and Huston, D. P. (2001). Understanding the pathogenesis of allergic asthma using mouse models. Ann Allergy Asthma Immunol *87*, 96-109; quiz 110.

Li, X. M., Chopra, R. K., Chou, T. Y., Schofield, B. H., Wills-Karp, M., and Huang, S. K. (1996). Mucosal IFN-gamma gene transfer inhibits pulmonary allergic responses in mice. J Immunol *157*, 3216-3219.

Liu, Y. J. (2001). Dendritic cell subsets and lineages, and their functions in innate and adaptive immunity. Cell *106*, 259-262.

Madrenas, J., Schwartz, R. H., and Germain, R. N. (1996). Interleukin 2 production, not the pattern of early T-cell antigen receptor-dependent tyrosine phosphorylation, controls anergy induction by both agonists and partial agonists. Proc Natl Acad Sci U S A *93*, 9736-9741.

Major, T., Wohlleben, G., Reibetanz, B., and Erb, K. J. (2002). Application of heat killed Mycobacterium bovis-BCG into the lung inhibits the development of allergen-induced Th2 responses. Vaccine *20*, 1532-1540.

Maloy, K. J., and Powrie, F. (2001). Regulatory T cells in the control of immune pathology. Nat Immunol *2*, 816-822.

Martin, L. B., Kita, H., Leiferman, K. M., and Gleich, G. J. (1996). Eosinophils in allergy: role in disease, degranulation, and cytokines. Int Arch Allergy Immunol *109*, 207-215.

Martin, R. J., Chu, H. W., Honour, J. M., and Harbeck, R. J. (2001). Airway inflammation and bronchial hyperresponsiveness after Mycoplasma pneumoniae infection in a murine model. Am J Respir Cell Mol Biol *24*, 577-582.

Maziak, W. (2003). The Th1-Th2 paradigm and asthma: how far should we go? J Asthma *40*, 201-205.

McKeever, T. M., Lewis, S. A., Smith, C., Collins, J., Heatlie, H., Frischer, M., and Hubbard, R. (2002). Early exposure to infections and antibiotics and the incidence of allergic disease: a birth cohort study with the West Midlands General Practice Research Database. J Allergy Clin Immunol *109*, 43-50.

McKenzie, S. E., and Schreiber, A. D. (1998). Fc gamma receptors in phagocytes. Curr Opin Hematol *5*, 16-21.

Medoff, B. D., Sauty, A., Tager, A. M., Maclean, J. A., Smith, R. N., Mathew, A., Dufour, J. H., and Luster, A. D. (2002). IFN-gamma-inducible protein 10 (CXCL10) contributes to airway hyperreactivity and airway inflammation in a mouse model of asthma. J Immunol *168*, 5278-5286.

Medzhitov, R., and Janeway, C., Jr. (2000a). Innate immune recognition: mechanisms and pathways. Immunol Rev *173*, 89-97.

Medzhitov, R., and Janeway, C., Jr. (2000b). The Toll receptor family and microbial recognition. Trends Microbiol *8*, 452-456.

Medzhitov, R., and Janeway, C. A., Jr. (1998). An ancient system of host defense. Curr Opin Immunol *10*, 12-15.

Meeus, F., Rossert, J., and Druet, P. (1993). Cellular immunity in interstitial nephropathy. Ren Fail *15*, 325-329.

Mellman, I., and Steinman, R. M. (2001). Dendritic cells: specialized and regulated antigen processing machines. Cell *106*, 255-258.

Meraz, M. A., White, J. M., Sheehan, K. C., Bach, E. A., Rodig, S. J., Dighe, A. S., Kaplan, D. H., Riley, J. K., Greenlund, A. C., Campbell, D.*, et al.* (1996). Targeted disruption of the Stat1 gene in mice reveals unexpected physiologic specificity in the JAK-STAT signaling pathway. Cell *84*, 431-442.

Meurs, H., McKay, S., Maarsingh, H., Hamer, M. A., Macic, L., Molendijk, N., and Zaagsma, J. (2002). Increased arginase activity underlies allergen-induced deficiency of cNOS-derived nitric oxide and airway hyperresponsiveness. Br J Pharmacol *136*, 391-398.

Mills, C. D. (2001). Macrophage arginine metabolism to ornithine/urea or nitric oxide/citrulline: a life or death issue. Crit Rev Immunol *21*, 399-425.

Monteleone, I., Vavassori, P., Biancone, L., Monteleone, G., and Pallone, F. (2002). Immunoregulation in the gut: success and failures in human disease. Gut *50 Suppl 3*, III60-64.

Morris, S. M., Jr. (2002). Regulation of enzymes of the urea cycle and arginine metabolism. Annu Rev Nutr *22*, 87-105.

Mosmann, T. R., and Coffman, R. L. (1989). TH1 and TH2 cells: different patterns of lymphokine secretion lead to different functional properties. Annu Rev Immunol *7*, 145-173.

Mostoslavsky, R., Alt, F. W., and Bassing, C. H. (2003). Chromatin dynamics and locus accessibility in the immune system. Nat Immunol *4*, 603-606.

Mowat, A. M., and Viney, J. L. (1997). The anatomical basis of intestinal immunity. Immunol Rev *156*, 145-166.

Mullis, K., Faloona, F., Scharf, S., Saiki, R., Horn, G., and Erlich, H. (1986). Specific enzymatic amplification of DNA in vitro: the polymerase chain reaction. Cold Spring Harb Symp Quant Biol *51 Pt 1*, 263-273.

Munder, M., Mallo, M., Eichmann, K., and Modolell, M. (1998). Murine macrophages secrete interferon gamma upon combined stimulation with interleukin (IL)-12 and IL-18: A novel pathway of autocrine macrophage activation. J Exp Med *187*, 2103-2108.

Nabel, G. J. (2002). HIV vaccine strategies. Vaccine *20*, 1945-1947.

Narumi, S., Tominaga, Y., Tamaru, M., Shimai, S., Okumura, H., Nishioji, K., Itoh, Y., and Okanoue, T. (1997). Expression of IFN-inducible protein-10 in chronic hepatitis. J Immunol *158*, 5536-5544.

Nave, H., Gebert, A., and Pabst, R. (2001). Morphology and immunology of the human palatine tonsil. Anat Embryol (Berl) *204*, 367-373.

Neurath, M. F., Finotto, S., and Glimcher, L. H. (2002). The role of Th1/Th2 polarization in mucosal immunity. Nat Med *8*, 567-573.

Neutra, M. R., Frey, A., and Kraehenbuhl, J. P. (1996). Epithelial M cells: gateways for mucosal infection and immunization. Cell *86*, 345-348.

Newport, M. J., Huxley, C. M., Huston, S., Hawrylowicz, C. M., Oostra, B. A., Williamson, R., and Levin, M. (1996). A mutation in the interferon-gamma-receptor gene and susceptibility to mycobacterial infection. N Engl J Med *335*, 1941-1949.

North, R. J., and Medina, E. (1998). How important is Nramp1 in tuberculosis? Trends Microbiol *6*, 441-443.

Ochiai, K., Tanabe, E., Ishihara, C., Kagami, M., Sugiyama, T., Sueishi, M., Koya, N., and Tomioka, H. (1999). Role of JAK2 signal transductional pathway in activation and survival of human peripheral eosinophils by interferon-gamma (IFN-gamma). Clin Exp Immunol *118*, 340-343.

Ohashi, P. S., Oehen, S., Buerki, K., Pircher, H., Ohashi, C. T., Odermatt, B., Malissen, B., Zinkernagel, R. M., and Hengartner, H. (1991). Ablation of "tolerance" and induction of diabetes by virus infection in viral antigen transgenic mice. Cell *65*, 305-317.

Ohmori, Y., and Hamilton, T. A. (1993). Cooperative interaction between interferon (IFN) stimulus response element and kappa B sequence motifs controls IFN gamma- and lipopolysaccharide-stimulated transcription from the murine IP-10 promoter. J Biol Chem *268*, 6677-6688.

Ohmori, Y., and Hamilton, T. A. (1995). The interferon-stimulated response element and a kappa B site mediate synergistic induction of murine IP-10 gene transcription by IFN-gamma and TNF-alpha. J Immunol *154*, 5235-5244.

Ohmori, Y., and Hamilton, T. A. (2001). Requirement for STAT1 in LPS-induced gene expression in macrophages. J Leukoc Biol *69*, 598-604.

Ohteki, T., Fukao, T., Suzue, K., Maki, C., Ito, M., Nakamura, M., and Koyasu, S. (1999). Interleukin 12-dependent interferon gamma production by CD8alpha+ lymphoid dendritic cells. J Exp Med *189*, 1981-1986.

Oltz, E. M. (2001). Regulation of antigen receptor gene assembly in lymphocytes. Immunol Res *23*, 121-133.

Pabst, R. (1996). The respiratory immune system of pigs. Vet Immunol Immunopathol *54*, 191-195.

Pabst, R., and Gehrke, I. (1990). Is the bronchus-associated lymphoid tissue (BALT) an integral structure of the lung in normal mammals, including humans? Am J Respir Cell Mol Biol *3*, 131-135.

Parronchi, P., Romagnani, P., Annunziato, F., Sampognaro, S., Becchio, A., Giannarini, L., Maggi, E., Pupilli, C., Tonelli, F., and Romagnani, S. (1997). Type 1 T-helper cell predominance and interleukin-12 expression in the gut of patients with Crohn's disease. Am J Pathol *150*, 823-832.

Payet, M., and Conrad, D. H. (1999). IgE regulation in CD23 knockout and transgenic mice. Allergy *54*, 1125-1129.

Pearl, J. E., Saunders, B., Ehlers, S., Orme, I. M., and Cooper, A. M. (2001). Inflammation and lymphocyte activation during mycobacterial infection in the interferon-gamma-deficient mouse. Cell Immunol *211*, 43-50.

Pinner, E., Gruenheid, S., Raymond, M., and Gros, P. (1997). Functional complementation of the yeast divalent cation transporter family SMF by NRAMP2, a member of the mammalian natural resistance-associated macrophage protein family. J Biol Chem *272*, 28933-28938.

Pinto, D., Robine, S., Jaisser, F., El Marjou, F. E., and Louvard, D. (1999). Regulatory sequences of the mouse villin gene that efficiently drive transgenic expression in immature and differentiated epithelial cells of small and large intestines. J Biol Chem *274*, 6476-6482.

Rais, M., Wild, J. S., Choudhury, B. K., Alam, R., Stafford, S., Dharajiya, N., and Sur, S. (2002). Interleukin-12 inhibits eosinophil differentiation from bone marrow stem cells in an interferon-gamma-dependent manner in a mouse model of asthma. Clin Exp Allergy *32*, 627-632.

Rankin, J. A., Picarella, D. E., Geba, G. P., Temann, U. A., Prasad, B., DiCosmo, B., Tarallo, A., Stripp, B., Whitsett, J., and Flavell, R. A. (1996). Phenotypic and physiologic characterization of transgenic mice expressing interleukin 4 in the lung: lymphocytic and eosinophilic inflammation without airway hyperreactivity. Proc Natl Acad Sci U S A *93*, 7821-7825.

Read, S., Malmstrom, V., and Powrie, F. (2000). Cytotoxic T lymphocyte-associated antigen 4 plays an essential role in the function of CD25(+)CD4(+) regulatory cells that control intestinal inflammation. J Exp Med *192*, 295-302.

Ricevuti, G. (1997). Host tissue damage by phagocytes. Ann N Y Acad Sci *832*, 426-448.

Riedler, J., Braun-Fahrlander, C., Eder, W., Schreuer, M., Waser, M., Maisch, S., Carr, D., Schierl, R., Nowak, D., and von Mutius, E. (2001). Exposure to farming in early life and development of asthma and allergy: a cross-sectional survey. Lancet *358*, 1129-1133.

Robine, S., Huet, C., Moll, R., Sahuquillo-Merino, C., Coudrier, E., Zweibaum, A., and Louvard, D. (1985). Can villin be used to identify malignant and undifferentiated normal digestive epithelial cells? Proc Natl Acad Sci U S A *82*, 8488-8492.

Robinson, D. S., Hamid, Q., Ying, S., Tsicopoulos, A., Barkans, J., Bentley, A. M., Corrigan, C., Durham, S. R., and Kay, A. B. (1992). Predominant TH2-like bronchoalveolar T-lymphocyte population in atopic asthma. N Engl J Med *326*, 298-304.

Romagnani, S. (1991). Type 1 T helper and type 2 T helper cells: functions, regulation and role in protection and disease. Int J Clin Lab Res *21*, 152-158.

Roth, K. A., Cohn, S. M., Rubin, D. C., Trahair, J. F., Neutra, M. R., and Gordon, J. I. (1992). Regulation of gene expression in gastric epithelial cell populations of fetal, neonatal, and adult transgenic mice. Am J Physiol *263*, G186-197.

Rousset, M. (1986). The human colon carcinoma cell lines HT-29 and Caco-2: two in vitro models for the study of intestinal differentiation. Biochimie *68*, 1035-1040.

Saam, J. R., and Gordon, J. I. (1999). Inducible gene knockouts in the small intestinal and colonic epithelium. J Biol Chem *274*, 38071-38082.

Sakaguchi, S., Sakaguchi, N., Asano, M., Itoh, M., and Toda, M. (1995). Immunologic self-tolerance maintained by activated T cells expressing IL-2 receptor alpha-chains (CD25). Breakdown of a single mechanism of self-tolerance causes various autoimmune diseases. J Immunol *155*, 1151-1164.

Salvi, S., and Holgate, S. T. (1999). Could the airway epithelium play an important role in mucosal immunoglobulin A production? Clin Exp Allergy *29*, 1597-1605.

Sambrook, J., and Russell, D. W. (2001). Molecular cloning : a laboratory manual, 3rd edn (Cold Spring Harbor, N.Y., Cold Spring Harbor Laboratory Press).

Sanderson, C. J. (1992). Interleukin-5, eosinophils, and disease. Blood *79*, 3101-3109.

Sands, B. E., Ogata, H., Lynch-Devaney, K., deBeaumont, M., Ezzell, R. M., and Podolsky, D. K. (1995). Molecular cloning of the rat intestinal trefoil factor gene. Characterization of an intestinal goblet cell-associated promoter. J Biol Chem *270*, 9353-9361.

Sarvetnick, N., Liggitt, D., Pitts, S. L., Hansen, S. E., and Stewart, T. A. (1988). Insulin-dependent diabetes mellitus induced in transgenic mice by ectopic expression of class II MHC and interferon-gamma. Cell *52*, 773-782.

Sato, A., Chida, K., Iwata, M., and Hayakawa, H. (1992). Study of bronchus-associated lymphoid tissue in patients with diffuse panbronchiolitis. Am Rev Respir Dis *146*, 473-478.

Schwartz, R. H. (1996). Models of T cell anergy: is there a common molecular mechanism? J Exp Med *184*, 1-8.

Sellon, R. K., Tonkonogy, S., Schultz, M., Dieleman, L. A., Grenther, W., Balish, E., Rennick, D. M., and Sartor, R. B. (1998). Resident enteric bacteria are necessary for development of spontaneous colitis and immune system activation in interleukin-10-deficient mice. Infect Immun *66*, 5224-5231.

Shevach, E. M. (2000). Regulatory T cells in autoimmmunity*. Annu Rev Immunol *18*, 423-449.

Shi, H. Z., Xiao, C. Q., Zhong, D., Qin, S. M., Liu, Y., Liang, G. R., Xu, H., Chen, Y. Q., Long, X. M., and Xie, Z. F. (1998). Effect of inhaled interleukin-5 on airway hyperreactivity and eosinophilia in asthmatics. Am J Respir Crit Care Med *157*, 204-209.

Shirakawa, T., Enomoto, T., Shimazu, S., and Hopkin, J. M. (1997). The inverse association between tuberculin responses and atopic disorder. Science *275*, 77-79.

Siebert, P. D., Chenchik, A., Kellogg, D. E., Lukyanov, K. A., and Lukyanov, S. A. (1995). An improved PCR method for walking in uncloned genomic DNA. Nucleic Acids Res *23*, 1087-1088.

Simon, T. C., Cho, A., Tso, P., and Gordon, J. I. (1997). Suppressor and activator functions mediated by a repeated heptad sequence in the liver fatty acid-binding protein gene (Fabpl). Effects on renal, small intestinal, and colonic epithelial cell gene expression in transgenic mice. J Biol Chem *272*, 10652-10663.

Simon, T. C., Roth, K. A., and Gordon, J. I. (1993). Use of transgenic mice to map cis-acting elements in the liver fatty acid-binding protein gene (Fabpl) that regulate its cell lineage-specific, differentiation-dependent, and spatial patterns of expression in the gut epithelium and in the liver acinus. J Biol Chem *268*, 18345-18358.

Singh, V. K., Mehrotra, S., and Agarwal, S. S. (1999). The paradigm of Th1 and Th2 cytokines: its relevance to autoimmunity and allergy. Immunol Res *20*, 147-161.

Stahl, P. D., and Ezekowitz, R. A. (1998). The mannose receptor is a pattern recognition receptor involved in host defense. Curr Opin Immunol *10*, 50-55.

Stephens, L. A., and Mason, D. (2000). CD25 is a marker for CD4+ thymocytes that prevent autoimmune diabetes in rats, but peripheral T cells with this function are found in both CD25+ and CD25- subpopulations. J Immunol *165*, 3105-3110.

Stripp, B. R., Sawaya, P. L., Luse, D. S., Wikenheiser, K. A., Wert, S. E., Huffman, J. A., Lattier, D. L., Singh, G., Katyal, S. L., and Whitsett, J. A. (1992). cis-acting elements that confer lung epithelial cell expression of the CC10 gene. J Biol Chem *267*, 14703-14712.

Strober, W., Fuss, I. J., and Blumberg, R. S. (2002). The immunology of mucosal models of inflammation. Annu Rev Immunol *20*, 495-549.

Suemori, S., Lynch-Devaney, K., and Podolsky, D. K. (1991). Identification and characterization of rat intestinal trefoil factor: tissue- and cell-specific member of the trefoil protein family. Proc Natl Acad Sci U S A *88*, 11017-11021.

Szabo, S. J., Sullivan, B. M., Peng, S. L., and Glimcher, L. H. (2003). Molecular mechanisms regulating Th1 immune responses. Annu Rev Immunol *21*, 713-758.

Takeda, K., Clausen, B. E., Kaisho, T., Tsujimura, T., Terada, N., Forster, I., and Akira, S. (1999). Enhanced Th1 activity and development of chronic enterocolitis in mice devoid of Stat3 in macrophages and neutrophils. Immunity *10*, 39-49.

Tanaka, K. (1994). Role of proteasomes modified by interferon-gamma in antigen processing. J Leukoc Biol *56*, 571-575.

Thomas, M. S., Kunkel, S. L., and Lukacs, N. W. (2002). Differential role of IFN-gamma-inducible protein 10 kDa in a cockroach antigen-induced model of allergic airway hyperreactivity: systemic versus local effects. J Immunol *169*, 7045-7053.

Toshchakov, V., Jones, B. W., Perera, P. Y., Thomas, K., Cody, M. J., Zhang, S., Williams, B. R., Major, J., Hamilton, T. A., Fenton, M. J., and Vogel, S. N. (2002). TLR4, but not TLR2, mediates IFN-beta-induced STAT1alpha/beta-dependent gene expression in macrophages. Nat Immunol *3*, 392-398.

Toyonaga, T., Hino, O., Sugai, S., Wakasugi, S., Abe, K., Shichiri, M., and Yamamura, K. (1994). Chronic active hepatitis in transgenic mice expressing interferon-gamma in the liver. Proc Natl Acad Sci U S A *91*, 614-618.

Trinchieri, G., and Gerosa, F. (1996). Immunoregulation by interleukin-12. J Leukoc Biol *59*, 505-511.

Turner, A. N., and Rees, A. J. (1996). Goodpasture's disease and Alport's syndromes. Annu Rev Med *47*, 377-386.

van den Broek, M. F., Muller, U., Huang, S., Zinkernagel, R. M., and Aguet, M. (1995). Immune defence in mice lacking type I and/or type II interferon receptors. Immunol Rev *148*, 5-18.

Vercelli, D. (2003). Arginase: marker, effector, or candidate gene for asthma? J Clin Invest *111*, 1815-1817.

Vidal, S., Gros, P., and Skamene, E. (1995). Natural resistance to infection with intracellular parasites: molecular genetics identifies Nramp1 as the Bcg/Ity/Lsh locus. J Leukoc Biol *58*, 382-390.

von Bethmann, A. N., Brasch, F., Nusing, R., Vogt, K., Volk, H. D., Muller, K. M., Wendel, A., and Uhlig, S. (1998). Hyperventilation induces release of cytokines from perfused mouse lung. Am J Respir Crit Care Med *157*, 263-272.

von Hertzen, L., Klaukka, T., Mattila, H., and Haahtela, T. (1999). Mycobacterium tuberculosis infection and the subsequent development of asthma and allergic conditions. J Allergy Clin Immunol *104*, 1211-1214.

Walker, C., Bode, E., Boer, L., Hansel, T. T., Blaser, K., and Virchow, J. C., Jr. (1992). Allergic and nonallergic asthmatics have distinct patterns of T-cell activation and cytokine production in peripheral blood and bronchoalveolar lavage. Am Rev Respir Dis *146*, 109-115.

Walter, D. M., McIntire, J. J., Berry, G., McKenzie, A. N., Donaldson, D. D., DeKruyff, R. H., and Umetsu, D. T. (2001). Critical role for IL-13 in the development of allergen-induced airway hyperreactivity. J Immunol *167*, 4668-4675.

Wang, J. M., Rambaldi, A., Biondi, A., Chen, Z. G., Sanderson, C. J., and Mantovani, A. (1989). Recombinant human interleukin 5 is a selective eosinophil chemoattractant. Eur J Immunol *19*, 701-705.

Wang, Z., Zheng, T., Zhu, Z., Homer, R. J., Riese, R. J., Chapman, H. A., Jr., Shapiro, S. D., and Elias, J. A. (2000). Interferon gamma induction of pulmonary emphysema in the adult murine lung. J Exp Med *192*, 1587-1600.

Weill, J. C., and Reynaud, C. A. (1996). Rearrangement/hypermutation/gene conversion: when, where and why? Immunol Today *17*, 92-97.

Wild, J. S., Sigounas, A., Sur, N., Siddiqui, M. S., Alam, R., Kurimoto, M., and Sur, S. (2000). IFN-gamma-inducing factor (IL-18) increases allergic sensitization, serum IgE, Th2 cytokines, and airway eosinophilia in a mouse model of allergic asthma. J Immunol *164*, 2701-2710.

Wills-Karp, M. (2000). Murine models of asthma in understanding immune dysregulation in human asthma. Immunopharmacology *48*, 263-268.

Wills-Karp, M., Luyimbazi, J., Xu, X., Schofield, B., Neben, T. Y., Karp, C. L., and Donaldson, D. D. (1998). Interleukin-13: central mediator of allergic asthma. Science *282*, 2258-2261.

Wirtz, S., and Neurath, M. F. (2000). Animal models of intestinal inflammation: new insights into the molecular pathogenesis and immunotherapy of inflammatory bowel disease. Int J Colorectal Dis *15*, 144-160.

Wood, N., Whitters, M. J., Jacobson, B. A., Witek, J., Sypek, J. P., Kasaian, M., Eppihimer, M. J., Unger, M., Tanaka, T., Goldman, S. J.*, et al.* (2003). Enhanced interleukin (IL)-13 responses in mice lacking IL-13 receptor alpha 2. J Exp Med *197*, 703-709.

Wucherpfennig, K. W., and Strominger, J. L. (1995). Molecular mimicry in T cell-mediated autoimmunity: viral peptides activate human T cell clones specific for myelin basic protein. Cell *80*, 695-705.

Wuthrich, R. P., and Sibalic, V. (1998). Autoimmune tubulointerstitial nephritis: insight from experimental models. Exp Nephrol *6*, 288-293.

Wynn, T. A. (2003). IL-13 effector functions. Annu Rev Immunol *21*, 425-456.

Ye, G., Barrera, C., Fan, X., Gourley, W. K., Crowe, S. E., Ernst, P. B., and Reyes, V. E. (1997). Expression of B7-1 and B7-2 costimulatory molecules by human gastric epithelial cells: potential role in CD4+ T cell activation during Helicobacter pylori infection. J Clin Invest *99*, 1628-1636.

Yoshida, M., Leigh, R., Matsumoto, K., Wattie, J., Ellis, R., O'Byrne, P. M., and Inman, M. D. (2002). Effect of interferon-gamma on allergic airway responses in interferon-gamma-deficient mice. Am J Respir Crit Care Med *166*, 451-456.

Yoshimoto, T., Okamura, H., Tagawa, Y. I., Iwakura, Y., and Nakanishi, K. (1997). Interleukin 18 together with interleukin 12 inhibits IgE production by induction of interferon-gamma production from activated B cells. Proc Natl Acad Sci U S A *94*, 3948-3953.

Zhang, W., Lucisano, Y. M., and Lachmann, P. J. (1997). Complement in IgA immune-complex-induced neutrophil activation. Biochem Soc Trans *25*, 462-466.

Zhou, C. Y., Crocker, I. C., Koenig, G., Romero, F. A., and Townley, R. G. (1997). Anti-interleukin-4 inhibits immunoglobulin E production in a murine model of atopic asthma. J Asthma *34*, 195-201.

Zhu, Z., Homer, R. J., Wang, Z., Chen, Q., Geba, G. P., Wang, J., Zhang, Y., and Elias, J. A. (1999). Pulmonary expression of interleukin-13 causes inflammation, mucus hypersecretion, subepithelial fibrosis, physiologic abnormalities, and eotaxin production. J Clin Invest *103*, 779-788.

Zimmermann, N., King, N. E., Laporte, J., Yang, M., Mishra, A., Pope, S. M., Muntel, E. E., Witte, D. P., Pegg, A. A., Foster, P. S.*, et al.* (2003). Dissection of experimental asthma with DNA microarray analysis identifies arginase in asthma pathogenesis. J Clin Invest *111*, 1863-1874.

9 Danksagung

Mein grosser Dank gilt Herrn Prof. Dr. Stefan Kaufmann für die Möglichkeit, diese Arbeit in einer ausserordentlich anregenden und großartigen wissenschaftlichen Umgebung anzufertigen. Ausserdem möchte ich ihm für das Vertrauen, die Unterstützung und die kompetente Betreuung danken.

Mein Dank gilt auch Herrn Prof. Dr. Roland Lauster für seine Bereitschaft diese Arbeit zu betreuen und zu begutachten.

Danken möchte ich allen, die durch viele fruchtbare Diskussionen, Anregungen und konstruktive Kritik diese Arbeit vorangetrieben haben und mir ausserdem über einige schwere Zeiten hinweg geholfen haben. Besonders erwähnen möchte ich hier Jens Zerrahn, dessen hervorragendes wissenschaftliches Verständnis mir häufig weiter geholfen hat, Immo Prinz, dem ich auch die wildesten Gele unter die Nase halten konnte, sowie Hans-Willi Mittrücker und Mischo Kursar, die nicht nur technisch und theoretisch zu dieser Arbeit beigetragen haben, sondern sie auch Korrektur gelesen haben.

Helen Collins danke ich ausserordentlich für ihre sowohl geistige als auch tatkräftige Betreuung und Unterstützung der Asthma-Versuche. Martin Witzenrath danke ich in diesem Zusammenhang für die Lungenfunktions-messungen.

Uwe Klemm und Karin Bordasch gebührt ein grosses Dankeschön für die viele Hilfe und die Betreuung der Mausarbeiten und die Geduld, mit der sie immer wieder probiert haben, weitere Transgene zu generieren.

Ein riesiger Dank geht in diesem Zusammenhang auch an Manuela Priemke, Jeanette Scherf, Daniela Groine-Triebkorn, Silke Matthias und Daniela Wittkowsky für die hervorragende Betreuung der Mäuse.

Bei Marion Herma möchte ich mich für ihre grosse Hilfe im Labor bedanken. So auch bei Frank Kaiser, Peter Geserik, Ute Guhlich, Isabell Dietrich, Jessica Bigot und Sandra Leitner, die als „Labor-Mitbewohner“ massgeblich mitverantwortlich für die angenehme Arbeitsatmosphäre waren.

Aber auch allen anderen Mitgliedern der Abteilung Immunologie des MPIIB sei gedankt für die Hilfsbereitschaft und die inspirierende und motivierende, einfach tolle Atmosphäre sowohl innerhalb aber auch ausserhalb des Instituts.

Danken möchte ich auch meinen Freunden Janek Kubelt, Stefan Vogel und Helge Schröder, die immer ein offenes Ohr für meine Probleme hatten und im richtigen Moment für Abwechslung sorgten.

Der grösste Dank jedoch gilt meinen Eltern, ohne deren Hilfe und Unterstützung diese Arbeit nicht möglich gewesen wäre, und meiner Frau Esther Daßio, die nicht nur das Abenteuer Forschung erträgt und mich dabei sogar unterstützt, sondern auch immer für mich da war. Meiner kleinen Tochter Clara möchte ich danken, dass sie mich mit ihrem Lächeln und ihrer Freude immer im richtigen Moment wieder aufgebaut hat.

10 Appendix

10.1 Plasmid maps

pcDNA3.1-Zeo

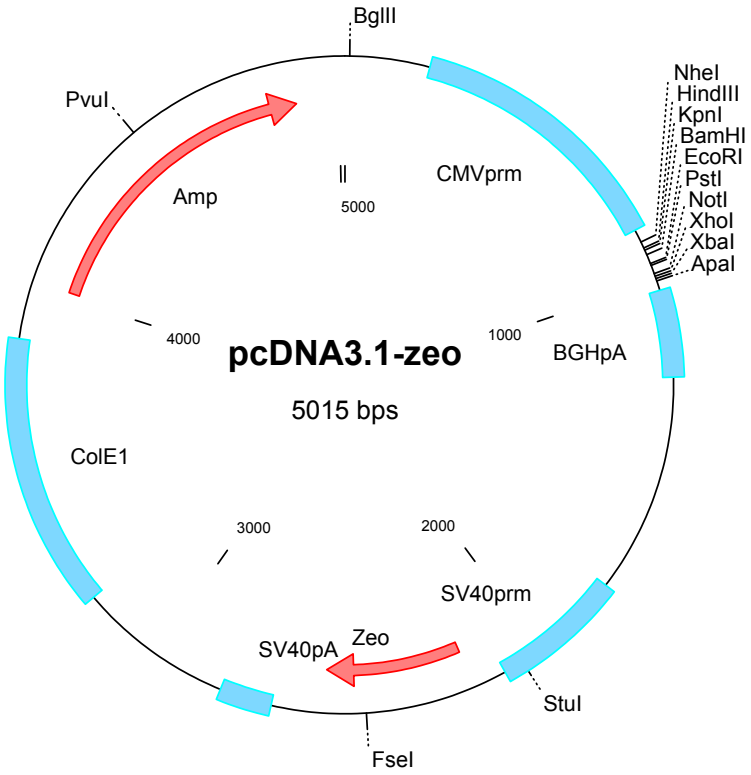

pcDNA3.1-Zeo-ΔCMV

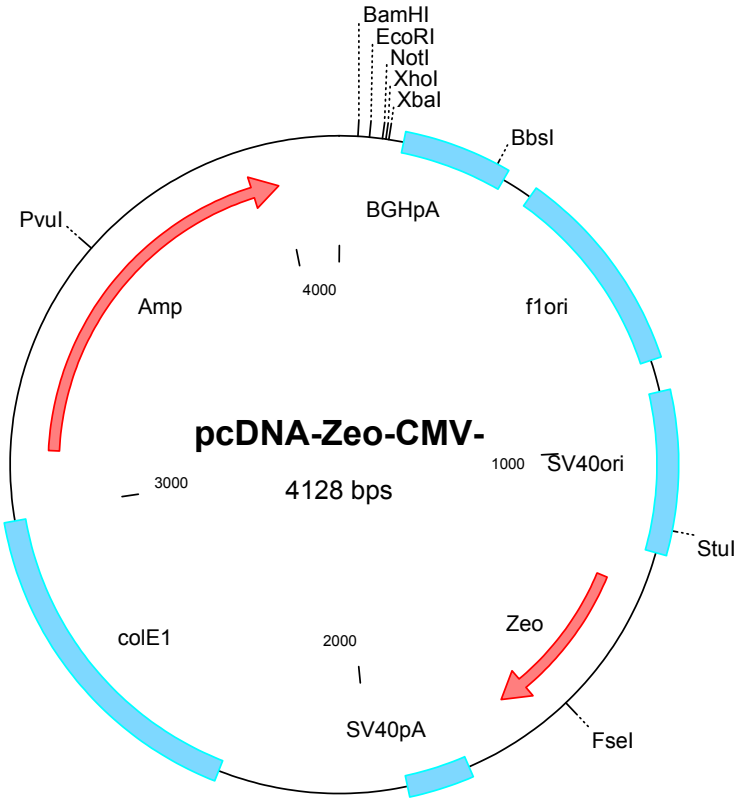

pCR2.1-TOPO

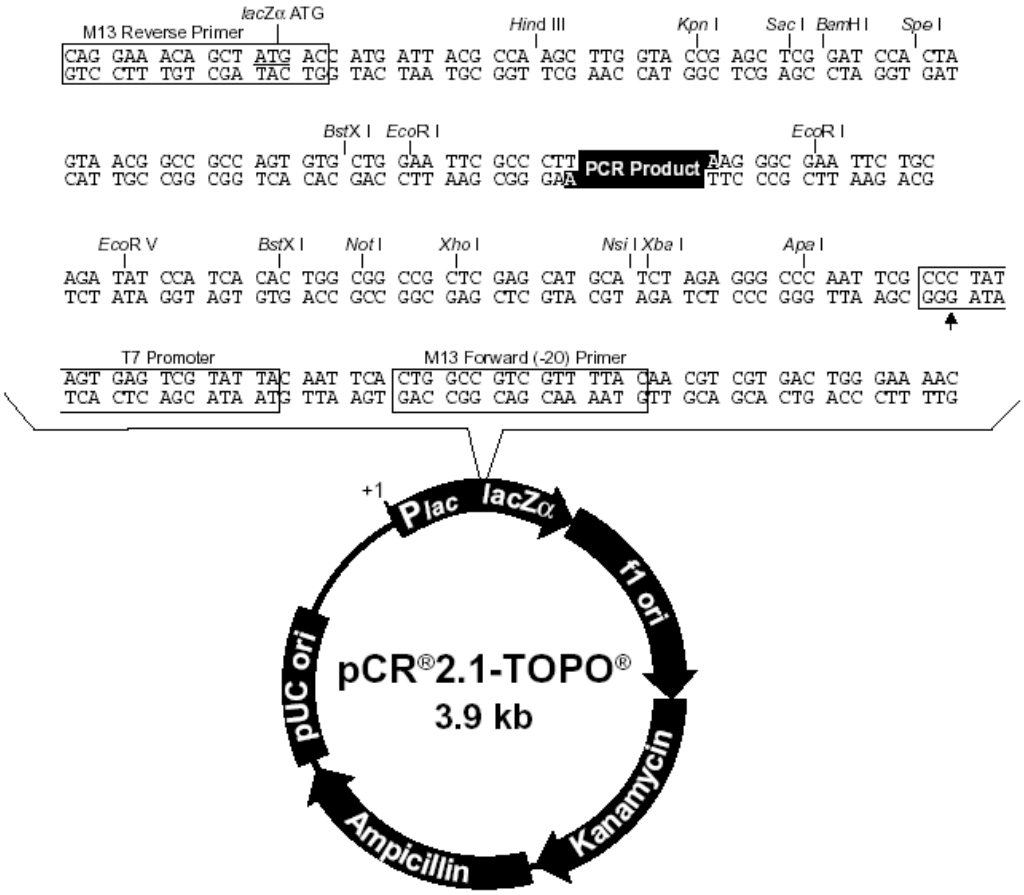

Comments for pCR®2.1-TOPO®
3931 nucleotides

LacZα fragment: bases 1-547
M13 reverse priming site: bases 205-221
Multiple cloning site: bases 234-357
T7 promoter/priming site: bases 364-383
M13 Forward (-20) priming site: bases 391-406
f1 origin: bases 548-985
Kanamycin resistance ORF: bases 1319-2113
Ampicillin resistance ORF: bases 2131-2991
pUC origin: bases 3136-3809

pPCR-Script Amp SK(+)

f1 (+) origin 135–441
β-galactosidase α-fragment 460–816
multiple cloning site 653–760
***lac* promoter 817–938**
pUC origin 1158–1825
ampicillin resistance (*bla*) ORF 1978–2833

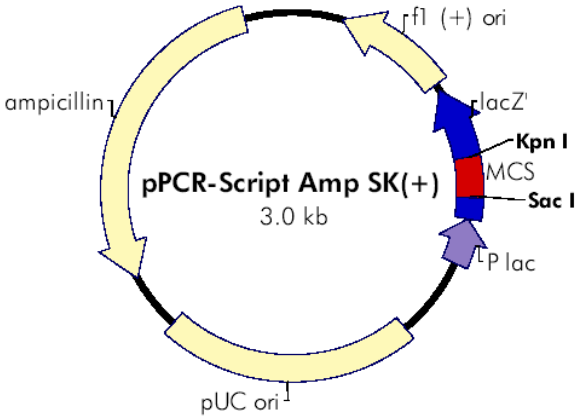

pPCR-Script Amp SK(+) Multiple Cloning Site Region
(sequence shown 598–826)

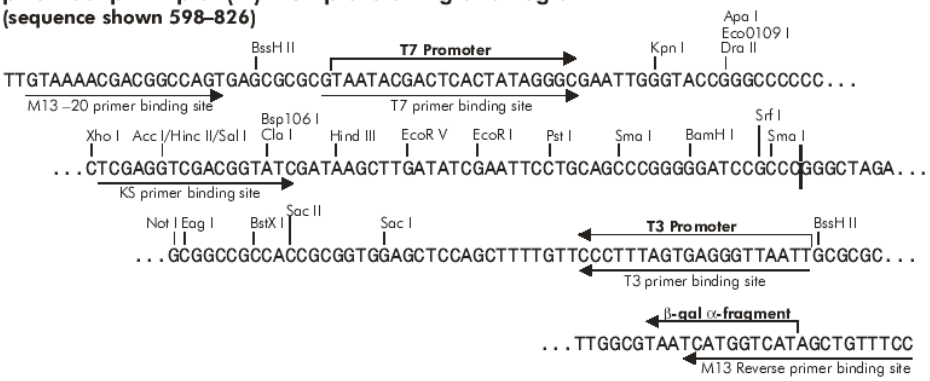

10.2 Suppliers

Supplier	Location	URL
Adobe Systems GmbH	Ohmstrasse 1 D-85716 Unterschleißheim	www.adobe.de
Agilent Technologies Deutschland GmbH	Herrenberger Strasse 130 D-71034 Böblingen	www.agilent.com
Amersham Biosciences Europe GmbH	Munzinger Strasse 9 D-79111 Freiburg	www. amershambiosciences. com
Applied Biosystems	Division Headquarters 850 Lincoln Centre Drive Foster City, CA 94404 USA	www.appliedbiosystems. com
American Type Culture Collection (ATCC)	P.O.Box 1549 Manassas, VA 20108 USA	www.atcc.org
Avidity	1899 Gaylord Street Denver, CO 80206 USA	www.avidity.com
Bachofer GmbH jetzt: Laborbedarf Saur	Wannweiler Straße 11 D- 72770 Reutlingen	www.h-saur.de
Bayer AG	D-51368 Leverkusen	www.bayer.com
Becton Dickinson GmbH (BD Biosciences): comprising products from Pharmingen and Clontech	Tullastrasse 8-12 D-69126 Heidelberg	www.bdbiosciences.com
Biochrom Labs, Inc.	1719 South 13th Street P.O. Box 996 Terre Haute, IN 47808 USA	www.biochrom.com
Bio-Rad Laboratories GmbH	Heidemannstrasse 164 D-80939 München	www.bio-rad.com
Curamed® Dr. Meindl u. Partner GmbH	Erlenstegenstrasse 5 D-90491 Nürnberg	www.curamed.de
De Novo Software	64 McClintock Crescent Thornhill, Ontario L4J 2T1 Canada	www.denovosoftware. com

Supplier	Location	URL
Eppendorf	Barkhausenweg 1 D-22339 Hamburg	www.eppendorf.com
Fuji Photo Film Europe GmbH	Heesenstrasse 31 D-40549 Düsseldorf	www.fujifilm.de
GeneCraft	Tresckowstrasse 10 D-48163 Münster	www.genecraft.de
Graph Pad Software, Inc.	11452 El Camino Real, #215 San Diego, CA 92130 USA	www.graphpad.com
Harvard Apparatus, Inc.	84 October Hill Road Holliston, Ma. 01746 USA	www.harvardapparatus.com
Heraeus Instruments	Kendro Laboratory Products GmbH Robert-Bosch-Strasse 1 D-63505 Langenselbold	www.heraeus-instruments.de
Hilgenberg GmbH	Strauchgraben 2 D-34323 Malsfeld	www.hilgenberg-gmbh.de
ICN Biomedicals GmbH.	Thüringer Strasse15 D-37269 Eschwege	www.icnbiomed.com
IKA Labortechnik IKA-Werke GmbH & Co.KG	Janke & Kunkel-Strasse 10 D-79219 Staufen	www.ika.net
Invitrogen GmbH: comprising products from Invitrogen, NOVEX and Gibco	Technologiepark Karlsruhe Emmy-Noether-Strasse 10 D-76131 Karlsruhe	www.invitrogen.com
Ismatec Laboratoriumstechnik GmbH	Futtererstrasse 16 D-97877 Wertheim-Mondfeld	www.ismatec.de
Leica Microsystems AG	Leica Mikrosysteme Vertrieb GmbH Lilienthalstrasse 39-45 D-64625 Bensheim	www.leica-microstystems.com
Merck	Frankfurter Strasse 250 D-64293 Darmstadt	www.merck.de
Metabion GmbH	Lena-Christ-Strasse 44 D-82152 Martinsried	www.metabion.de

Supplier	Location	URL
Microm International GmbH	Robert-Bosch-Strasse 49 D-69190 Walldorf	www.microm.de
Microsoft Deutschland GmbH	Katharina-Heinroth-Ufer 1 D-10787 Berlin	www.microsoft.de
Millipore GmbH	Am Kronberger Hang 5 D-65824 Schwalbach	www.millipore.de
Mobitec	Lotzestrasse 22a D-37083 Göttingen	www.mobitec.de
Molecular Devices GmbH	Gutenbergstrasse 10 D-85737 Ismaning/ München	www.moleculardevices. com
Molecular Probes Europe BV	Poortgebouw Rijnsburgerweg 10 2333 AA Leiden The Netherlands	www.probes.com
Narishige International Ltd.	Unit 7, Willow Business Park, Willow Way, London SE26 4QP United Kingdom	www.narishige.co.jp
New England Biolabs GmbH (NEB)	Bruningstr.asse 50 Geb.G810 D-65926 Frankfurt am Main	www.neb.com
Nunc GmbH und Co.KG	Hagenauer Straße 21A D-65203 Wiesbaden	www.nuncbrand.com
Olympus Deutschland GmbH	Wendenstrasse 14-18 D-20097 Hamburg	www.olympus.de
QIAGEN GmbH	QIAGEN Strasse 1 D-40724 Hilden	www.qiagen.com
R&D Systems GmbH	Borsigstrasse 7 D-65205 Wiesbaden	www.rndsystems.com
Roche Diagnostics GmbH Roche Applied Science	Sandhofer Strasse 116 D-68305 Mannheim	www.roche-applied- science.com
Rosetta Inpharmatics LLC	12040 115th Avenue N.E. Kirkland, WA 98034 USA	www.rii.com
Carl Roth GmbH & Co.KG	Schoemperlenstrasse 1-5 D-76185 Karlsruhe	www.carl-roth.de

Supplier	Location	URL
Schleicher & Schuell BioScience GmbH MicroScience GmbH	Hahnestrasse 3, D-37586 Dassel/ Relliehausen	www.schleicher-schuell.de
Scientific Software Group	P.O. Box 708188 Sandy, Utah 84070 USA	www.scisoftware.com
Serag Wiessner	Zum Kugelfang 8-12 D-95119 Naila	www.serag-wiessner.de
SERVA Electrophoresis GmbH	Carl-Benz-Str. 7 P.O.B. 10 52 60 D-69115 Heidelberg	www.serva.de
Thermo Shandon, Inc.	171 Industry Dr. Pittsburgh, PA 15275 USA	www.shandon.com
Sigma-Aldrich Chemie GmbH	Eschenstrasse 5 D-82024 Taufkirchen bei München	www.sigmaaldrich.com
Stratagene Europe	P.O. Box 12085 1100 AB Amsterdam The Netherlands	www.stratagene.com
Validyne	8626 Wilbur Avenue Northridge, CA 91324 USA	www.valdyne.com
Zapf Instruments	Emmy-Noether-Straße 5 D-31157 Sarstedt	www.zapf-instruments.de
Zeiss: Unternehmensbereich Mikroskopie	Rankestr. 26 10789 Berlin	www.zeiss.de